

A THESIS

ON

"THE DYNAMIC BENDING PROPERTIES OF TEXTILE
FIBRES AND THE EFFECTS OF TEMPERATURE AND
HUMIDITY THEREON"

PRESENTED TO
THE UNIVERSITY OF GLASGOW
IN ACCORDANCE WITH THE
REGULATIONS GOVERNING THE AWARD OF THE
DEGREE OF DOCTOR OF PHILOSOPHY

BY

WILLIAM MORTIMER KUBIE

OCTOBER, 1961.

ProQuest Number: 13850782

All rights reserved

INFORMATION TO ALL USERS

The quality of this reproduction is dependent upon the quality of the copy submitted.

In the unlikely event that the author did not send a complete manuscript and there are missing pages, these will be noted. Also, if material had to be removed, a note will indicate the deletion.



ProQuest 13850782

Published by ProQuest LLC (2019). Copyright of the Dissertation is held by the Author.

All rights reserved.

This work is protected against unauthorized copying under Title 17, United States Code
Microform Edition © ProQuest LLC.

ProQuest LLC.
789 East Eisenhower Parkway
P.O. Box 1346
Ann Arbor, MI 48106 – 1346

ACKNOWLEDGEMENTS

The author wishes to express his gratitude to Professor R. Meredith, D.Sc., F.Inst.P., F.T.I., F.R.S.E., for his continued advice and guidance throughout the course of this work.

He is indebted to the Royal College of Science and Technology, Glasgow, for the award of a Walter Duncan Research Scholarship and a supplementary grant, and to the Courtaulds' Scientific and Educational Trust Fund for the award of a Courtaulds' Post Graduate Scholarship.

ABSTRACT

The dynamic bending properties of dry wool, silk, Fibrolane, ramie, Fortisan, acetate fibre, Tricel, two types of Acrilan and polypropylene were investigated in vacuo, over a temperature range of -70°C to $+170^{\circ}\text{C}$.

An electrostatic technique was used, wherein fibres are sustained in lateral vibration by an applied alternating voltage from an audio frequency oscillator.

Transition phenomena, characterised by rapid changes in dynamic elastic modulus, accompanied by peaks in the loss modulus-temperature curve, are discussed in relation to the molecular structures of the fibres. High temperature transitions were generally the result of secondary bond breakdown in non-crystalline regions, while low temperature transitions were due to main or side chain activities in non-crystalline regions.

Further support for a "coiled-coil" α -keratin wool structure is established, and a "coiled-coil" β -keratin structure is proposed for Fibrolane. A comparison of the protein fibres with nylon 66, shows the latter to be more closely related to silk in some respects, and to wool and Fibrolane in others.

Lack of experimental evidence of hydrogen bond breakdown in ramie and Fortisan is explained, particularly by a comparison with viscose rayon.

Acetate fibre and Tricel showed marked resemblances in their dynamic responses to temperature, but the influence of hydrogen bonding in the former was still detectable.

Significantly different dynamic responses of two chemically identical types of Acrilan are related to a difference thought to exist in their respective manufacturing processes. A modification to a previous interpretation of the response of the chemically related Orlon is proposed.

Three transitions in polypropylene could not all be associated with similar transitions in polyethylene. A helical chain configuration, methyl groups and lack of branching in the former, were thought to be largely responsible.

The dynamic bending properties of wool, nylon 66 and viscose rayon at 20°C were investigated in a partial vacuum, over a range of 0 to 90% relative humidity. Fibre internal friction is calculated by applying a factor which corrects for the effect of external damping caused by the presence of water vapour.

Changes in the elastic and loss moduli are discussed in terms of molecular structure, and in the case of wool and viscose rayon, with special regard to the two-phase sorption process.

A method for predicting the location, and estimating the magnitude of a loss modulus peak of nylon at different temperature-humidity conditions is suggested.

A good correlation between temperature and humidity experiments is obtained with regard to dispersion mechanisms.

CONTENTS

	<u>Page</u>
<u>INTRODUCTION</u>	1
Characteristics of Dynamic Mechanical Behaviour	2
Internal Friction 	5
Dynamic Bending Modulus.. 	6
Some Basic Theories of Mechanical Properties:	
Dynamic Mechanical Properties and	
Phase Transitions 	8
Frequency Transitions	15
Temperature Transitions.. 	17
Effect of Humidity 	19
<u>LITERATURE SURVEY</u>	22
Static Tensile and Torsional Deformations:	
Natural, Regenerated and Synthetic Fibres	22
Dynamic Tensile and Torsional Deformations:	
Natural and Regenerated Fibres	25
Synthetic Fibres	32
Rubbers, Plastics and other Filamentous	
Polymers	41
The Flexion of Textile Materials by Static Methods:	
Natural, Regenerated and Synthetic	
Fibres	52
The Flexion of Textile Materials by Dynamic Methods:	
Natural and Regenerated Fibres	53

<u>EXPERIMENTAL</u>	60
Apparatus and Instruments: Changing Temperature at 0% r.h.	61
The Mounting Head	61
Fibre Excitation	62
Heating System	63
Cooling Unit	64
Fibre Selection, Preparation and Conditioning	65
Procedure	66
Quantities Measured and Methods of Measurement	67
Apparatus and Instruments: Changing Humidity at 20°C	71
The Mounting Head, Fibre Excitation, The Humidity Chambers	71
Fibre Selection, Preparation and Conditioning	72
Procedure	72
Quantities Measured and Methods of Measurement	74
Calibration and Instrument Checks	75
<u>INVESTIGATIONS AND RESULTS</u>	76
Temperature Experiments	77
Effect of Pressure on Amplitude	77
Effect of Amplitude on Dynamic Bending Modulus and Loss Tangent	78

Effect of Frequency on Dynamic Bending Modulus and Loss Tangent	80
Effect of Temperature on Dynamic Bending Properties	82
Thermal Expansion	87
Humidity Experiments	89
Fibre Dimensions and Swelling	90
The Damping Correction Factor and Dynamic Parameters for a Partial Vacuum	91
<u>DISCUSSION AND CONCLUSIONS</u>	96
Temperature Experiments:	
<u>Protein Fibres:</u>	96
Wool	98
Silk	105
Fibrolane	110
The Proteins and Nylon 66	113
<u>Cellulose Fibres:</u>	116
Ramie and Fortisan	116
<u>Modified Regenerated Cellulose Fibres:</u>	123
Acetate Fibre and Tricel	123
<u>Synthetic Fibres:</u>	129
Acrilan A and Acrilan B	129
Acrilan and Orlon	135
Polypropylene	136
Polypropylene and Polyethylene	140

Humidity Experiments	143
Wool	143
Nylon 66	148
Predicting and Estimating the Hydrogen Bond Dispersion in Nylon 66	152
Viscose Rayon	154

the crystal axis.

Amorphousness parameter of a

crystalline parameter of a

$0.577 + 10^4$.

temperature.

molecular activation energy.

Flexural rigidity.

Flexural rigidity of fibre with

flexural rigidity of fibre with

constant 1.575 for the function

of function.

series.

dynamic strain amplitude.

series.

LIST OF SYMBOLS

A	area of cross section, constant.
E_1	dynamic modulus.
E_2	dynamic loss modulus.
$E^{\mathbb{E}}$	complex modulus.
E_b $E_b 20^\circ\text{C}$	dynamic bending modulus at 20°C .
F_1	correction factor for moisture swelling.
I	moment of inertia about a line perpendicular to the plane of bending and passing through the neutral axis.
K	dimensionless parameter of m.
K'	dimensionless parameter of m.
L	$0.577 + \ln m$.
T	temperature.
U	molecular activation energy.
Y	flexural rigidity.
Y_1	flexural rigidity of fibre with shape factor ξ'
Y_0	flexural rigidity of fibre with shape factor ξ'_0
c	constant: 1.875 for the fundamental mode of vibration.
e	strain.
e_0	dynamic strain amplitude.
f	stress.
f_0	dynamic stress amplitude.
i	$\sqrt{-1}$

- k Boltzmann's constant (1.379×10^{-16} ergs/degree).
- l length.
- m $\left(\frac{\rho_a A \omega}{4 \pi \mu}\right)^{\frac{1}{2}}$, fibre mass.
- m_1 mass per unit length.
- r reaction rate
- t time
- β ratio of the density of water vapour to the fibre density.
- δ loss angle.
- ξ' shape factor for irregular cross sections.
- ξ'_0 shape factor for circular cross sections.
- η coefficient of internal friction (ratio of out of phase component of stress to the rate of change of strain).
- μ coefficient of viscosity of air, water vapour.
- ν_0 resonant frequency in vacuo (c/s).
- $\Delta\nu_0$ bandwidth in vacuo (c/s).
- ρ fibre density.
- ρ_a density of air, water vapour.
- ω angular frequency (radians/sec.).
- ω_a resonant angular frequency in air, partial vacuo (radians/sec.).
- ω_0 resonant angular frequency (radians/sec.).
- $\Delta\omega_a$ bandwidth in air, partial vacuo (radians/sec.).

INTRODUCTION

The term "dynamic bending properties" infers the modes of response of materials to periodic variations of bending stress or strain. The stress or strain is usually varied sinusoidally with time. The determination of the dynamic properties, in general, of textile materials, is of two-fold importance:

1) in the understanding of molecular processes which underlie the response of polymers to mechanical forces. The information derived therefrom, when combined with that obtained from static or quasi-static investigations, serves to give a broader basis on which to expound a more complete theory of the rheological behaviour of fibres. The results of the study of the dynamic elastic and viscoelastic components as functions of frequency, temperature, and humidity, help to define both the magnitude and nature of the molecular barriers resisting forces of deformation, and the relative contributions of the elastic and viscous components of the total strain, during deformation. Perhaps the most important aspect of dynamic investigations is that they do provide a means of identifying the relative contributions of the elastic and viscous components of a viscoelastic

material such as a fibre.

2) in assessing the suitability for purpose of the fibres to their end uses. Materials are often subjected to sudden shocks, impacts, loads or are otherwise deformed under high rates of loading such as in tyre cords, fan beltings and parachute materials, and must possess the necessary mechanical properties to withstand these conditions. In contrast to the severity of these conditions, certain materials are required to possess good draping and handling qualities, in which case the bending properties of the constituent fibres might be expected to bear some relationship to those of the finished article.

Thus the dynamic properties of fibres yield useful theoretical information, which may also be put to practical use. Like ~~any~~ other physical properties, the dynamic mechanical behaviour must be measured, and the quantities used to characterise this behaviour are now discussed.

Characteristics of Dynamic Mechanical Behaviour

The two quantities used to characterise dynamic mechanical behaviour are elastic modulus and internal friction which represent the elastic and viscous responses

respectively of a viscoelastic material such as a fibre, to a deformation. In the case of the elastic component the energy imposed is conserved, and is in phase with the displacing force, while in the case of the viscous component, the imposed mechanical energy is dissipated as heat, and is out of phase with the displacing force by $\pi/2$ radians. The two quantities combined give the complex modulus and the relationship may be expressed as

$$E^* = E_1 + iE_2$$

where E^* is the complex modulus

E_1 is the dynamic modulus

E_2 is the loss modulus

i is the operator.

The derivation of this relationship is outlined below.

Assuming small deformations, thereby avoiding non-linear effects, such as powers of strain or rate of strain higher than the first, the value of the strain in the specimen at any particular moment, responding to a sinusoidally varying displacement is given by

$$e = e_0 \sin \omega t \quad \dots\dots\dots(1)$$

where e_0 is the dynamic strain amplitude

ω is the angular frequency

t is the time

The stress at this point will have a certain phase lead δ and is given by

$$f = f_0 \sin(\omega t + \delta) \dots\dots\dots(2)$$

where f_0 is the stress amplitude

ω is the same angular frequency

δ is the loss angle.

This may be rewritten

$$f = f_0 \sin \omega t \cos \delta + f_0 \cos \omega t \sin \delta \dots\dots(3)$$

which indicates that the stress actually consists of two components, $f_0 \cos \delta$ in phase with strain, and $f_0 \sin \delta$ out of phase with strain and lagging by $\pi/2$ radians.

Let E_1 be the elastic component, of size $\frac{f_0 \cos \delta}{e_0} \dots\dots(4)$

Let E_2 be the viscous component, of size $\frac{f_0 \sin \delta}{e_0} \dots\dots(5)$

Let E^* be the total modulus and equal to $\frac{f_0}{e_0}$

then substituting in equation (3)

$$f = e_0 E_1 \sin \omega t + e_0 E_2 \cos \omega t \dots\dots\dots(6)$$

From (4) $\frac{E_1}{\cos \delta} = \frac{f_0}{e_0} = E^* \dots\dots$ hence $E_1 = E^* \cos \delta \dots\dots(7)$

(5) $\frac{E_2}{\sin \delta} = \frac{f_0}{e_0} = E^* \dots\dots$ hence $E_2 = E^* \sin \delta \dots\dots(8)$

$$\text{From (7)} \quad E_1^2 = E^*{}^2 \cos^2 \delta$$

$$(8) \quad E_2^2 = E^*{}^2 \sin^2 \delta$$

$$(7)+(8) \quad E^*{}^2 = E_1^2 + E_2^2$$

Introducing the operator i , this may be re-written

$$E^* = E_1 + iE_2$$

The Internal Friction

The loss modulus E_2 , which represents the internal frictional loss, can be expressed in several ways.

By defining the coefficient of internal friction, η , as the ratio of the out of phase component of the stress to the rate of change of strain, and hence dividing the second term in equation (6) by the differential of $e_0 \sin \omega t$,

$$\eta = \frac{E_2}{\omega} \quad \text{and} \quad E_2 = \omega \eta$$

Another expression is the loss tangent, $\tan \delta$ which by dividing equation (8) by equation (7) gives:

$$\tan \delta = \frac{E_2}{E_1}$$

Hence loss modulus in terms of loss tangent is given by

$$E_2 = E_1 \tan \delta$$

Although not used in this investigation two further methods

of measuring internal friction deserve mention. One is the specific damping capacity which is defined as the ratio of the energy dissipated per cycle of vibration to the strain energy when the strain is a maximum and is equal to $2\pi \tan \delta$.

The other, known as the logarithmic decrement and equal to $\pi \tan \delta$, is used in free vibration experiments. It is obtained experimentally from the natural logarithm of the ratio of the amplitudes of successive oscillations, as the amplitude diminishes.

The Dynamic Bending Modulus

Hsu¹ made a rigorous analysis of the theory of vibration of viscoelastic bars and applied the theory to fibres, to obtain the standard expression for the dynamic bending modulus, which is used in this investigation.

$$\text{i.e.} \quad E_1 = \frac{\rho A}{I_c^4} \cdot l^4 \cdot \omega_0^2 \quad \dots \dots \dots (9)$$

where E_1 is the dynamic bending modulus (dynes/cm²).

ρ is the density in gm/cc.

I is the moment of inertia of the cross section about a line perpendicular to the plane of bending and passing through the neutral axis.

c is a constant for the fundamental mode of vibration and has the value 1.875.

l is the length in cm.

ω_0 is the resonant frequency in radians/second

This equation can now be transformed into quantities which are experimentally more easily measurable. It may be written in the form

$$E_1 = \frac{1.295 \pi^3 \rho^2 l^4 \nu_0^2}{\xi' m_1} \dots\dots\dots(10)$$

where ν_0 = frequency in cycles/second (at resonance)

ξ' = a shape factor depending on the cross sectional shape.

m_1 = mass/unit length (gm/cm.)

The derivation is thus:

$$E_1 = \frac{\rho A}{I c^4} \cdot l^4 \omega_0^2$$

Since $\omega_0 = 2\pi \nu_0$ and for a circular cross section $I = \frac{A^2}{4\pi}$

$$\begin{aligned} E_1 &= \frac{\rho \cdot 4\pi}{A \cdot 1.875^4} \cdot l^4 4\pi^2 \nu_0^2 \\ &= \frac{16\pi^3 \rho^2 \cdot l^4 \nu_0^2}{A \rho 1.875^4} \\ &= \frac{16\pi^3}{1.875^4} \cdot \frac{\rho^2}{m_1} l^4 \nu_0^2 \\ &= \frac{1.295 \pi^3 \rho^2 l^4 \nu_0^2}{m_1} \end{aligned}$$

The shape factor ξ' is introduced in the denominator to account for a moment of inertia differing from that of a

circular cross section. The proof for the relation $= \frac{I_1}{I_0}$ where I_1 is the moment of inertia of an irregular cross section, about an axis perpendicular to the plane of bending and passing through the neutral axis, and I_0 is the moment of inertia of a circular section will follow (See "Shape Factor, p.69).

The loss tangent is expressed as the ratio $\frac{\Delta \nu_0}{\nu_0}$ where $\Delta \nu_0$ is the difference between two frequencies straddling the resonant frequency ν_0 , at which the amplitude of vibration is $\frac{1}{\sqrt{2}}$ of that at resonance. These quantities are directly measurable experimentally.

The foregoing discussion serves to explain some parameters of dynamic properties, and in particular those with which this investigation is directly concerned. In order to present a broader basis on which to interpret the results of the investigation, further fundamental aspects are discussed.

Some Basic Theories of Mechanical Properties:

Dynamic Mechanical Properties and Phase Transitions.

With regard to the understanding of molecular processes responding to external forces, the following theory, based on that of Maxwell², may be advanced.

When a polymeric material such as a fibre is subjected to a static stress, the strain can take place

by one or more of several mechanisms. The most rapid response is that of bending of the bond angles along the polymer chain. If there were no other forces involved which restrained this motion, it should take place instantaneously. Another method of deformation is by the uncoiling of chains and chain segments. In the unstressed condition, the polymer chains are considered to be in a randomly coiled configuration, moving about their lowest energy positions under the action of thermal agitation. When a stress is applied, it tends to uncoil the chains from their normal configuration. This uncoiling is resisted by secondary bonds between chain segments. In order that these bonds break, they must reach their activation energy under the combined action of applied stress and thermal agitation. Therefore the breaking and reforming of bonds is time dependent. The rate at which such a process takes place (r) varies with the absolute temperature (T) according to the relationship

$$r = Ae^{-U/kT}$$

where A = a constant

U = molecular activation energy of the bonds involved

k = Boltzmann's constant

A third mechanism by which chain molecules can deform is

by chain slipping and again the same process of reaching the activation energy of the bonds involved takes place. This type of deformation is not recoverable upon removal of the stress. Chain-chain slipping does not take place when the chains are held together by primary chemical bonds such as chemical cross links, or by crystallites acting as cross links between chains.

The above gives an indication as to the type of response which may be expected when a fibre is subjected to a continually increasing applied static stress, at a constant humidity and temperature. When small forces, which do not involve the above mentioned third form of deformation are applied, significant molecular responses may be observed, if a dynamic force is applied in any particular direction relative to the fibre axis and the frequency is varied over a very wide range. Similar phenomena may be observed as the temperature or humidity to which the material is exposed is varied, and these are discussed later in terms of transition phenomena with particular reference to their effects on the loss modulus.

Before so doing it may be advantageous to discuss phase transitions in general, and the mechanisms by which they take place.

While such transitions, as indeed all important properties of polymers, depend on the motions which their bonded atoms undergo, under the action of thermal, mechanical and other forces, the general discussion is confined to thermal agitation for the sake of clarity. The theories advanced are based on those proposed by Mark³ and Gordon⁴.

Phase changes or transitions may thus be defined as phenomena which occur as the complex molecular structure of a polymer is altered by external agencies, thereby conferring different mechanical and other properties on the individual phases. They are in principle equilibrium phenomena, which can be reproduced reversibly regardless of whether the critical transition temperatures are approached from higher or lower temperatures.

Molecules in fibre forming polymers, as in all states of aggregation, unlike our crude and lifeless models of them, are endowed with thermal motion. The types of motion to be found, before breakdown of the main chains, are rotational in the case of chain segments, and vibrational in the case of secondary bonds. Such movements are normally arrested in the crystalline domains, while it is precisely the arresting or freezing of the motions in amorphous regions which gives rise to transitions. The rotational

movements may be visualised as large oscillatory movements about bonds which have to surmount energy barriers to facilitate this movement. At low temperatures, free volume space is reduced and rotations are frozen, a process which is aided by the number, type and strength of the secondary bonds in the structure. The vibrational movements of the secondary bonds may be visualised as similar to those of tiny flexible steel springs being stretched and released repeatedly. As the disturbing force increases, the bonds will ultimately yield. Conversely, these bonds will re-unite as the disturbing force diminishes. The transition due to secondary bonds will normally occur at higher temperatures than that due to segmental motions.

It is not to be imagined that only two transitions can be observed as a fibrous polymer is cooled (from below melting point in the case of melting polymers). It often occurs that with decreasing temperatures, a different arrangement of the centres of gravity of individual molecules or a different orientation becomes more stable. This leads to the existence of various polymorphic phases which may be separated from each other by transition points.

Certain polymers in the melt, when cooled, have individual molecules which form strong bonds with each other before they have time to assume the relative geometric

arrangement required for the formation of the densest 3-dimensional lattice and a glassy type polymer results, which exhibits what is commonly termed a glass transition at a certain critical temperature. Below this temperature, rigidity is introduced into the molecular system, while above, the polymer is rubbery. Glass transitions are realisable in some polymers. In others, however, such as highly cross linked materials (e.g. phenolics) and, more commonly found in textile fibres, rigid materials (e.g. cellulose), bond dissociation energies are lower than rotational barriers. Pyrolysis will then occur before a rubbery stage can be reached on heating.

A glass transition in such "amorphous" linear polymers as have been described, is regarded as taking place in the following manner. (Tobolsky⁵ draws a very striking analogy of the process). Since the wriggling segmental motion is due to thermal energy and the existence of free volume, as the temperature is reduced the free volume becomes very small compared with the thermal energy barrier heights for rotational and translation jumps of the polymer segments to take place. At a critical temperature or within a narrow temperature range, the wriggling and diffusional motions of the polymer molecules are

frozen, and the polymer segments and atomic groups can make only vibrational motions as in an ideal solid. The polymer has now entered the glassy state from the rubbery state.

Summarising, it is reasonable to say transition phases are many and varied. These reflect the fact that the gradual consolidation of a three dimensional network in which the individual units have a shape departing widely from spherical symmetry and are attracted to each other by a variety of relatively weak, anisotropic forces, is a complicated and multistep process of settling down to an ultimate arrangement of highest consolidation through a series of states of intermediate stability.

To exemplify phase changes more precisely, transition phenomena with reference to the dynamic Young's modulus and loss modulus, as affected by temperature and frequency changes are discussed. While polymorphic **characteristics** may be expected, in order to avoid complexity, only two phase changes are considered; one due to a generalised segmental motion, the other due to arbitrary secondary forces. Humidity effects are also discussed.

Frequency Transitions (at constant temperature and relative humidity).

It has earlier been implied that on the application of a small static stress, an uncoiling of the main chains in the amorphous regions is resisted by secondary bonds between them which will eventually yield completely. (Molecules in crystalline domains are relatively unaffected due to their high degree of packing and subsequent strong interactive forces). If the direction of the disturbing stress is reversed, and the frequency of this reversal is gradually increased the characteristic vibration of the secondary bonds will come into effect and, due to insufficient time for large relaxations, the tendency to relax diminishes. On further increasing the frequency, a rate of stress reversal will be reached at which and beyond which, these bonds will behave rigidly, being unable to adjust themselves to the rapidly changing stress. This gradual change from viscoelastic to elastic behaviour is a transition phenomenon. It also explains why the dynamic Young's modulus is greater than the static Young's modulus - the strain responding to a given stress becoming smaller as the resisting force of the bonds becomes greater.

The molecular chain segments flow quite freely at low frequencies. As the imposed "elastic vibration"

increases in frequency, it will also eventually match the average relaxation frequency of the molecular chain segments. (Relaxation frequency is definable as the average rate at which rotational jumps of molecular chain segments occur.) At and beyond this frequency, the motion of the molecular chain segments will be arrested, and a second high frequency transition is realised.

On passing through these transitions the rate of increase of dynamic Young's modulus is greatest because it is in these regions that the secondary bonds, and chain segments respectively become rigid, and due to the resistance offered to the disturbing stress the strain is smaller.

The loss modulus, being a measure of the internal friction, is proportional to the stress resisted by the secondary bonds and chain segments times their respective displacements, or the energy dissipated. Below each transition frequency, the resistance to stress is negligibly small, while the displacement of the structural elements is relatively large. Above each transition frequency, when motions are arrested, the resistance to the disturbing force is large and the displacement negligibly small. The product in each case will therefore tend to be small in comparison to that at transition frequencies where there is both considerable resistance and displacement prior to "freezing".

Hence at these transition frequencies, the energy dissipated and hence the loss modulus will pass through a maximum.

Temperature Transitions (at constant frequencies and relative humidity).

At sufficiently high temperatures, the thermal energy to which the secondary bonds in the amorphous regions are subjected, causes their rupture at a point where their dissociation energies are reached. On cooling the bonds will tend to reform, until a stage is reached where they are rigid. This change will give rise to a transition. On further cooling, the molecular chain segments which have flowed with ease at elevated temperatures will eventually be arrested as the free volume space and rotational barriers are reduced and increased respectively. A second low temperature transition is realised.

The effect of the high temperature transition on dynamic elastic modulus and loss modulus is similar to that of the low frequency transition while the low temperature transition has a similar effect to that of the high frequency transition. Indeed, it has been shown by Onogi and Ui⁶ that the low temperature and high frequency transition in polyvinylidene-vinylchloride fibres exhibit equal loss

maxima and that below the low temperature transition the dynamic modulus is equal to that above the high frequency transition.

When the secondary bonds are relaxed, their resistance to stress is small, and as their gradual consolidation continues, the dynamic modulus and loss modulus will increase. The dynamic modulus will pass through a maximum rate of increase at the transition temperature while below this temperature the dynamic modulus will continue to increase, but at a lesser rate until the low temperature transition is reached. This is due to the fact that the stress is transferred more to the molecular chain segments which flow freely and show little resistance. As the motions of the chain segments become restricted on further reducing the temperature, the resultant strain to an applied stress becomes smaller and the rate of increase of dynamic modulus reaches a maximum as the low temperature transition is realised.

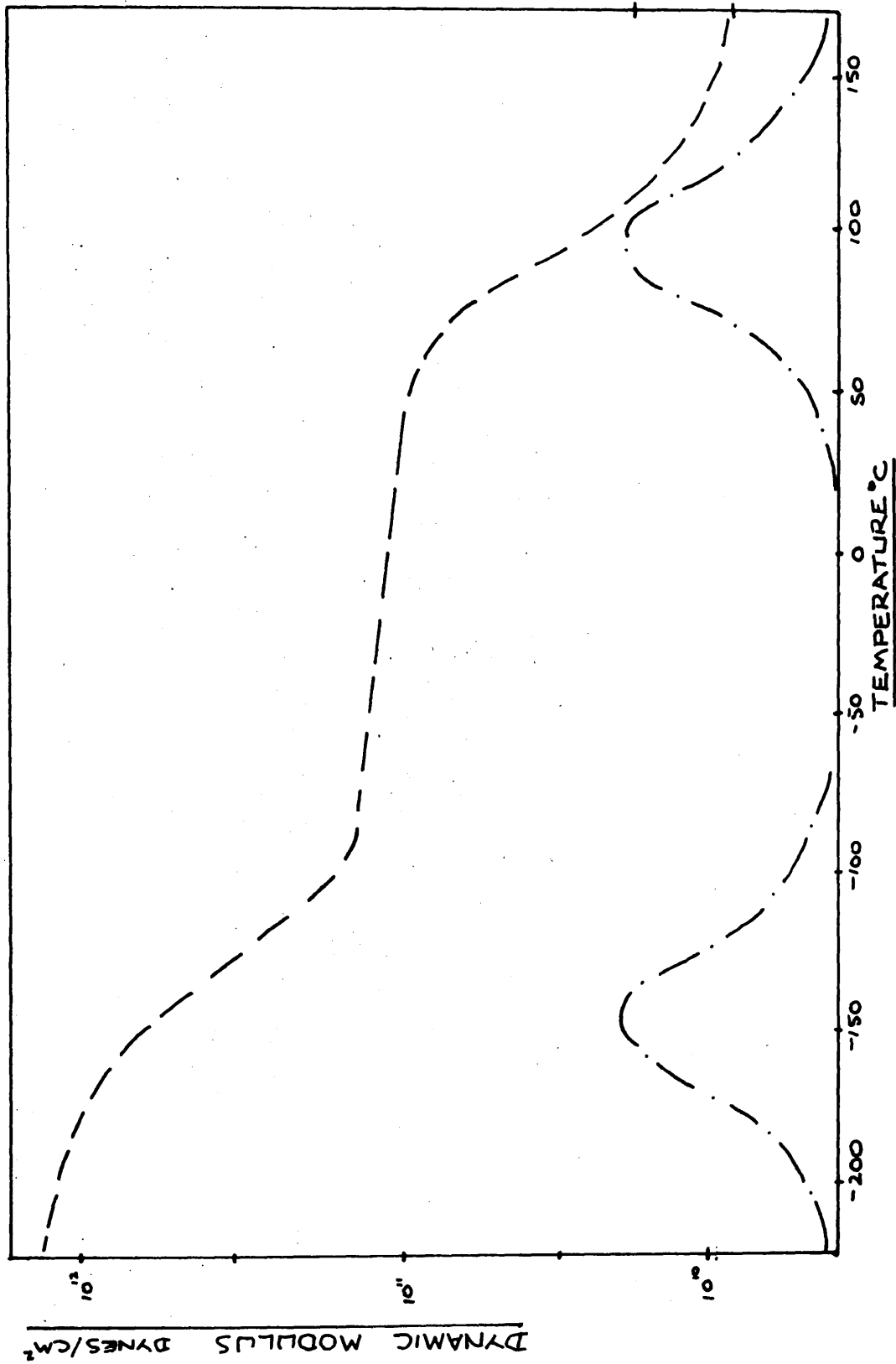
The loss modulus for the same reasons described in the case of frequency transitions, passes through a maximum at the high and low temperature transitions.

Figs.1 and 2 typify the dependence of dynamic modulus and loss modulus on frequency and temperature.

FIG. 2.

LOSS MODULUS ARBITRARY
UNITS

DYNAMIC MODULUS LOSS MODULUS



The Effect of Humidity

When moisture is absorbed by a fibre, it is normally the result of water molecules penetrating into the amorphous regions. The action of the molecules is to break apart existing secondary bonds and if a transition is to be realised and represented by a maximum in the loss modulus curve, it will be due to a gradual increase in dissipated energy, as the stress imposed upon the bonds increases, and a subsequent drop in energy dissipated when bond resistance has been overcome. Again an arbitrary secondary bond has been considered, because it is known that several types exist. For instance Feughelman⁷ states that the molecular forces holding wool together which are affected by the presence of moisture are Van der Waals forces, salt linkages and hydrogen bonds. Thus it may be expected that more than one transition can exist, or that these separate transitions are combined by one occurring immediately after another, with a certain amount of overlap. Alternatively, a transition may not be realised since unlike a temperature or frequency range, the humidity range is limited, namely between 0% relative humidity and 100% relative humidity. Working with horn keratin, which will be expected to show similar characteristics to wool, Warburton⁸ found that the logarithmic decrement increased gradually from 0% to 15% regain, and

rather more quickly thereafter, but a maximum did not occur. Quistwater and Dunell⁹ on the other hand produced a curve for nylon 66, in which the loss modulus had a maximum at 60% relative humidity, while Kawai and Tokita¹⁰ found that polyvinyl alcohol showed a point of inflection between 25 and 65% relative humidity, the loss modulus being relatively constant at a low value below 25%, and relatively constant at a higher value above 65% relative humidity.

The other mechanism by which a loss maximum occurs, is the arresting of molecular chain segments in the amorphous regions. Again considering a generalised segmental motion, as moisture is adsorbed not only will it tend to break the secondary bonds, but it will occupy free volume which had previously been available for bond rotation. Again, since the humidity range is confined, it is to be expected that either a second loss maximum will occur, or a single maximum consisting of two components, one due to the secondary bonds, the other to segmental motion.

The dynamic modulus will generally decrease with gradual moisture adsorption, as many workers (e.g. van Wyk¹¹, Warburton⁸, Speakman¹²) have found to be the case. Meredith¹³ describes the fall of torsional rigidity of several fibres, with increase in regain as being consistent with the idea that this fall is caused by the breaking of

hydrogen bonds between chain molecules in the non-crystalline regions, and that at saturation regain one molecule of water is bound to each accessible polar group which would otherwise be linked to a similar polar group in a neighbouring chain molecule by means of an hydrogen bond.

Speakman¹² attributes the fall in the rigidity of wool to the breaking of hydrogen bonds between CO and NH groups of neighbouring chain molecules, as water is absorbed. It is possible from Feughelman's hypothesis, to relate this fall to salt linkages and Van der Waals forces being broken as well as to the breakage of hydrogen bonds. It would further be expected that as in a temperature or frequency transition, a maximum rate of change of dynamic modulus accompanies a maximum in the loss modulus, if such is to be realised in humidity experiments.

Literature Survey

It appears to be little more than a decade since the first studies of the dynamic bending properties of fibre forming or filamentous materials were carried out, while for more than twenty-five years, considerable research has been devoted to the general dynamic behaviour of such materials. Tensile and torsional properties yield useful information, and in order to have a complete dynamic theory, must be considered together with bending properties. To provide a maximum of useful information, the following chapter therefore makes reference to static, and, in greater detail, to dynamic investigations involving the three main types of mechanical deformation and the effects of varying frequency temperature and humidity conditions.

The Tensile and Torsional Deformation of Polymers and Textiles.

1. Static Deformations.

Natural, Regenerated and Synthetic Fibres.

The stiffness-temperature behaviour of various filaments, including viscose and acetate rayon and synthetics, was investigated by Brown¹⁴, where stiffness referred to the

modulus at 1% strain. All filaments, with the exception of viscose rayon showed a second order transition temperature which was associated with the amorphous phase. Below the transition temperature, the polymer chains exhibited a high resistance to deformation, their segments being relatively immobile. Above this temperature, the chains were mobile in the amorphous regions but those in the crystalline regions were immobile and exerted an intermediate stiffness.

Bryant and Walter¹⁵ used an Instron Tester to measure the stiffness modulus of a wide range of wet and dry fibres, including wool, cotton, viscose and acetate rayons, polyethylene, acrylics, and polyesters. The swelling action of water was found to lower the glass transition temperature and a correlation between the value of the glass transition temperature of dry fibres and the extent of the lowering of this temperature in water was drawn. It was attributed to a dependence on secondary bonding along the polymer chains.

The initial tensile modulus of cellulose fibres was measured by Guthrie¹⁶ over a temperature range of 22° to 100°C. While the effect of moisture was to greatly reduce the modulus, temperature had only a secondary effect on wet fibres. Synthetic fibres, however, were extremely sensitive to temperature changes.

Suleimanova and Kargin¹⁷ found that cellulosic fibres were highly deformable due to their molecular structure. The different deformabilities of the various cellulosic fibre types were attributed to differences in orientation and packing of the chains. Moisture was found to have considerable effects on the mechanical properties.

The tensile properties of silk, nylon and Vinyon were investigated by Kaswell¹⁸ at temperatures ranging from -70 to $+70^{\circ}\text{C}$. The initial Young's modulus of nylon was four times as great at -57°C as at 21°C .

Rigby¹⁹ found that Young's modulus and stress relaxation of dry wool fibres were independent of temperature in the range 10° to 80°C at strains of 1 to 20% and Young's modulus was independent of the rate of straining over the range 0.75 to 250% per minute.

Peters and Woods²⁰, who examined the change of initial Young's modulus of wet and dry wool with temperature over the range 0° to 100°C , observed an increase in modulus with decreasing temperature, the rate of increase being smaller towards both ends of the range covered.

Bueche²¹ determined the initial modulus of polyethylene at several temperatures between 30° and 140°C

and observed a sharp drop at about 120°C. He proposed a theory relating modulus to crystallinity with varying temperature, a fall in modulus being accompanied by a decrease in crystallinity.

2. Dynamic Deformations.

a) Natural and Regenerated Fibres

Meyer and Lotmar²² appear to be the first to have subjected fibres to forced vibrations by means of an acoustic method. At high frequencies, they found that the dynamic Young's modulus of linen, ramie and hemp increased slightly with increasing static tension.

The dynamic tensile moduli of twenty three yarns and their dependence on static and dynamic strain, were measured by Tipton²³. The modulus generally increased with static strain and decreased with dynamic strain. In the case of monofilaments, the increase in modulus with increasing static strain was ascribed to an increase in molecular orientation. Small initial drops in modulus, at very small strains, were said to be due to increases in moisture regain, which occur on straining a yarn. Highly twisted yarns did not exhibit a drop in modulus, but an increase which was attributed to a lateral compression of fibres and a resultant lowering of regain. The decrease

in modulus with increasing dynamic strain was attributed to the fact that the forces of contact between adjacent fibres in a yarn increase and tend to cause movement and slippage amongst a greater number of fibres.

Palandri²⁴, using a forced longitudinal vibration method, found that the dynamic Young's modulus of yarns made from long fibres, was independent of dynamic strain amplitude and of frequency above 100 c/s in the range 20 to 200 c/s. In the case of yarns made from short fibres, the dynamic Young's modulus was found to decrease with increasing dynamic strain amplitude.

The dynamic elastic moduli of cellulose fibres and rayon were measured as a function of extension by de Vries²⁵ at 65% relative humidity and 20°C. The modulus remained fairly constant up to a certain critical extension, which varied according as to whether viscose, acetate or Lilienfeld rayon was under examination. Beyond this extension, the modulus increased for all materials but the rate of increase again depended on the material under tests. The decrease in compliance ($1/\text{modulus}$) was proportional to the increase in the natural strain. The results of the dynamic experiments suggested a correlation between the modulus and the chain molecule orientation. de Vries²⁶ further established a relationship between the dynamic elastic modulus and

birefringence of viscose, acetate and cuprammonium rayons such that, beyond a certain yield value of extension, the modulus was equivalent to the birefringence as a measure of the orientation of the filament.

Hamburger²⁷ found that for viscose rayon, cellulose acetate and nylon yarns, the **dynamic** Young's modulus increased with static tension beyond the yield point, but remained constant up to the yield point.

By means of several longitudinal vibration methods Fujino²⁸ et al measured the viscoelastic properties of viscose, acetate and cuprammonium rayons, silk and nylon 6, under a static tension of 0.4 gm. per denier and dynamic strain of less than 1%. Generally speaking the real part of the complex dynamic modulus was constant over the frequency range 2×10^{-1} to 2×10^5 c/s. with only a slight increase in the supersonic range. The imaginary part of the complex modulus seemed to increase at both ends of the frequency range. It was concluded that for any textile fibre the anomalous dispersion is not as great as that of various rubber-like materials in the same frequency range.

Kawai and Tokita²⁹ measured the dynamic Young's modulus of silk at 8°C and 71% relative humidity. Over

a frequency range of 2 to 14×10^2 c/s., a constant value of 9.8×10^{10} dynes per sq. cm. was obtained.

Dunell and Dillon³⁰ measured the dynamic modulus and energy losses of single fibres of viscose and acetate rayons, silk, feather keratin and nylon by a forced longitudinal vibration method. Both factors were independent of frequency in the range 1 to 100 c/s. Measured values of energy dissipated per cycle were found to be proportional to the square of the dynamic strain amplitude in accordance with theoretical prediction.

Lyons³¹, however, noted that for cotton and viscose rayon cords, the loss modulus was not strictly independent of the dynamic strain amplitude at large values of the latter. In the frequency range of 65 to 360 c/s, and at a dynamic strain amplitude of 0.3%, no significant dependence of the dynamic Young's modulus on frequency was observed, but with increasing dynamic strain amplitude, the dynamic Young's modulus was found to decrease.

Chaikin and Chamberlain³² found that the dynamic elastic modulus at 100 kc/s. was four times as great for viscose rayon and Tenasco and about two and a half times as great for wool, human hair and nylon, as the static modulus. Higher values at higher rates of strain were attributed to the fact that weak secondary bonds had no

time to break and the stress was transferred directly to the main chains, while at lower rates of strain ^{the mechanism of deformation is} they were due to the unfolding of molecular chains in the non-crystalline regions, which involved rotation of segments of the chains around single bonds having low activation energy barriers; at slow deformations, the weak secondary bonds broke when stress was applied.

Asmussen and Andersen³³ found that the dynamic Young's modulus was higher than the static modulus, when investigating the effect of longitudinal vibrations on cellulosic fibres. Humidity had a lesser effect on the dynamic than on the static modulus.

Andersen³⁴ observed that the dynamic Young's modulus of viscose rayon and cotton in a frequency range of 25 to 40 c/s. was much less affected by changing relative humidity than the static modulus. By increasing the static strain the modulus of cotton became much more humidity dependent, while the rayon was unaffected. Increasing temperature caused a fall of both the static and dynamic moduli of rayon, but only the static modulus of cotton increased.

A sound velocity method was employed by Ballou and Silverman³⁵ to determine the tensile moduli of viscose and acetate rayons, nylon and other yarns at frequencies of

10,000 c/s. Viscose rayon showed a decrease in modulus with increasing humidity and temperature; finishes in general had little effect, although boiling in soap solution tended to lower the modulus.

It was also observed by Chaikin and Chamberlain³² that for viscose rayon, human hair and nylon, a significant decrease in Young's modulus occurred in the case of viscose and human hair, while nylon showed a smaller decrease as the relative humidity was raised from 25 to 65%.

Dunell and Price³⁶ produced curves of dynamic Young's modulus and loss factor against temperature for viscose rayon, which were similar in shape to those for high polymers. The percentage increase in modulus and changes in energy loss factor were much smaller, however, in the case of viscose rayon. Young's modulus increased by 40% as the temperature was lowered from 0 to -80°C , and a well defined energy loss maximum, ascribed to CH_2OH side chains, which did not involve breaking of hydrogen bonds was observed at -40°C .

Tokita³⁷ discovered another dispersion in dry viscose rayon at 80°C . As the relative humidity was increased, the temperatures at which the dispersion occurred shifted to lower values. At constant temperature of 20°C and relative

humidity of 66%, and over a frequency range of 0.047 c/s. to 100 kc/s., no loss maximum was found.

Russel and van Kerpel³⁸ used a torsion pendulum technique to determine the dynamic rigidity modulus and damping of cellulose acetate and cellulose triacetate. Damping peaks and associated modulus changes were observed at 175°C and -48° for triacetate and 195°C and -55°C for acetate, while the remainder of the two curves took similar shapes. The variation in temperature of the high temperature transition with acetyl content was studied by Nakamura³⁹ who found, in agreement with Russel and van Kerpel³⁸ that the transition temperature decreased with increasing acetyl content. Nakamura, working at audio frequencies also found a mechanical loss peak at 60°C in the case of cellulose triacetate and considered this to correspond with the 30°C transition which is obtained in dilatometric measurement. He found no peak in the secondary acetate curve, which could be correlated with a 55°C transition obtained by dilatometric methods.

Tokita and Kanamaru⁴⁰ experimented with modified viscose and acetate rayons and found that the dynamic torsional modulus of the viscose was almost constant with temperature over the range 25 to 90°C but tended to drop above 60°C. Curves representing internal friction showed

two peaks at 40°C and 65°C for the viscose and 30°C and 50°C for the acetate.

Torsional oscillations were used by Mackay and Downes⁴¹ to determine the effect of the sorption process on the dynamic rigidity of dry wool, suddenly exposed to an atmosphere of 61% relative humidity. An almost immediate drop in rigidity occurred which was explained by the fact that the outer part of the fibre had reached equilibrium while the inner part had not, and fibre diameter was consequently relatively unaltered. Moreover a transient stress had arisen from the differential swelling during penetration. Subsequent to the drop, the inner fibre swelled and modulus increased continuously with humidity. Where the fibre was not subjected to such sudden humidity changes, the size of the dip was greatly reduced, and modulus gradually decreased with increasing humidity.

b) Synthetic Fibres

Ree et al.⁴² observed that internal friction of Saran fibres altered with frequency in the range 1.75 to 31.5 c/s. They further observed that internal friction increased as temperature decreased from 44° to 14.8°C; below which it decreased. Both the dynamic Young's

modulus and the static modulus increased sharply below 17°C at which temperature a second order transition probably occurred.

Smith and co-workers⁴³ measured the dynamic modulus of Orlon yarn at rates of strain varying from 1% to 300,000% per minute. The dynamic modulus increased with frequency in the lower ranges, but became constant above 10 kc/s.

Eyring et al.⁴⁴ subjected polyamide filaments to forced vibration over a frequency range of 0.06 to 6 c/s. and a temperature range of 0 to 65°C. The application of a sinusoidally varying strain to highly orientated filaments resulted in an energy loss per cycle which was practically independent of frequency but decreased almost exponentially with increasing temperature at constant frequency.

The dependence of dynamic Young's modulus and shear modulus of nylon 66 monofilaments on their degree of orientation was investigated by Adams.⁴⁵ Young's modulus at 66% relative humidity was the same for draw ratios 1 and 1.4, but thereafter increased continually with draw ratio. At humidities greater than 40% relative humidity, shear modulus increased with draw ratio, while at lower humidities it decreased with draw ratio.

Using a longitudinal vibration method, Fujino et al.⁴⁶

examined the viscoelastic properties of several high polymers and found that the effect of increasing the draw ratio was to increase the dynamic tensile Young's modulus. The effect was attributed to lateral bonding between chains in the amorphous regions and not to the development of crystallisation. Kawaguchi⁴⁷ measured dynamic parameters of nylon and Terylene filaments and compared results with those predicted from theory. The **degree** of orientation was assumed to be principally responsible for affecting the mechanical properties, while the influence of crystallisation was negligible in comparison. It was proposed that Young's modulus would increase to a maximum value of 5 times that of the isotropic body as the draw ratio was increased. On the other hand, the torsional modulus would decrease with increasing draw ratio, the completely orientated amorphous polymer exhibiting zero torsional modulus.

Thompson and Woods⁴⁸ measured the dynamic tensile modulus and loss factor of polyethylene terephthalate filaments having different degrees of crystallinity. At a frequency of 1 c/s. the main transition temperature rose from 80°C to 125°C, with increasing crystallinity. A second transition at about -40°C, was observed, which was less affected by changes in crystallinity of the polymer. Kawaguchi⁴⁹ examined a series of polyethylene terephthalate

filaments over a temperature range of -70 to 150°C and a frequency range of 100 – 200 c/s. The main softening region at 120°C was influenced by the degree of crystallinity while two mechanical loss maxima at 80°C and -40°C were also observed; the latter decreased in height and moved to lower temperatures as crystallinity increased. The effect of increasing the water content of the polymer was to increase the height of the low temperature loss maximum, without affecting the temperature at which the phenomenon occurred.

The same author⁵⁰ studied the dynamic and loss moduli of a series of polyamides and related polymers over a temperature range of -140 to 200°C . At least four dispersion regions were indicated, characterised by peaks in the loss tangent curve; at -120 , -40 , $+90^{\circ}\text{C}$ and near the melting temperature. The α peak reflected the onset of motion of large chain parts, caused by breaking of intermolecular bridges in the amorphous regions. The data on the β process supported the view of Woodward et al.⁵¹ that it is the result of segmental motion involving non-hydrogen bonded amide groups. An attempt was also made to correlate the area under the β peak with the density of amide groups in the series of polyamides, but further

work was necessary to draw firm conclusions. It was further observed that in general the magnitude of elastic modulus rose with an increase in amide group concentration.

Schmieder and Wolf^{52,53} investigated the frequency and temperature dependence of several high polymers in dynamic torsional experiments. For crystalline polymers such as polyamides and polyethylene they found three loss peaks. A peak above room temperature was ascribed to motion of the activated amorphous segments, while the low temperature peaks were said to be due to the rotation of CH_2 links in the amorphous regions.

Woodward and co-workers⁵¹ studied nylons 66 and 610, and a copolymer in the audio frequency range and at temperatures of -193°C to near the melting point. Dispersions were observed in all cases at 225, 77, -23 and -77°C . The α peak was due to chain mobility in the crystalline regions; the α' peak was attributed to the onset of motion of large chain parts, the β (second order transition) to segmental motion involving amide groups in the amorphous regions which are not hydrogen bonded. The dependence of the peak on the polyamide tested and its proximity to the low temperature peak of polyethylene and certain methacrylate esters, was in agreement with a proposal that it was caused

by the onset of co-operative movement of the CH_2 groups between amide linkages in the amorphous part.

Woodward et al.⁵⁴ investigated specimens of poly-hexamethylene adipamide containing between 0 and 6.4% by weight of water, over a wide temperature range. It was found that with increasing water content, the loss peak and associated modulus dispersion at -100°C in the dry material decreased; the loss peak and modulus dispersion at 100°C in the dry material shifted to lower temperatures reaching a value of 7°C for 6.4% water content. A third damping peak appeared at about -30°C , and the modulus in the -120 to -20°C region increased while above and below this range the reverse was true.

Price et al.⁵⁵ investigated the dynamic mechanical properties of nylon, polyethylene and viscose and acetate rayons, by a forced longitudinal vibration method in a frequency range of 5 to 50 c/s. The dynamic modulus increased with decreasing relative humidity which was lowered from 98 to 28%. It was found that the dissipation of energy, per cycle, increased with increasing relative humidity.

Quistwater and Dunell⁹ measured the dynamic tensile and loss modulus of nylon 66 filaments at a constant temperature of 35°C , and over a range of 11 to 96% relative

humidity. The tensile modulus increased with decreasing relative humidity, but was only slightly dependent on the frequency over the range covered. The loss modulus was effectively independent of frequency at relative humidities between 50 to 60%. At lower humidities a decrease in energy loss and at higher humidities an increase in energy loss, occurred with increasing frequency. At an arbitrary value of $\omega = 100 \text{ sec.}^{-1}$ the values of the loss parameter and tensile modulus were plotted against relative humidity. A maximum in the energy loss ($\omega\eta = E_2$) lay at 60% relative humidity. Plotting loss tangent against relative humidity, the maximum shifted to 20% relative humidity. Small variations of energy dissipation with changes in frequency were such as to suggest that the dispersion region extended over a wide frequency range and that at low humidity, an energy loss maximum could be expected at a frequency below 1 c/s. It was thought that an increase in the amount of water absorbed by the polymer with increasing relative humidity, led to a plasticisation and consequent increase in freedom of motion of chain segments in the amorphous regions of the fibre.

The same authors⁵⁶ extended their work by measuring the same properties at 9° and 60°C over the same humidity and frequency range (10^{-4} to 10^6 c/s.). The dynamic

tensile modulus at 9°C was independent of frequencies at humidities lower than 60% but increased with increasing frequencies at higher humidities. The tensile modulus was similarly affected by frequency at 60°C. At this temperature, a well defined maximum in the energy loss was observed, similar to that obtained at 35°C but at a somewhat lower moisture content. This effect was expected if both the increase in temperature and moisture content facilitated segmental chain motion, and if such motion produced increased energy dissipation up to a point at which further increase in ease of motion corresponded to such a decrease in intermolecular forces that energy loss decreased again. If a maximum occurred in energy loss at 9°C, (it was not well defined), it was near 100% relative humidity.

The dynamic mechanical and electrical properties of polyethylene were measured over a wide temperature range by Robinson and Oakes⁵⁷. Peaks at -100, 0 and 70°C were associated with movement of certain CH₂ links in the main polymer chains, side chain mobility and large scale mobility of the polymer chains in both the crystalline and amorphous phase, respectively. Temperature differences between mechanical and electrical loss peaks were observed and attributed to the fact that the former were obtained at

200 c/s. and the latter at 11,000 c/s.

Reddish⁵⁸ investigated the dielectric properties of polyethylene terephthalate over a wide frequency range (10^2 to 10^7 c/s.) and a temperature range of -80 to 180°C . Three dielectric processes were identified, and it was suggested that one of these is correlated with mechanical and thermal properties of the polymer and is therefore due to the relaxation of dipoles in the main polymer chain. A second process was attributed to the presence of OH groups and a third which occurred at low frequencies and high temperatures was associated with the conduction of charge through the material.

Ward⁵⁹ employed a nuclear magnetic resonance method to study polyethylene terephthalate and related polymers which contained in the glycol residue, between four and ten methylene groups. A temperature range of -180 to 200°C was covered. Second moment data from both the single broad absorption below the glass transition temperature, and the broad component of the composite signal above the glass transition temperature suggested that most of the methylene groups in the structure (i.e. even the crystallites) underwent hindered rotations at high temperatures.

The nuclear magnetic resonance absorptive and dynamic mechanical properties of Terylene, nylon and plastics were studied by Nohara.⁶⁰ In the temperature range -70 to 200°C

it was observed that the p-phenylene group in Terylene was hindered at about 110°C , whereas the two methylene groups still rotated at lower temperatures.

(c) Rubbers, Plastics and other filamentous Polymers

Ecker⁶¹ surveyed and interpreted theories of the high elasticity of macromolecular substances, and referred to methods of measuring plastic-elastic behaviour of high polymers by means of forced longitudinal vibrations.

Nolle^{62,63} used five methods to study the changes in dynamic Young's modulus and loss tangent, over a frequency range of 0.1 c/s. to 100 kc/s. and a temperature range of -60 to 100°C , of various rubber-like materials. Young's modulus increased with decreasing temperature and increasing frequency, while there was no indication that it was a function of amplitude when measured by a vibrating reed method, with the exception of natural rubber whose resonant frequency depended strongly on the amplitude of vibration. In general there were temperature regions in which the loss tangent showed maxima, which were accompanied by maximum rates of change of moduli in the same temperature region. Dynamic modulus approached a maximum value as the temperature became very low and frequency very high.

The frequency and temperature dependence of the elastic losses of natural rubber, polyvinyl chloride (P.V.C.) and butadiene-styrene co-polymers (G.R.S.) were studied by Sack et al.⁶⁴ who used three vibrating reed methods. Natural rubber at temperatures above 20°C and P.V.C., exhibited frequency independent losses, the mechanisms of which were not fully clear. The results for rubber below 20°C, and for G.R.S. were explained by a relaxation theory. The behaviour of the elastic losses also reflected the existence of second order transitions below which rotation of chain segments were hampered.

The shear wave velocity and attenuation of G.R.S. Butyl, Hevea, Hycar and Paracril rubbers were measured by Cunningham and Ivey⁶⁵ in a frequency range of 0.2 to 7 mc/s. and temperature range of -60 to 20°C. To a fair approximation in the range investigated it was concluded that the real and imaginary parts of the dynamic Young's modulus were three times the corresponding values of the dynamic shear modulus. It was found also that the classical Stokes' assumption that the bulk viscosity was negligible in comparison to the shear viscosity, was reasonable for some, but not all the rubbers.

Fukada⁶⁶ showed that the calculated values of

dynamic shear modulus and loss tangent from creep experiments with polymethyl methacrylate agreed satisfactorily with those observed.

Maxwell² investigated polymethyl methacrylate and his results indicated that over a temperature range of -20 to 80°C , and a frequency range of 6×10^{-4} to 1.6×10^2 c/s., three relaxation mechanisms were involved.

Gordon⁶⁷ found a main peak at 160°C when examining the same polymer, while at 70°C , a shoulder in the energy curve occurred and was attributed to the CO_2Me side chains.

Yamamoto and Wada⁶⁸ studied the dynamic Young's modulus and loss factor of polymethyl methacrylate, polystyrene, nylon 6 and a polyester over a temperature range of -70 to 90°C , at very high frequencies. The γ transition in polymethyl methacrylate produced a loss factor dispersion at -20°C .

Kawaguchi⁶⁹ found that the dynamic and dielectric properties of polycaproamide were intrinsically correlated. Over a range of -60 to 200°C , three dispersions were observed. A change in dynamic modulus and the associated loss maximum at 80°C was attributed to hydrogen bonding while one observed at -45°C was associated with dipole interaction between amide links.

Deutch, Hoff and Reddish⁷⁰ studied the dynamic and

dielectric properties of various acrylic polymers and found these also to be intrinsically correlated. They proposed the hypothesis that each mechanical and dielectric dispersion region in a given polymer was associated with a defineable structural feature i.e. a group of atoms in the polymer such that each group gave rise to a mechanical dispersion and if polar, also to a dielectric dispersion in the same temperature region. The possibility of tracing the same dispersion from one polymer to another, provided they all contained the same group, was suggested.

Hoff, Robinson and Willbourn⁷¹ detected four dispersions in acrylic ester polymers. The main softening process was associated with slipping of chain segments past one another and was shown to be influenced by the shape and size of the side chains. The presence of polar atoms in both side and main chains, by influencing the interchain cohesive forces, had their effect on the main softening region. A secondary maximum was influenced by side chain flexibility; two low temperature processes at -30 and -150°C were similarly influenced.

Sharpe and Maxwell⁷² attempted to relate shear modulus, Young's modulus and Poisson's ratio for various plastics. Generally, at 30°C , agreement between predicted and experimental values of Poisson's ratio was reached. It

was observed that polystyrene approached the theoretical value of Poisson's ratio of a true elastic solid, while cellulose triacetate butyrate approached that of a liquid.

Newman⁷³ measured the dynamic Young's modulus of crystalline polystyrene over a temperature range of 20 to 160°C. A maximum in damping was found at 120°C.

According to Sauer and Kline⁷⁴ polystyrene exhibited a large rise in internal friction at 80°C and an accompanying drop in modulus. Molecular movement involving entire chains was thought to be responsible. No loss peaks were evident in the temperature range covered. Teflon and polypropylene showed two peaks, a room temperature peak and dispersion regions at -75 and 100°C respectively. The low temperature peak in the case of Teflon was associated with alternative configuration of the main C-C links in amorphous regions between crystallites and was indicative of a glass like transition.

Sauer et al.⁷⁵ subjected rod like specimens of crystalline and amorphous polypropylene to transverse vibrations and measured the dynamic elastic modulus and internal friction over a temperature range from -100°C to near the melting point. Three dispersions were observed - a high temperature transition associated with large scale

motion of polymer chains, a room temperature transition associated with the primary glass transition of the amorphous phase of the polymer, and a low temperature transition attributed to the onset of small scale chain motion in the amorphous regions. The low temperature transition occurred at about -50°C in amorphous polypropylene, and -110°C in polyethylene. This difference, it was suggested, was a result of hindrances to main chain rotation caused by the presence of a methyl group on every other carbon atom.

Baccareda and Butta⁷⁶ determined the dynamic elastic modulus and damping characteristics of several polythenes having different degrees of crystallinity, over a temperature range of -70 to $+50^{\circ}\text{C}$ and at frequencies of between 5 and 30 kc/s. A transition temperature at -24°C , independent of the degree of crystallinity was noted, being sharper the more amorphous the material. At temperatures above this, Young's modulus increased with increasing crystallinity in the case of uncross-linked or weakly cross-linked polymers. This was attributed to overlapping of crystallites which under these conditions formed a more rigid framework than the molecular segments in the amorphous regions. Below the transition temperature, Young's modulus seemed to be lower in the more crystalline than in the more

amorphous samples. It was suggested that this could be due to stronger intermolecular forces existing in the glass like state of the amorphous regions.

Dynamic torsional measurements by Nielsen⁷⁷ on a number of polyethylene co-polymers showed that the temperature of the α transition decreased from over 100°C for the pure polymer to 0°C for a co-polymer containing 26.7% vinyl acetate. A β peak was detected at -25°C , which was independent of the quantity of vinyl acetate while a low temperature peak at -110°C increased in height or temperature with increasing amounts of co-polymer.

Kline et al.⁷⁸ studied the effect of the extent of chain branching of polyethylenes on the various dispersions found between -193 and 107°C by driving rod like specimens in their transverse modes. The α dispersion at 97°C shifted to higher temperatures with decreased branching in accord with the shift in melting temperature with degree of crystallinity. The β transition at -43°C decreased in magnitude with decreased branching and for polyethylene which has negligible branching, it was almost entirely absent. This suggested a direct relation between the number of branch points and the size and shape of the peak. The γ dispersion region near -103°C was sharper and shifted to higher temperatures with decreased branching:

this was attributed to a narrowing of the relaxation times associated with the movement of a small number of CH_2 units.

The effect of cross-linking polyethylene by means of pile radiation was studied over a temperature range of -193 to 177°C by Deeley et al.⁷⁹ Definite changes in the dynamic modulus were observed. Three mechanical loss peaks, at -108 , -8 and 82°C were noted. The low temperature peak increased in height and peak temperature as dosage increased but at higher dosages a marked decrease in the damping occurred. The peak at -8°C decreased in height and shifted to higher temperatures while the 82°C peak, attributed to the melting of the crystalline portions of the sample, decreased in height and shifted to lower temperatures as irradiation dose increased.

Irradiated polyethylene was also investigated by Butta and Charlesbury⁸⁰. Three distinct transitions were found associated with the glassy state (T_g) softening of amorphous regions (T_s) and melting of the crystallites (T_m). With increasing dosage, T_m decreased, T_g increased, while T_s showed a minimum value for a radiation dose equal to the critical value. At temperatures above the melting point of the crystallites T_m , lightly cross-linked samples showed rubber like elasticity, but highly cross-linked samples showed the same dynamic behaviour as highly cross-linked

amorphous material.

Schmieder and Wolf^{52,53} conducted dynamic torsional experiments on a series of rubbers, amorphous and crystalline polymers including polyethylene, polyvinyl chloride, polyisobutylene and polyamides. Three damping peaks were observed in polyethylene and polyamides; low temperature peaks were attributed to rotation of CH_2 groups in amorphous regions, and the high temperature peaks to strains on amorphous segments which consequently had diffusional motion. Amorphous polymers showed transition regions and a second, lower temperature dispersion caused by side chains. When long and mobile side chains were present a third damping peak occurred.

Koppelman⁸¹ measured the elastic, shear, torsional and longitudinal wave moduli of plasticised polyvinyl chloride over a frequency range of 10^{-1} to 4×10^6 c/s. The dispersion regions of the different moduli were found to be at different frequencies, and thus the relaxation behaviour depended upon the type of stress applied. The relation between the moduli outside the dispersion regions (but not within) could be explained by simple elastic theory. It was also found that the distribution of relaxation times was displaced to higher frequencies in the case of shear modulus, than in the case of compression modulus. At

temperatures above freezing point the inner structure and apparent activation energy changed considerably with temperature, while at higher temperatures the changes were smaller and the chain segments probably moved more freely.

Fitzgerald⁸² measured the complex shear modulus of polyvinyl stearate between 50 and 5,000 c/s. and found several sharp resonances in the compliance. The apparatus consisted of two small discs of the sample clamped between metal surfaces and subjected to sinusoidal dynamic vibration in a direction perpendicular to the static clamping stresses. Using the same apparatus, Sheldon⁸³ measured the complex shear compliance of fractionated poly n-dodecyl methacrylate. A method of reduced variables gave superimposed curves for the real and imaginary components of the complex compliance, against frequency, and for creep compliance against time, except for an anomaly below -28°C , interpreted as due to crystallisation of the side groups.

It was shown by Kawai and Tokita¹⁰ that the dynamic Young's modulus of amorphous films of polyvinyl alcohol increased only slightly as the relative humidity was raised to 35%, whereafter, a rapid decrease occurred, while the loss tangent was almost constant up to 25% and increased rapidly up to 65% relative humidity above which it remained relatively unaltered. The interpretation of the response

of dynamic Young's modulus was that water molecules were initially attracted to the C-H radicals in the amorphous regions, but at higher humidities the existing hydrogen bonds were broken.

Shinohara⁸⁴ investigated the temperature dependence of the torsional rigidity and loss angle of graft polymers of nylon 6. All samples showed a relaxation peak at 80°C. A second peak was observed which increased in height as the degree of grafting increased. It was thought probable that the two peaks of the graft co-polymer were due to the onset of segmental motion of the trunk nylon polymer and the grafted vinyl polymer.

An electrostatic form of vibroscope was employed by Stauff and Montgomery⁸⁵ to determine the effect of air damping on resonant frequencies of forced vibrations of stretched glass filaments, by observing the shift in frequency with reduced or increased atmospheric pressures. It was found that the finer the filament the greater the shift in resonant frequency between that measured in air and that in a vacuum. The frequency shifts agreed well with those predicted from Stokes' theories. The torsional modulus of glass was found to be dependent on the atmosphere in which it was measured, by Eischen⁸⁶. This dependence was attributed to changes in the surface energy.

The Flexion of Textile Materials

1. By Static Methods

a) Natural, Regenerated and Synthetic Fibres

Sen⁸⁷ measured the static bending modulus of a fringe of jute fibres by clamping them at one end and causing a deflection at the other with an applied load. With a similar technique, Khayatt and Chamberlain⁸⁸ found that wool had a slightly lower bending than tensile modulus, and that the effect of descaling the fibres was to reduce both moduli by similar amounts; and Roder⁸⁹ measured the flexural rigidity of a variety of fibres including viscose and acetate rayons, Orlon, Dacron and polyamides.

Kawakami and Ikeda⁹⁰ established a method of measuring the flexural rigidity of filaments, their system being based on the theoretical treatment of the bending of a beam by T. Bousinesq. Reliable values in the denier range 1.5 to 15 were obtained with silk, nylon and glass filaments.

Carlene⁹¹ and Prins⁹² used loop methods to determine flexural rigidities of yarns. Carlene investigated the variation of flexural rigidity of viscose rayon with mass per unit length, while Prins showed that the flexural

rigidity of a yarn was equal to the sum of the flexural rigidities of the individual filaments in an unsized yarn of low twist.

Isshi⁹³ described a bending tester for fibres, yarns and fabrics, which measured bending moments. The bending moment of cotton yarns showed steep initial increases but later tended to fall with curvature. The bending moment of cotton fabrics had a slight convex tendency to the curvature, and increased nearly in proportion to the breadth of fabric.

Dynamic and static methods for determining flexural rigidity and bending moduli of viscose rayon and Perlon were employed by Friedermann⁹⁴ who concluded that the bending modulus of Perlon, while independent of denier, increased with increasing draw ratio. Dynamic methods yielded higher values for flexural rigidity than static methods, the ratio of these values varying according to the particular type of viscose or Perlon under test.

2. By Dynamic Methods

a) Natural and Regenerated Fibres

Peirce⁹⁵ used a Searle's double pendulum to measure the bending modulus of cotton fibres in a fringe. Using a free vibration system, he found values of 27×10^{10} and 14×10^{10} dynes per sq. cm. for the dynamic bending moduli

of dry and wet cotton respectively.

Lochner⁹⁶ made the first experiments on the dynamic bending properties of single fibres. For wool and acetate in forced vibration, the damping capacity was greater in bending than in torsion. Absolute values of dynamic bending modulus for quartz, acetate, ardil, nylon and casein are quoted.

The dynamic bending modulus and damping capacity of wool, untreated, acid carbonised, and carbonised and neutralised, were measured by Lincoln⁹⁷ at different moisture regains. Bending modulus was found to decrease with increasing regain, while damping capacity increased almost linearly with increasing regain. The damping capacity of dry wool was found to be unaffected by carbonising treatment, while wool at 10% regain showed a much higher damping capacity when carbonised than when untreated or when carbonised and neutralised.

van Wyk¹¹ established that the dynamic bending moduli of wool, mohair and human hair were reduced to one third of their values, from dryness to saturation. The shape of the curve relating bending modulus to adsorbed water was found to be similar to that of torsional rigidity. It was shown that due to fibre swelling the stiffness of the fibres was reduced by approximately one half of the extent to which the bending modulus was reduced on the adsorption of water.

Warburton⁸ recorded slightly higher results for the bending modulus of horn keratin in adsorption than in desorption over a range of 0 to 30% regain. The variation of bending modulus with regain was very much greater than that of the tensile modulus as observed by Woods⁹⁸ but compared better with the variation of torsional rigidity as measured by Speakman⁹⁹. Dusenbury et al.¹⁰⁰ compared the dynamic elastic properties of goose feather barbs and down filaments by means of a vibroscope. The extensional properties, the bending and torsional moduli, of the former were found to be greater. The effect of air damping was found to be relatively small but significant in the determination of ~~cross sectional area~~ and bending modulus, but the observable effects in the case of torsion were much smaller. It was observed that the effects on cross sectional area, bending modulus and torsional modulus caused by drying the samples from 65 to 0% relative humidity, were much greater than those caused by air damping.

Guthrie¹⁰¹ and co-workers investigated the bending and torsional rigidities of several fibres including viscose rayon, nylon, Terylene, Orlon etc., the former by both static and dynamic methods, the latter by only a dynamic method. The values of dynamic bending rigidities were higher than those obtained in static experiments, while for most fibres,

the tensile modulus lay between the dynamic and static moduli of bending. Certain continuous filaments yielded higher bending and lower torsional rigidities than their respective staples. Values of 4.4, 4.6, and 10×10^{10} dynes per sq.cm. were obtained for the dynamic bending moduli of wool, Fibrolane and the acrylic X51 respectively under conditions of 65% relative humidity and 20°C.

The influence of air damping on resonant frequency was calculated with the help of equations deduced by Stokes, by Karrholm and Shröder¹⁰². Experimental verification was performed on model circular viscose rayon using a cantilever vibration method. It was shown that Young's modulus by bending was 1.5 times that by stretching. Values of the moduli for wool, nylon and human hair, were obtained. Two values of resonant frequency were recorded around the principle axes of inertia in the case of the elliptical hairs, the ratios of these frequencies being equal to the ratios between the axes of the ellipse.

Karrholm¹⁰³ studied the effect of varying amounts of formaldehyde added to viscose rayon on the bending, stretching and torsional moduli, and found that a maximum value for each was obtained for a 5% formaldehyde content. The results indicated that below 5%, the number of cross-links increased steadily, whereas above 5%, the length of the

cross-link was greater.

Okajima and Suzuki¹⁰⁴ used a vibrating reed method to measure the bending modulus of viscose rayon. The mean resonant frequency of four readings taken at right angles to one another was used as a basis from which to calculate the bending modulus.

Schroder¹⁰⁵ described a simple mechanical device which determined the dynamic bending stiffness of single fibres. Tyre cord rayon was found to be less stiff than cotton fibres used in tyre cords, but the latter showed a larger scatter over 10 readings. This was attributed to the irregularity naturally inherent in the cotton.

Horio et al.¹⁰⁶ measured the effect of frequency over a range of 20 to 200 c/s. on the bending modulus and viscosity coefficient of round viscose filaments. Modulus increased slightly with frequency, the dependence becoming more prominent as the orientation of the cellulose increased. This dependence was consistent with relaxation mechanisms and a slight increase in modulus with frequency could have suggested an energy dispersion at low frequencies (below 1 c/s.) and at high frequencies (above 10^4 c/s.). The loss tangent increased linearly with orientation at frequencies up to 90 c/s., above which it was independent of orientation. It was proposed that with increasing orientation, the larger

number of cross-bonds caused higher resistance to chain slippage at low frequencies, while at higher frequencies, they could not adjust themselves to rapid changes, and behaved as fixed parts of the chain segments.

Horio and Onogi¹⁰⁷ used a forced vibration technique to obtain a value of 3.3×10^{10} dynes per sq.cm. for the bending modulus of cellulose acetate filaments. It was also noted that the modulus was independent of frequency over a range of 45 to 11,000 c/s.

(b) Synthetic Fibres

Wakelin et al.¹⁰⁸ found that as the draw ratio increased from one (undrawn) to six, the bending moduli of nylon 66 and Dacron increased by factors of 3.5 and 5.8 respectively. It was concluded that the higher the draw ratio, the less isotropic the materials remained, since the ratios of Young's modulus to three times shear modulus were 3 and 5 for the nylon and Dacron filaments respectively while for homogeneous, isotropic materials having a Poisson's ratio of 0.5, this ratio, should be unity.

Marlow¹⁰⁹ compared the effect of draw ratio on the bending modulus of nylon filaments with the tensile modulus obtained by Adams⁴⁵. The considerable agreement between the two sets of results indicated that in bending, the

EXPERIMENTAL

The basic principle involved in dynamic bending experiments consists of forcing a fibre in the form of a cantilever into sustained lateral vibration and measuring the resonant frequency and the bandwidth. There are several ways of doing this e.g.,

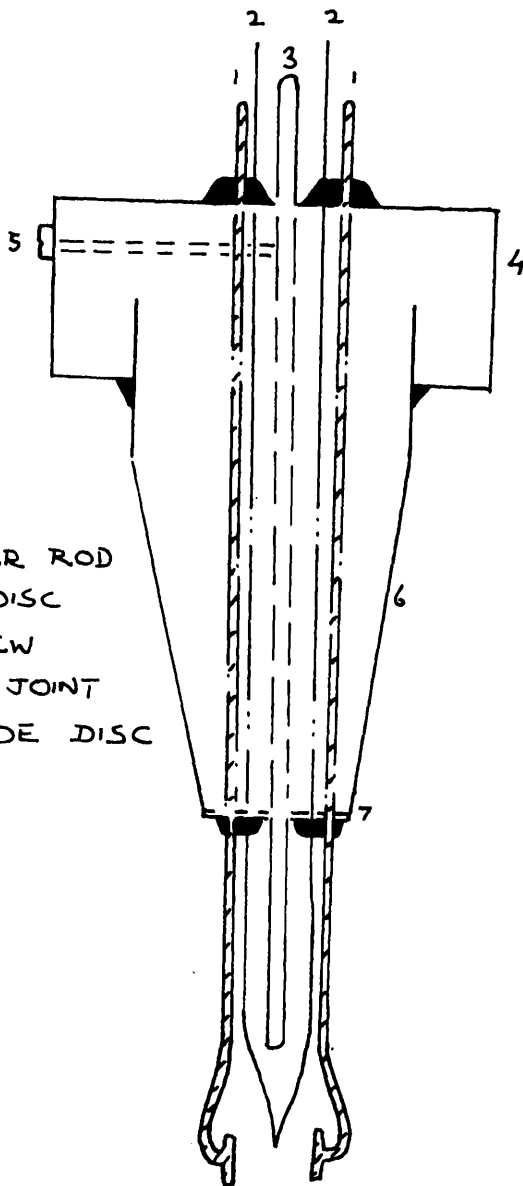
- (1) by attaching one end of the fibre to the diaphragm of a telephone earpiece (c.f. Guthrie et al.¹⁰¹ and Lincoln⁹⁷), or to an electromagnetically excited clamp (c.f. Karrholm and Schröder¹⁰²), or to a piezo electric gramophone cutting head (cf. Lochner⁹⁶). In such cases the clamped end of the fibre is usually mechanically driven.
- (2) by mounting the fibre rigidly and placing in a sound field (c.f. Lochner⁹⁶) or alternating electrostatic field (c.f. Wakelin et al.¹⁰⁸). In such cases a disturbing force is exerted along the fibre length. Lochner⁹⁶ showed experimentally that the latter methods were better in that the shift in resonant frequency due to air friction was smaller.

In the present investigation, an electrostatic method is used, in which the free end of a negatively charged fibre situated between two electrodes is caused to vibrate by an

alternating voltage. The effect of temperature in the range -70 to 170°C on the resonant frequency and bandwidth of bone dry fibres was observed in the first series of experiments which was performed in vacuo. In the second series, the resonant frequency and bandwidth of fibres at constant temperature and in a humidity range of 0% to 90% relative humidity were measured, at reduced pressures which were governed by humidity. All measurements of resonant frequency are made in the fundamental mode of vibration.

Apparatus and Instruments: Changing Temperature - 0%
Relative Humidity

The Mounting Head. (see figure 3): This consists of a non-porous disc of Bakelite, into which and below which, is fitted a ground glass plug of about 2 cm. diameter at its broader end, and joined to the Bakelite disc by means of Araldite cement to give a heat and moisture resistant, vacuum tight joint. Copper wires (18 s.w.g.) which connect the electrodes to the circuit pass through and are fixed to the Bakelite top, again with Araldite. The spacing of the electrodes is adjustable by simple bending, a distance of 2 to 3 mm. apart being suitable to give reasonably sized vibration of most fibres. A copper-constantan (40 s.w.g.)



- 1 ELECTRODES
- 2 THERMOCOUPLE
- 3 CENTRAL COPPER ROD
- 4 BAKELITE TOP DISC
- 5 SECURING SCREW
- 6 GROUND GLASS JOINT
- 7 BAKELITE GUIDE DISC
- ARALDITE

MOUNTING HEAD

thermocouple, whose hot junction is situated in close proximity to the mounted fibre, and measures the temperature inside the glass vessel also passes through the Bakelite top, is similarly sealed with Araldite, and is positioned behind a central earthed copper wire (18 s.w.g.) on to which the fibre is mounted by means of Durofix. This material is used in preference to mechanical clamping to avoid distortion of the fibre cross-section. Durofix has the added advantages of being heat and moisture resistant, quick drying, and if carefully applied, of allowing clean emergence of the fibre from its point of fixation and consequent accuracy in the measurement of fibre length. The earthed copper rod is sealed to the Bakelite top with Araldite, or where its vertical movement is required, with sealing wax. Vertical movement is obtained by manual adjustment and at the desired position the rod is secured by means of a screw inserted horizontally in the Bakelite top.

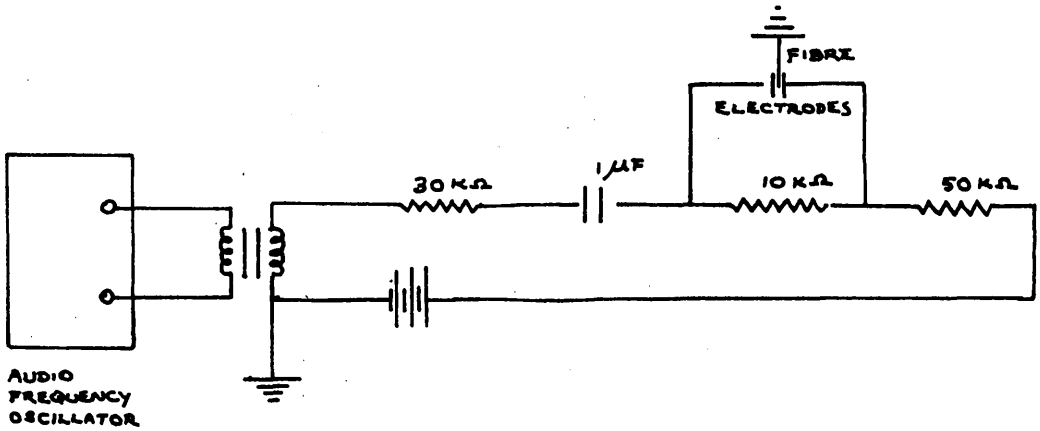
At the bottom end of the ground glass joint, a fitted Bakelite disc acts as a guide and stabiliser by means of appropriate holes drilled into it, to the electrodes, central rod and thermocouple wires.

Fibre Excitation: The mounted fibre, with its free end situated between the electrodes, is charged to a potential

of 120 volts by means of a dry battery in the electric circuit (see figure 4). A step-up transformer amplifies the voltage from a Jackson Audio Frequency Oscillator, modified by fitting condensers in series, to read to an accuracy of 0.1 c/s. at 100 c/s. and 0.25 c/s at 400 c/s. The voltage can be varied to a maximum of 400 volts, but it was found that fine denier fibres vibrated with sufficiently large amplitudes at 50 volts, while thicker wool and ramie fibres required 150 volts, in vacuo.

The frequency range was confined to one of 100 c/s. to 400 c/s. although the method would work satisfactorily from 30 to 1,000 c/s. The lower limit is set by the amplitude of vibration, which decreases with increasing fibre length at a constant applied voltage. Since high frequencies require short fibre lengths, the upper limit depends upon the shortest fibre length which can be satisfactorily measured.

Heating System: The mounting head is inserted into the top end of a vertical glass tube fitted with a ground glass joint and a side arm near the bottom of the tube which is connected to the vacuum pump. The tube is heat insulated, by successive layers of asbestos paper and asbestos string. A ground glass joint at the bottom end of the tube has a flask annexed to it, which houses the phosphorus pentoxide



CIRCUIT DIAGRAM

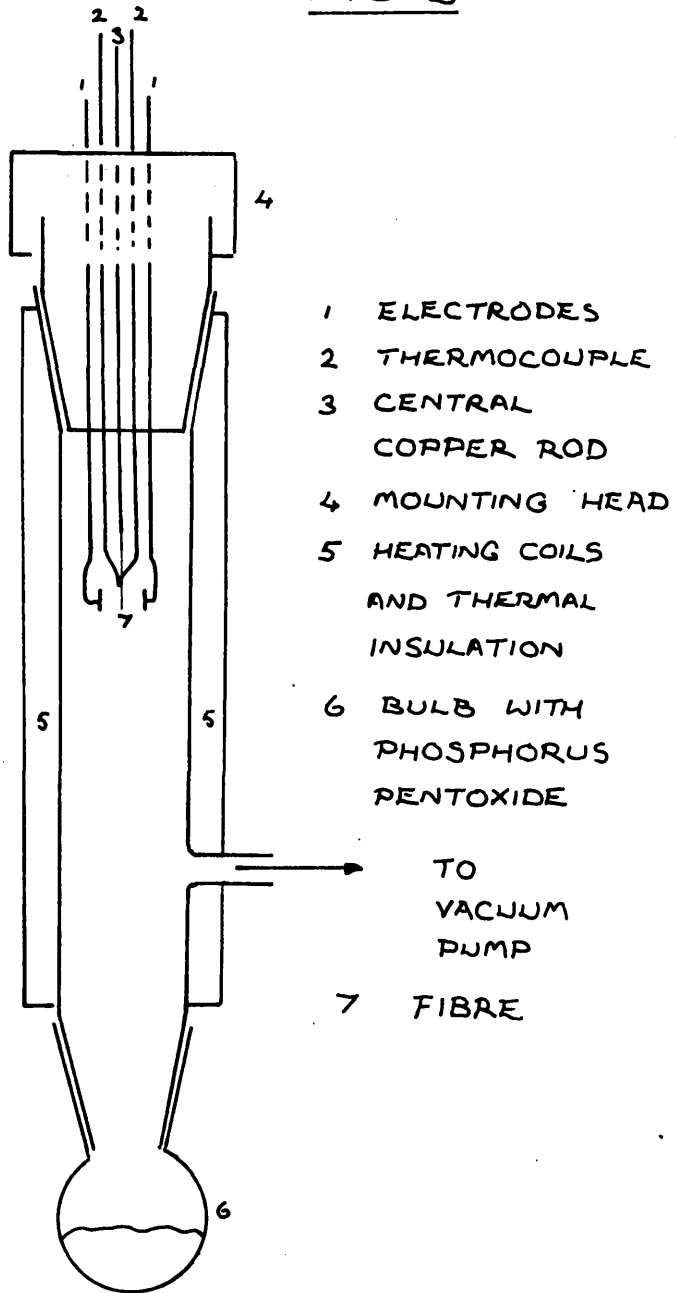
required to dry specimens.

Heating is provided by supplying the output of a constant voltage transformer (230 volts) through a variac (by means of which temperature can be quickly altered from room temperature to 170°C) and a bridge type full wave metal rectifier, to heating coils which consist of Nichrome resistance wire uniformly wound around the glass tube. The purpose of the rectifier is to eliminate possible interference of the applied alternating voltage used to excite the fibre, by the electric field from a 50 c/s. alternating current in the coils.

Insulation is provided by a layer of asbestos paper (between the glass tube and the resistance wire) and successive layers of asbestos string. An earthed piece of metallic paper between two layers of string prevents the accumulation of electric charges. The unit is assembled in such a way as to have two windows ($\frac{1}{2}$ " x $\frac{3}{8}$ ") on opposite sides, to enable viewing of the fibres. By directing a stream of cool air at the assembly, it can be rapidly cooled from high to room temperature. (See figures 5 and 5A).

Cooling Unit: Temperatures down to -70°C are reached by means of a Townsend and Mercer Minus Seventy Thermostat Bath which uses solid carbon dioxide as the cooling agent

FIG. 5.

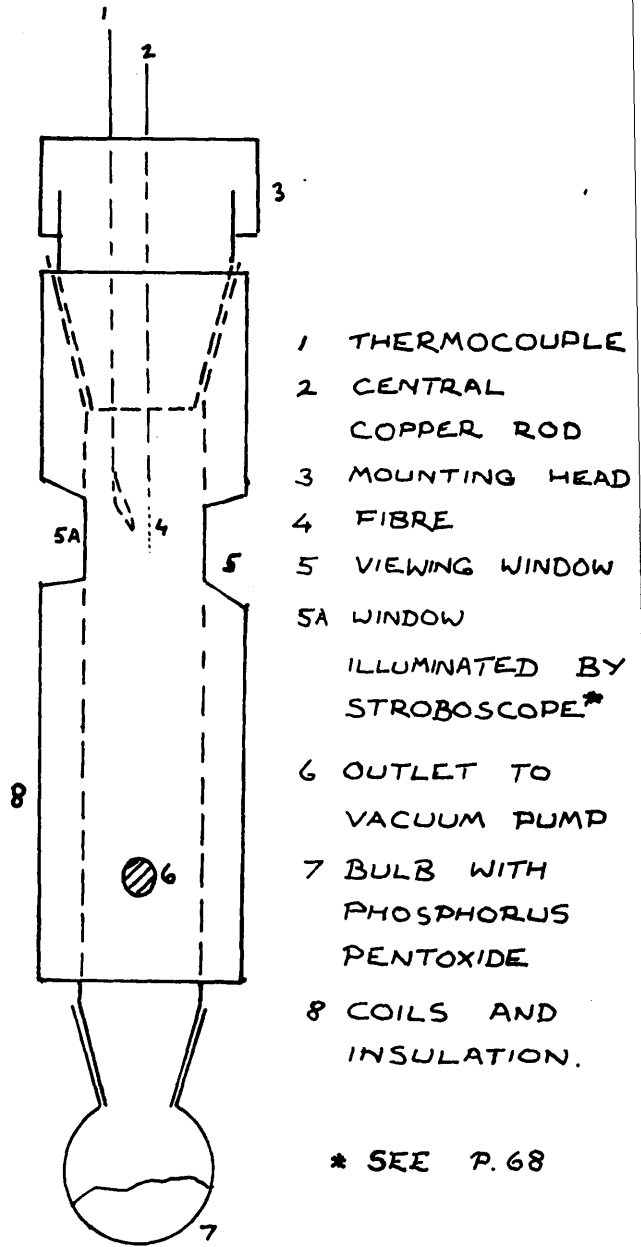


HEATING SYSTEM

FRONT VIEW

(NOT SHOWING COMPLETE COVERAGE OF INSULATION)

FIG. 5A



HEATING SYSTEM
SIDE VIEW

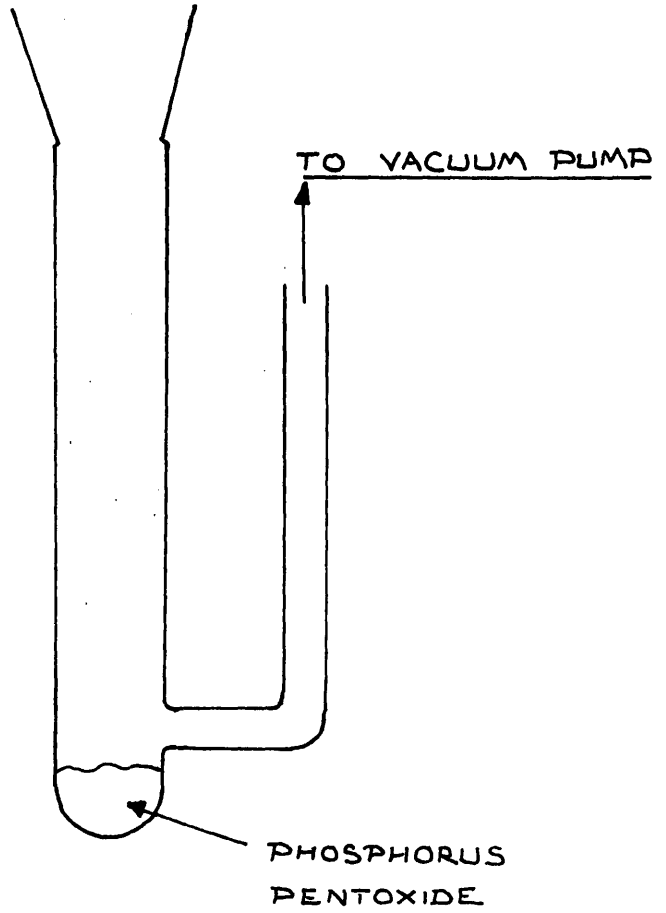
and petroleum ether as the heat transfer medium. The bath has a double glass window at the front through which the fibre, now removed to a second glass tube is viewed. The "cooling" tube (see figure 6) has a ground glass joint at its top end to accommodate the mounting head and a vertical side arm which is connected to the vacuum pump. Phosphorus pentoxide is housed at the lower end of the tube which throughout the high temperature experiment is connected to the vacuum system.

Viewing often becomes difficult at very low temperatures as the petroleum ether tends to become cloudy and condensed moisture forms on the surface of the window. This was overcome by directing a stream of room air at the lower end of the window.

Fibre Selection, Preparation and Conditioning

Selection: By careful microscopic examination, straight fibres of uniform thickness are selected for use in the vibration experiments. Consequent calculations of Young's moduli demand these prerequisites, since they are based on the vibration or bending of straight and uniform bars. Some difficulty is encountered with wool and ramie but suitable specimens up to about 1 cm. in length were obtained.

FIG. 6.



COOLING TUBE

this temperature for 10 minutes. This removes internal strains and enables the effect of temperature to be clearly shown. The tensioning weight is then quickly removed and after replacing the mounting head in the heating system, resonant frequency is checked at successive time intervals to ensure that no moisture has been adsorbed during the removal of the weight. Measurements of resonant frequency and bandwidth are taken at 5 to 10°C intervals as the temperature is lowered speedily, about two minutes being allowed at each temperature to allow the fibre to reach equilibrium with its surroundings. At room temperature, the mounting head is transferred to the cooling tube and a similar procedure is adopted until the lowest temperature in the experiment is reached. All measurements of resonant frequency and bandwidth are made in vacuo.

Quantities Measured and Methods of Measurement

Resonant Frequency: The free end of the fibre is viewed with a low power microscope (2.5 x 15 in. magnification and 2" objective lens). The frequency at which the amplitude of vibration is a maximum is the resonant frequency, and is read directly from the audio-frequency oscillator. The amplitude of vibration is measured against a scale in the eyepiece, having 100 divisions, of 0.05 mm. each.

Bandwidth: At two frequencies straddling the resonant frequency, the amplitude of vibration is $\frac{1}{\sqrt{2}}$ of the maximum. The difference between these two frequencies is the bandwidth.

To facilitate viewing of the vibrating fibre, a Philips Stroboscope (Type PR9103) is employed.

Fibre Length: After the temperature experiments are completed, the length of the fibre is measured at 20°C while in the cooling tube. The low power travelling microscope, which reads to 0.01 mm., is again employed.

Fibre Weight: The fibre is removed from the central copper rod by means of a razor blade and is conditioned for 24 hours at 20°C and 65% relative humidity. It is then weighed on a modified double cantilever balance which reads to 0.02 microgrammes. The actual length of fibre weighed is the difference between the total length and the residue remaining on the copper rod on removal of the fibre. The mass per unit length is calculated by proportion and the dry value is obtained by applying the appropriate correction factor for moisture regain¹¹³.

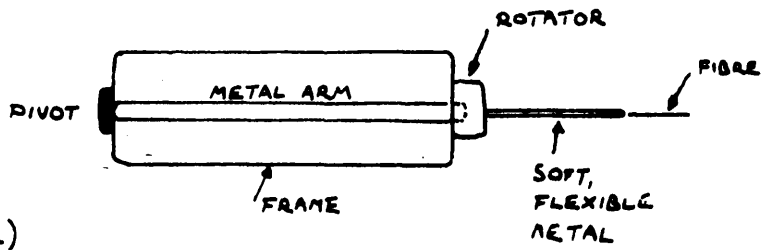
Fibre Cross-Section: After weighing, a three-stage method

is used to identify the cross-sectional shape. (When desired, areal dimensions are measured by means of a 400 X microscope with a square eyepiece scale)

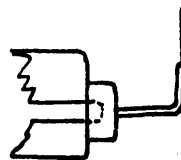
- 1) attaching the fibre to a rotatable arm (see figure 6A) and viewing horizontally at different points along the length and from different angles.
 - 2) bending the arm through 90° and focussing vertically on the fibre tip. An accurate idea of fibre shape and dimensions is obtained.
 - 3) removing the fibre, drawing it through a conical hole in a cork, and adopting a similar procedure to that of Steffens¹¹⁴. The mounting medium is UHU, a clear and uniform quick drying adhesive, not unlike Durofix. The fibre is readily identified and readings confirm those in stage 2), except in the case of fine fibres of uniform cross section where the shape may be confused with imperfections in the mounting medium. In such instances readings from stages 1) and 2) are used.
- Shape Factor: The formula for the flexural rigidity of a fibre bending about a neutral axis is given by

$$Y = \frac{\xi' A^2}{4\pi} \cdot E_1 \quad \dots\dots\dots(11)$$

where Y = flexural rigidity
 A = cross-sectional area
 E_1 = bending modulus
 ξ' = a shape factor depending on the cross-sectional shape.



(a)
HORIZONTAL
FIBRE VIEWING.



(b)
VERTICAL
FIBRE VIEWING.

CROSS SECTION
MEASURING DEVICE
(SIDE VIEW).

Since the flexural rigidity is defined as the couple required to produce unit curvature

$$Y = E_1 I \quad \text{where } I \text{ is the moment of inertia}$$

$$\text{Thus } I = \frac{\xi' A^2}{4\bar{I}} \quad \text{and} \quad \xi' = \frac{4\bar{I} I}{A^2}$$

(Note: for a circular cross-section, $I = \frac{A^2}{4\bar{I}}$ and $\xi'_0 = 1$.)

Consider two fibres of the same material and of equal cross-sectional area, one irregular in shape and having a shape factor ξ' and flexural rigidity Y_1 , the other circular in shape and having a shape factor ξ'_0 , and flexural rigidity Y_0 . The bending moduli E_1 will be the same.

$$\text{Then since } Y_1 = E_1 I_1 \quad \text{and} \quad Y_0 = E_1 I_0$$

where I_1 and I_0 are the respective moments of inertia of the irregular and circular cross sections

$$\frac{Y_1}{Y_0} = \frac{I_1}{I_0} = \frac{\xi'}{\xi'_0} \quad \text{from equation (11)}$$

$$\text{but } \xi'_0 = 1 \quad \therefore \xi' = \frac{I_1}{I_0}$$

de Witt Smith¹¹⁵ approximates the actual shape to the most similar shape of which the moment of inertia can be conveniently calculated. To illustrate the magnitudes and the range of shape factors which may be expected, his data are

given in Table 1.

Apparatus and Instruments : Changing Humidity - 20°C

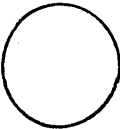
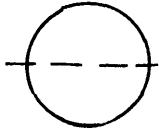
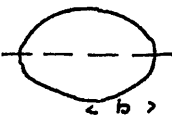
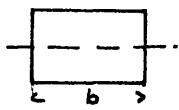
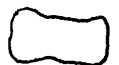
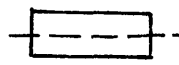
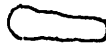
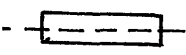
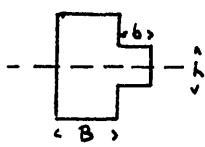
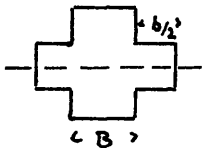
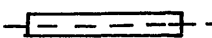
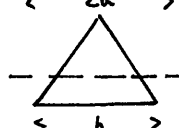
The Mounting Head: The assembly is similar to that used in the temperature experiments with the exception that the ground glass plug is about 2.5 cm. at its broad end (and the unit consequently larger) and does not require a thermocouple.

Fibre Excitation: The fibre is driven as in the temperature experiments. Higher voltage output is required to give reasonable amplitudes of vibration, which are diminished by external damping, especially at higher humidities.

The Humidity Chambers (See figure 7): A central horizontal glass tube with side arms, connected to the vacuum pump, accommodates a further six vertical glass tubes, into five of which, mounting heads are fitted. In this way five fibres can be tested simultaneously. The vertical glass tubes have ground glass joints at the top to accommodate the mounting heads, and side arms with high pressure rubber tubing (about 2 inches in length) sealed to them by sealing wax. High vacuum silicone grease is used to ensure a vacuum tight seal between the free end of the rubber tubing

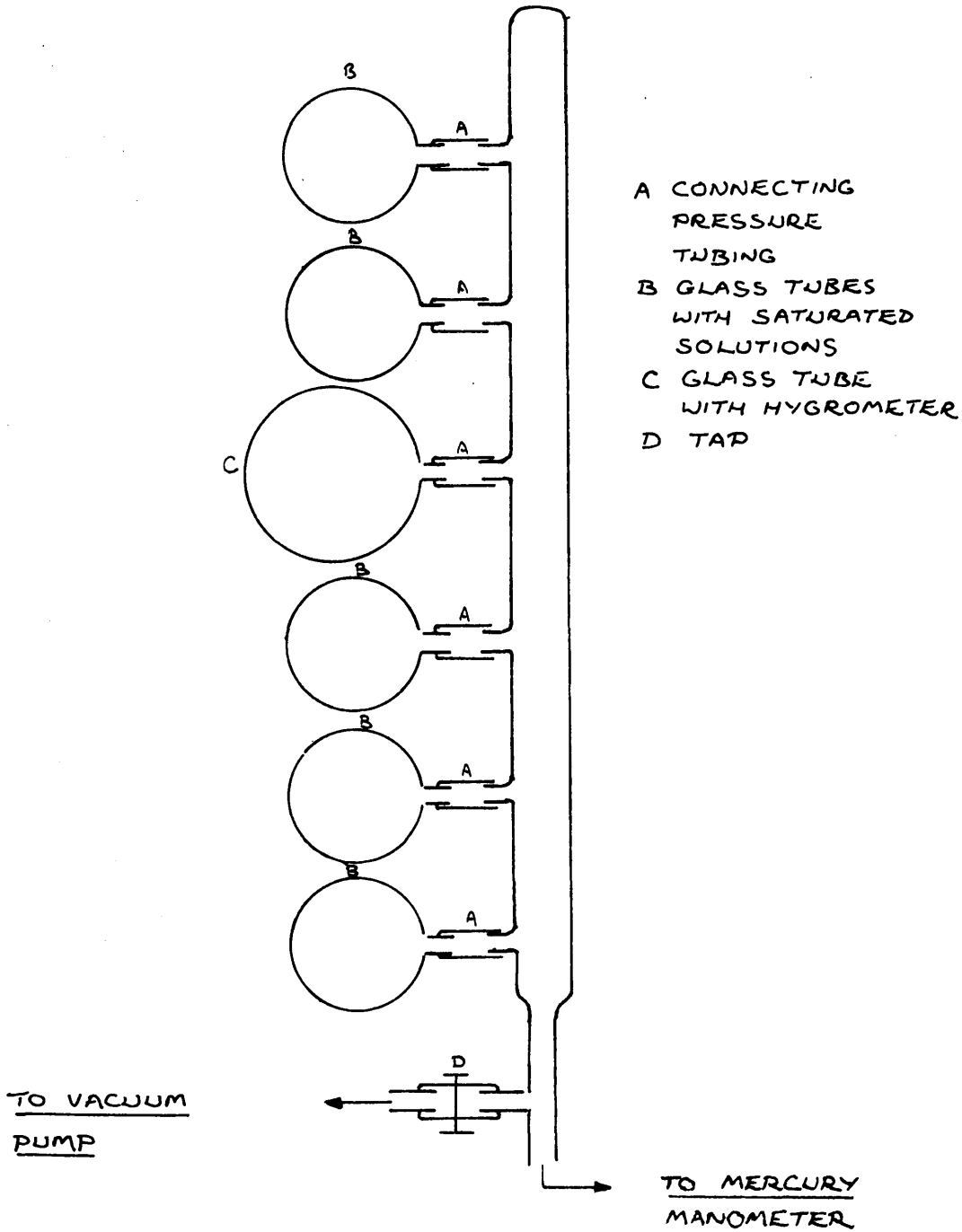
Table 1.

Shape Factors of Typical Fibre Cross-Sections

Shape	Ratio major minor axis	Beam Section Resembling actual Fibre Section	Dimensions Microns	Formula M. of I	Shape Factor
	1.0		$d = 23.2$	$\frac{\pi d^4}{64}$	1
	1.18		$a = 10.56$ $b = 12.67$	$\frac{\pi a^3 b}{4}$	0.82
	1.98		$h = 14.51$ $b = 29.02$	$\frac{bh^3}{12}$	0.52
	3.05		$h = 11.85$ $b = 35.55$	$\frac{bh^3}{12}$	0.34
	3.88		$h = 10.26$ $b = 41.04$	$\frac{bh^3}{12}$	0.26
	1.11		$h = 12.97$ $H = 25.94$ $b = 6.48$ $B = 12.97$	$\frac{BH^3 + bh^3}{12}$	1.41
	1.10		$h = 11.85$ $H = 23.7$ $b = 11.85$ $B = 11.85$	$\frac{BH^3 + bh^3}{12}$	1.04
	7.00		$h = 7.75$ $b = 54.25$	$\frac{bh^3}{12}$	0.15
	-		-	$\pi(a_3 b - a_1^3 b_1)$	0.3 approx.
	-		-	$\frac{bh^3}{36}$	1.5 approx.

HUMIDITY CHAMBERS

(NOT SHOWING MOUNTING HEADS IN B AND HYGROMETER IN C.)



and the side arms of the horizontal tube. The vertical tubes are thus easily removable. The desired humidity is obtained by using an appropriate saturated salt solution which is contained in the bottom of the tubes. A recording Hygrometer (Gregory electrolytic) is fitted into the sixth tube, which is centrally placed, to check the humidity.

Fibre Selection, Preparation and Conditioning

Selection and Preparation:- as in temperature experiments.

Conditioning: Mounted fibres are conditioned for 48 hours at room temperature and in vacuo over phosphorus pentoxide. Dryness is checked by the resonant frequency method as before. 24 hours are allowed for the fibre to reach equilibrium with its surrounding medium for all relative humidities above 0%.

Procedure

The resonant frequency and bandwidth of the dry fibres (0% relative humidity) in vacuo, are noted. The pressure is also measured by means of a mercury manometer, which is closed at one end, the height difference being read with a cathetometer (2.5 x 15 in. magnification and 2 in. objective lens) to an accuracy of 0.01 mm. The tubes

with the fibres are removed from the central horizontal tube, ^{having been} and sealed to exclude the possibility of moisture adsorption by the fibres from the atmosphere. This ensures that the complete set of readings from 0 to 90% relative humidity is obtained on the adsorption cycle. (A room atmosphere of 65% relative humidity to which, without the above necessary precaution, the fibres would be exposed, would mean that on going from 0 to 10% relative humidity for example, in the run, the fibres may adsorb sufficiently to necessitate desorption before equilibrium is reached during conditioning at 10% relative humidity).

A second auxiliary set of vertical tubes, containing a saturated salt solution to give the appropriate relative humidity (e.g. zinc chloride 10%), and having standard ground glass stoppers in place of mounting heads is now attached to the central tube. The pressure in the system is reduced by means of the vacuum pump, which is disconnected from the system only when reactions due to boiling of the solution have ceased. The mounting heads are then safely transferred to the system without fear of contamination by droplets of the solution on re-application of the vacuum pump. The pressure is again reduced until the lowest possible pressure is reached, whereupon the system is

isolated by means of a tap, and the vacuum pump disconnected. After 24 hours in partial pressure, measurements are recorded as before, and the process is repeated up to the highest humidity.

Quantities Measured and Methods of Measurement

Resonant Frequency and Bandwidth:- as in temperature experiments.

Fibre Length, Cross-section and Specific Gravity: The

fibre length and cross-section of the 3 fibres to be examined are measured at 20°C, 65% relative humidity.

Values at remaining humidities are got from data given by King¹¹⁶ for specific gravity, Speakman⁹⁹ for fibre length, and Warburton⁸ for diameter in the case of wool.

In the case of nylon, the data by Starkweather Jnr.¹¹⁷ for specific gravity, and Abbott and Goodings¹¹⁸ for length and diameter are used, while for viscose, the data of Meredith¹³ for length and diameter and the same author¹¹⁹ for specific gravity are used.

Calibrations and Instrument Checks

Audio-Frequency Oscillator: The modified Jackson Oscillator was standardised and calibrated against a Standard Muirhead (Type D-0650-B) Oscillator by Lissajous figures.

Waveform: The alternating voltage across the electrodes was analysed on a Cathode Ray Oscilloscope and found to be sinusoidal throughout the frequency range 100 to 500 c/s.

Thermocouple: The thermocouple is calibrated on a Scalamp Galvanometer against a Standard Mercury Thermometer above room temperature. The temperature read from the galvanometer, plus the room temperature gives the actual temperature. A Standard Alcohol Thermometer was used directly to read temperatures below room temperature.

Vacuum: In temperature experiments, pressures were recorded on a Pirani (Type 7-2A) Vacuum Balanced Gauge.

In humidity experiments, pressures were recorded on a mercury manometer, as described earlier. The manometer was standardised against a Macleod Gauge.

Investigations and Results

Single fibres were used throughout the investigations, their sources and characteristics being given below.

<u>Fibre</u>	<u>Average fineness</u> <u>(microgrammes/cm.)</u>	<u>Source</u>
+ Wool, Lincoln	24.6	Staple fibre, 40's quality, length 5-15"
Silk,	1.3	tex 1.2(11)/s/20 t.p.m. yarn.
Fibrolane	5.7	tex 25/z/150 x 2/s/120 t.p.m. yarn.
Ramie	8.5	staple fibre, length 3-7" .
* Viscose rayon	2.7	tex 11(40)/s/96 t.p.m. yarn.
Fortisan	1.6	tex 200(1100)/z/100 t.p.m. yarn.
Acetate fibre	6.5	tex 33(50)/s/62 t.p.m. yarn.
Tricel	13.6	staple fibre, average length, $\frac{4.8}{32}$ " .
‡ Acrilan A	3.6	staple fibre, average length, $\frac{1.24}{32}$ " .
‡ Acrilan B	3.7	staple fibre, average length, $\frac{1.24}{32}$ " .
* Nylon 66	3.8	tex 11(34)/z/30 t.p.m. yarn.
Polypropylene	4.8	tex 22(40)/s/56 t.p.m. yarn.

+ Used in both temperature and humidity experiments.

* Used in humidity experiments only.

Other fibres: used in temperature experiments only.

‡ Two chemically identical forms of Acrilan, but products of differing manufacturing processes.

Temperature Experiments

All temperature experiments are performed in vacuo, thereby eliminating effects caused by air damping. Before proceeding it is therefore necessary to establish what vacuum pressures must be attained before external damping effects can be completely ignored. A convenient method of making such a study is to observe the amplitude of fibre vibration at resonance as the pressure of the medium surrounding the fibre is reduced.

Effect of Pressure on Amplitude.

Dry specimens of wool and Fortisan are examined in successive experiments. The vacuum pressure is observed from the Pirani gauge and noted, and at each pressure the amplitude of fibre vibration at resonance is measured. The results in Table 2 show that for each fibre the amplitude increases with decrease in pressure until a pressure of 0.02 mm. mercury is attained, below which the amplitude remains constant.

Karrholm and Schroder¹⁰² deduced that the influence of air damping decreases with increasing fibre diameter using circular viscose filaments while Stauff and Montgomery⁸⁵ reached a similar conclusion using stretched glass

Table 2

Effect of Pressure on Amplitude

	Pressure, mm.Hg.	Amplitude of Vibration at Resonant Frequency, mm.
Fortisan _{20°C}	0.150	1.10
	0.080	1.45
	0.055	1.62
	0.038	1.70
	0.028	1.85
	0.022	1.92
	0.018	2.00
	0.015	2.00
0.010	2.00	
Wool _{20°C}	0.032	1.025
	0.025	1.030
	0.020	1.032
	0.017	1.032

filaments. Since Fortisan is the second finest filament used in this investigation, and only slightly heavier than silk, it is reasonable to assume that no fibre tested is subject to amplitude variations below 0.02 mm. mercury. As a precautionary measure, subsequent temperature experiments are performed at 0.01 mm. mercury pressure.

It has previously been implied that where large deformations are involved, non-linear effects in the specimen may occur. Clearly, the amplitude of vibration at the free end affects the amplitude of dynamic strain at the fixed end. It is therefore necessary to establish whether the dynamic bending modulus and loss tangent are affected by different deflections of the free end of the fibre.

Effect of Amplitude on Dynamic Bending Modulus
and Loss Tangent.

Dry specimens are forced into resonance at which point measurements of resonant frequency and bandwidth are made. The amplitude of vibration of the fibre is recorded. By increasing the voltage output from the audio-frequency oscillator, the amplitude of vibration is enlarged, and the same readings are taken. Table 3 illustrates that over a reasonable temperature range the

Table 3.

Effect of Amplitude on Dynamic Bending Modulus and Loss Tangent

Amplitude, mm. Resonant Frequency, c/s Loss Tangent

Wool. Length = 0.92 cm.

88°C

0.550	179.3	0.0175
0.825	180.0	0.0180
0.925	179.5	0.0175

38°C

0.350	188.6	0.0257
0.550	189.0	0.0250
0.650	189.0	0.0254

Fortisan Length = 0.60 cm.

165°C

0.650	166.3	0.0460
1.000	166.4	0.0450
1.400	166.5	0.0450

121°C

0.800	187.4	0.0225
1.300	187.3	0.0218
1.750	187.3	0.0220

84°C

0.800	198.2	0.0130
1.200	198.3	0.0129
1.650	198.3	0.0130

amplitude of vibration does not affect the resonant frequency (and hence the dynamic bending modulus) or the loss tangent. Sufficient accuracy can be achieved by vibrational amplitudes of 0.5 mm. (10 eyepiece divisions), while a convenient maximum amplitude of 1.5 mm. (30 eyepiece divisions) is governed by the spacing of the electrodes. Hence, for the purposes of this investigation, the dynamic parameters are independent of the amplitude of vibration.

The effect of frequency on dynamic properties may be quite considerable as has been previously indicated, and with respect to the present investigation, three factors must be taken into consideration.

- 1) As the dynamic properties vary with temperature, so do the natural frequencies of specimens under observation change; consequently the imposed frequency required for resonance will be subject to a corresponding variation.
- 2) Considering two filaments of the same material, then providing their physical dimensions are identical, they will have exactly the same resonant frequencies. However, it is indeed a rare phenomenon that such a situation should exist, and in consequence different samples of

the same material will have different resonant frequencies.

3) Add to this the fact that when taking samples from a group or bundle, without rigidly controlling the length of specimen, further differences in resonant frequency will occur.

It is plain therefore that a range of frequencies will be covered for each fibre tested, and it is necessary to determine whether or not the dynamic bending modulus and energy loss are dependent on frequency.

Effect of Frequency on Dynamic Bending Modulus
and Loss Tangent.

The resonant frequency, bandwidth and length of a dry fibre are measured in vacuo. A portion of the fibre is severed, and the measurements are recorded once more. The process may be repeated several times, but since the audio frequency oscillator is accurate only in the range 100 to 400 c/s., a wide range of fibre lengths cannot be covered. It is found that within this range the product of length and the ~~reciprocal of the~~ square root of resonant frequency is relatively constant. Such variations as do

occur may be attributable to small, inherent irregularities in the fibre. The fact that straight lines passing through the origin are obtained suggests, however, not only that the dynamic bending modulus is independent of frequency in the range 100-400 c/s., but also that the inherent irregularities, with carefully selected fibres, may be very small.

Values of loss tangent for several of the fibres are relatively constant and show no definite tendency either to increase or decrease at different frequencies.

The results, (Table 4 and figure 8) are in accordance with prediction since frequency dispersions occur over very wide ranges. The results of Fujino et al.²⁸ (Table 5) indicate this quite clearly. Dynamic Young's modulus was independent of frequency except in the supersonic range, where it showed a tendency to rise while the loss tangent tended to increase at very low and very high frequencies except in the case of silk.

Those variables which may arise as a consequence of experimental conditions and techniques may be summed up thus:

- 1) Measurements of dynamic properties will be accurate provided a vacuum pressure of less than 0.02 mm. mercury is employed.
- 2) Within the range of amplitudes of maximum vibration

Table 4.

Effect of Frequency on Bending Modulus and Loss Tangent

	Length, l, cm.	Resonant Frequency, c/s.	$\frac{1}{\sqrt{\nu_0}}$	$\frac{1 \cdot \sqrt{\nu_0}}{\sqrt{\nu_0}}$	Loss Tangent
Wool	0.69	286.8	0.060	11.50	
	0.77	225.0	0.066	11.65	
	0.87	182.6	0.073	11.98	
	1.08	121.1	0.091	11.93	
Silk	0.43	172.4	0.077	5.60	
	0.45	155.8	0.081	5.65	
	0.50	121.0	0.091	5.58	
Fibrolane	0.50	258.0	0.063	8.00	
	0.56	210.3	0.071	7.98	
	0.72	127.3	0.089	8.95	
Ramie	0.52	256.0	0.063	8.30	0.0075
	0.59	196.5	0.073	8.10	0.0076
	0.70	134.5	0.087	8.09	-
Fortisan	0.50	343.3	0.054	9.25	0.0120
	0.70	180.5	0.073	9.58	0.0140
	0.80	133.2	0.087	9.18	0.0101
Acetate Fibre	0.48	330.0	0.055	8.72	
	0.62	177.3	0.075	8.30	
	0.70	149.0	0.082	8.50	
Tricel	0.57	324.0	0.056	10.23	
	0.68	227.0	0.066	10.29	
	0.83	157.1	0.080	10.30	
Acrilan A	0.55	240.0	0.065	8.50	0.0475
	0.63	182.0	0.074	8.40	0.0465
	0.76	121.0	0.091	8.35	0.0478
Acrilan B	0.56	258.0	0.061	9.10	0.0475
	0.66	182.0	0.074	8.90	0.0435
	0.82	120.0	0.092	8.90	0.0435
Polypropylene	0.60	225.0	0.067	9.00	
	0.64	210.0	0.069	9.34	
	0.84	121.0	0.091	9.25	

FIG. 8.

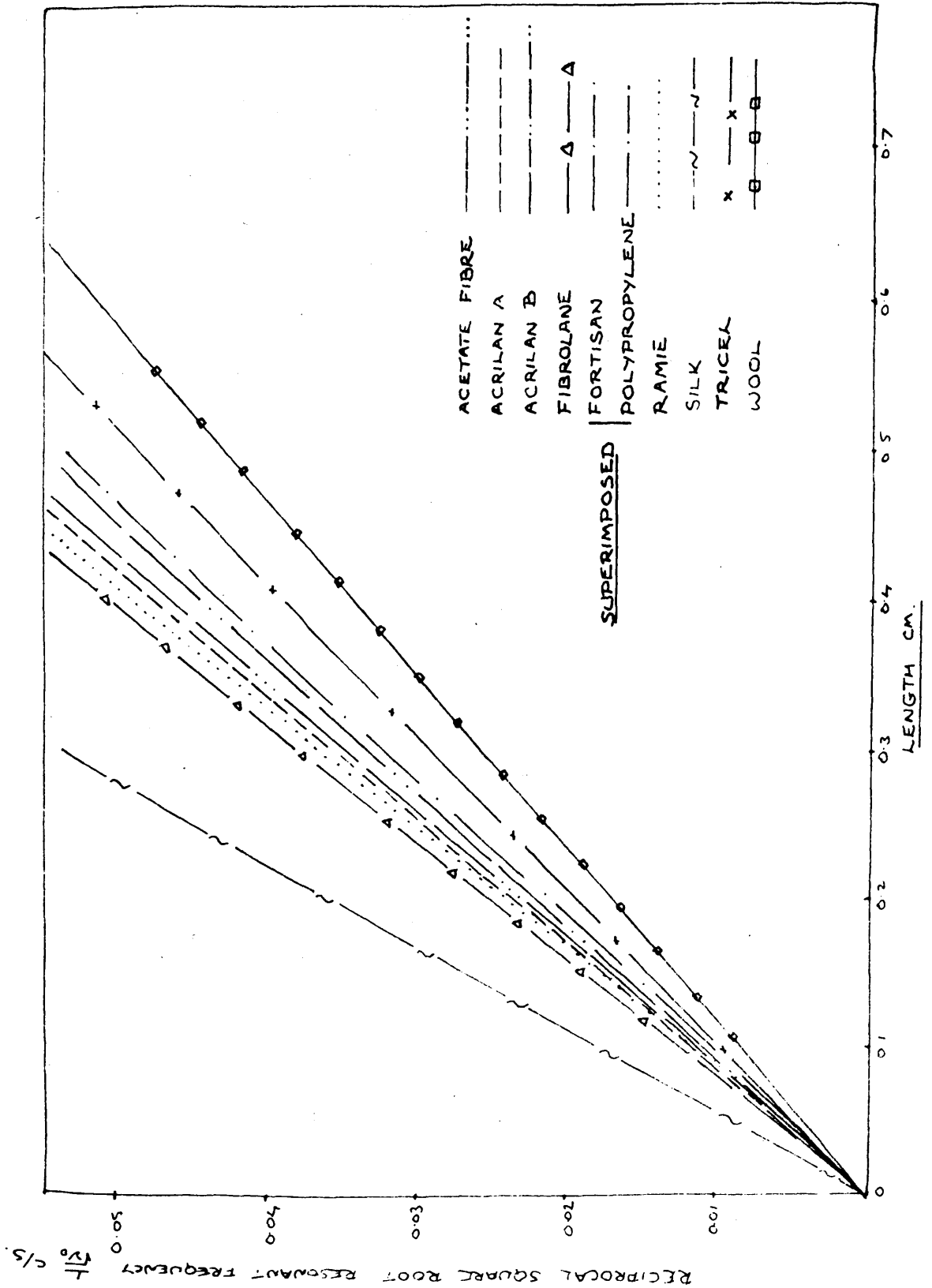


Table 5.

Effect of Frequency on Dynamic Properties

at 20°C and 65% Relative Humidity.

Fibre	Static Stress, 10 ⁸ dynes/cm ²	Dynamic Young's Modulus .			Loss Tangent		
		10 ¹⁰ dynes/cm ²			1 c/s	100 c/s	100 kc/s
		1 c/s	100 c/s	100 kc/s			
Viscose Rayon	6.3	13	14	14	0.05	0.03	0.045
Cuprammonium Rayon	6.7	19	19	21	0.045	0.03	0.05
Cellulose Acetate	4.1	5	5	6	0.03	0.03	0.04
Raw Silk	5.1	16	15	15	0.02	0.02	0.025
Degummed Silk	5.4	12	13	15	0.03	0.03	0.03
Nylon 6	4.1	5	5	6	0.09	0.075	0.10

0.5 mm. to 1.5 mm., resonant frequency and bandwidth can be recorded with accuracy and free from non-linear effects.

3) Dynamic properties are independent of frequency within the range 100 to 400 c/s.

The effect of temperature may now be studied provided that the above conditions and limitations are realised.

The Effect of Temperature on Dynamic Bending Properties.

The effect of temperature on the resonant frequency and bandwidth of 10 fibres (nylon and viscose rayon are investigated only in humidity experiments) is measured according to the procedure previously described; i.e. by conditioning a dry fibre for ten minutes at the highest temperature of the experiment and taking measurements at small temperature intervals down to the lowest temperature. This conditioning ensures that irreversible dimensional and structural changes do not take place in the subsequent experiments performed below the conditioning temperature, and that the transitions which may take place are truly reversible, regardless as to whether the critical transition temperatures are approached from higher or lower

temperatures. (This was verified with wool, Acrilan, and polypropylene fibres, by measuring the dynamic parameters on an increasing temperature cycle immediately following the decreasing temperature cycle. Without conditioning, such reproducibility, as was obtained with these fibres - neglecting small experimental errors - may not be obtained, especially with thermoplastic fibres.)

The results are shown in Figs.9 to 32 and Tables 6 to 53. Figs.9-18 deal with the effect of temperature on loss tangent, and Figs.19-28 deal with the effect of temperature on relative bending modulus.

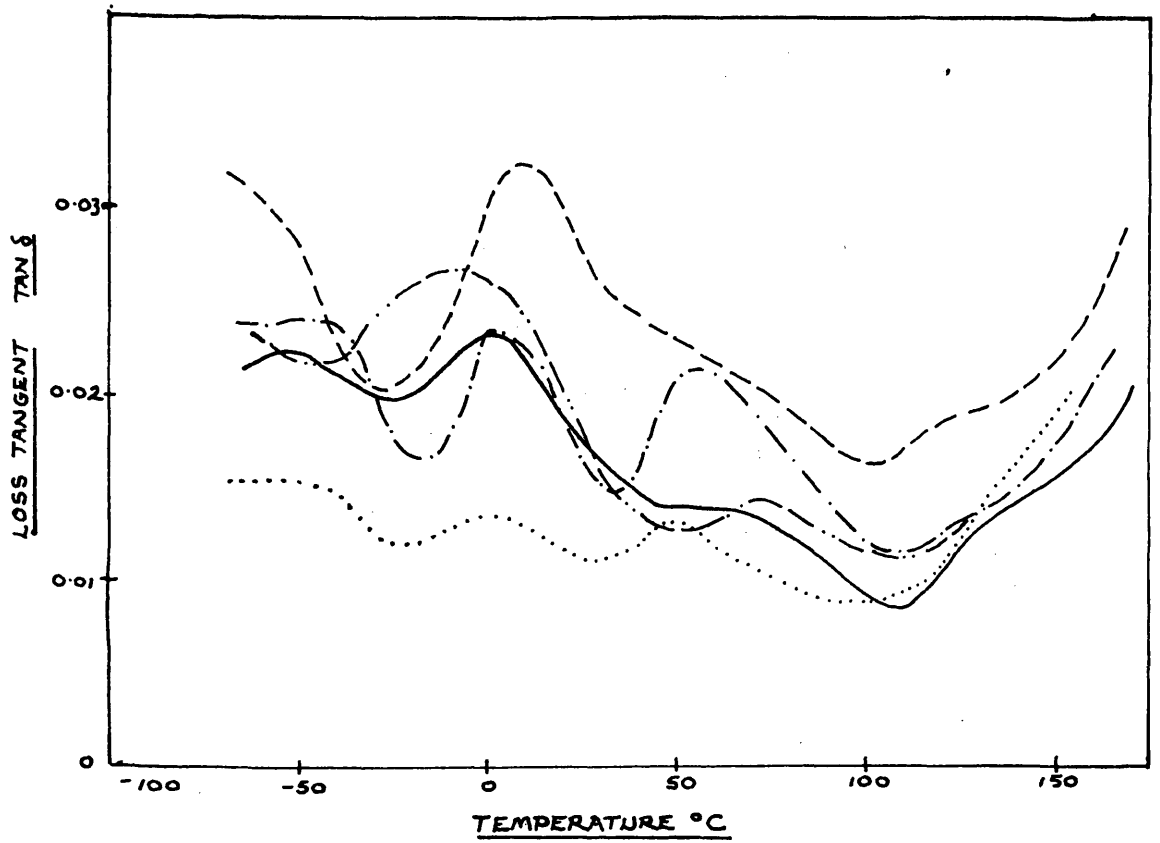
The relative bending modulus is the ratio of the square of the resonant frequency at a given temperature to the square of the resonant frequency at 20°C.

Fig.29 shows the effect of temperature on mean loss tangent for a number of fibres. Two or more specimens of each fibre (designated Fibre 1, 2, etc.), were tested for dynamic behaviour. Differences in the location and height of maxima and minima in the loss tangent curve were observed. The means of both location and height were calculated from the experimental data. The shapes of the mean loss tangent curves between maxima and minima were also estimated from experimental data.

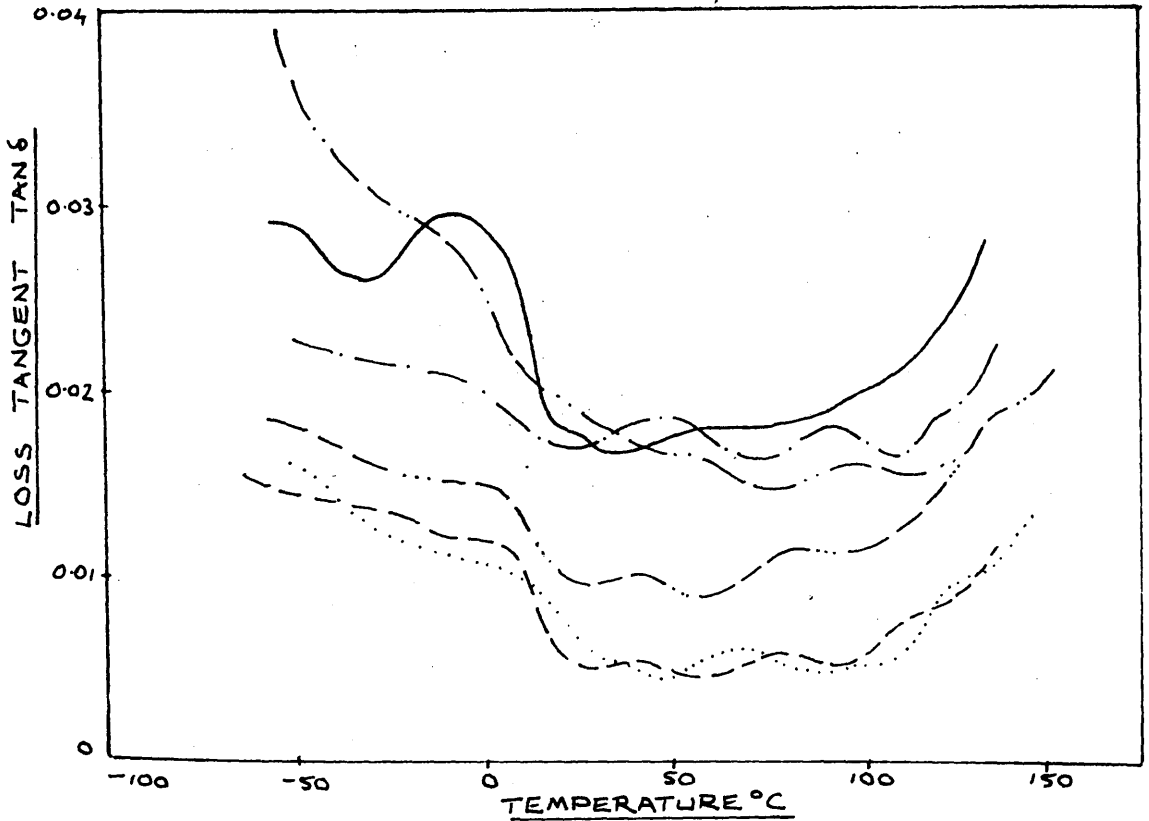
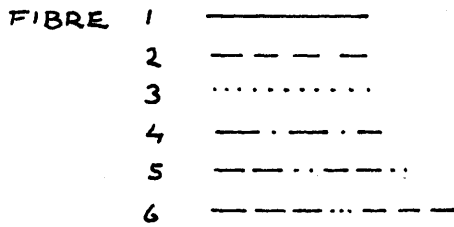
Fig.30 shows the effect of temperature on the mean

WOOL

FIBRE 1 —————
2 - - - - -
3
4 - · - · -
5 - · - · -

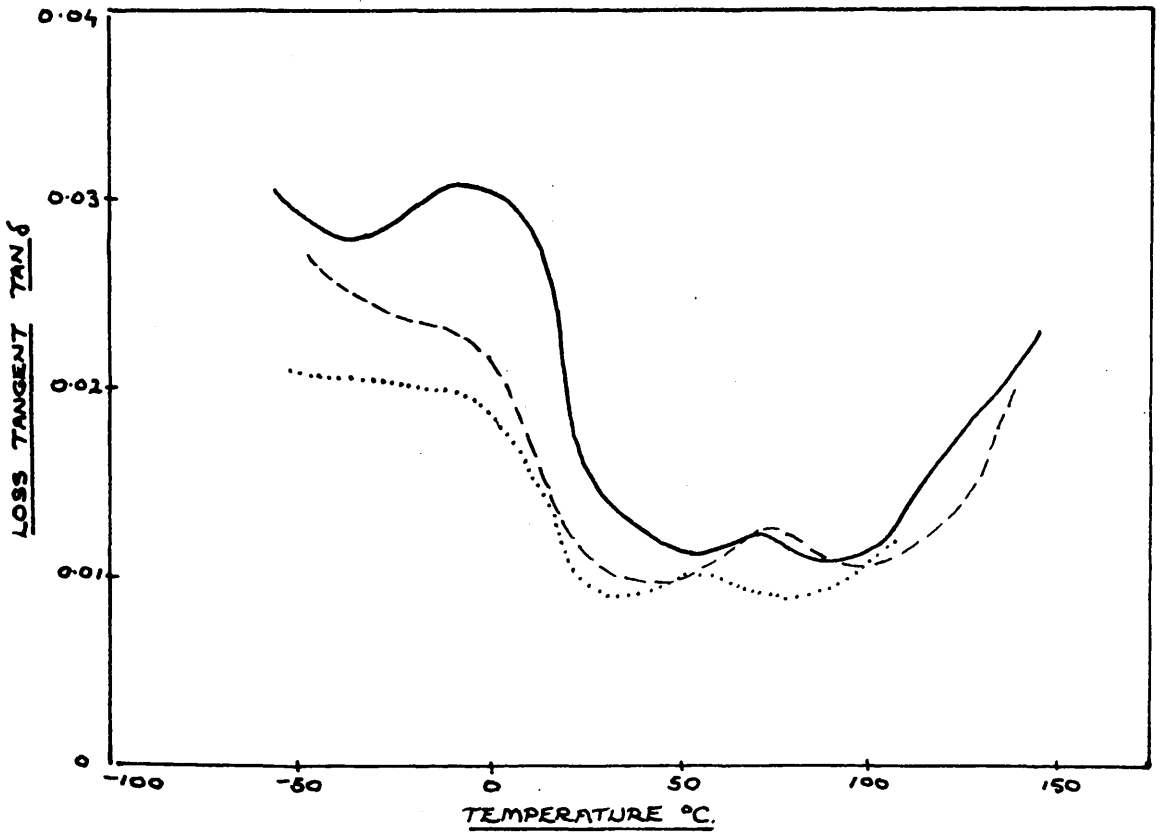


SILK



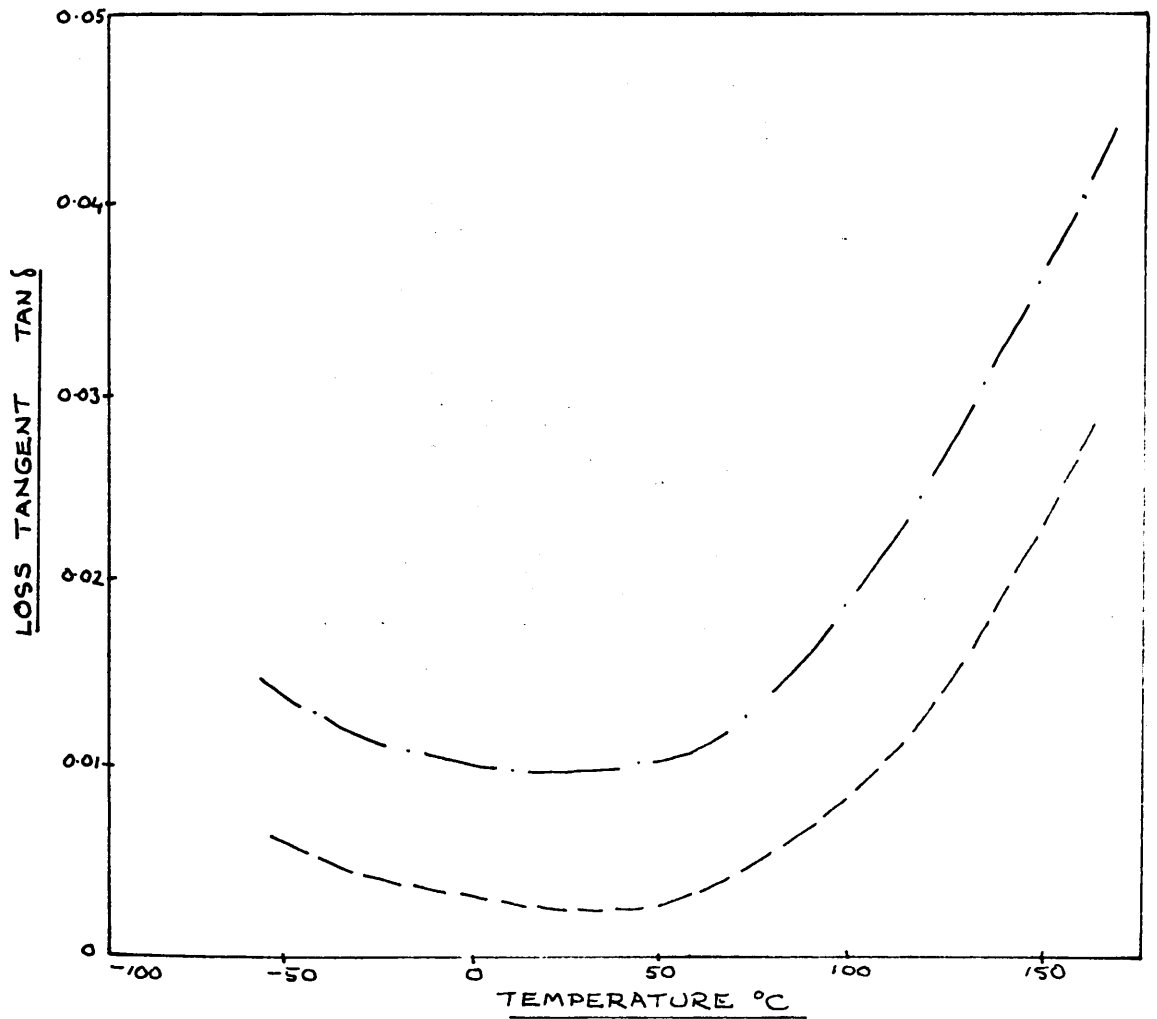
FIBROLANE

FIBRE 1 ———
2 - - - -
3 ······



RAMIE

FIBRE 1 - . - . -
FIBRE 2 - - - - -



FORTISAN

FIBRE 1 — · — ·
2 — — —

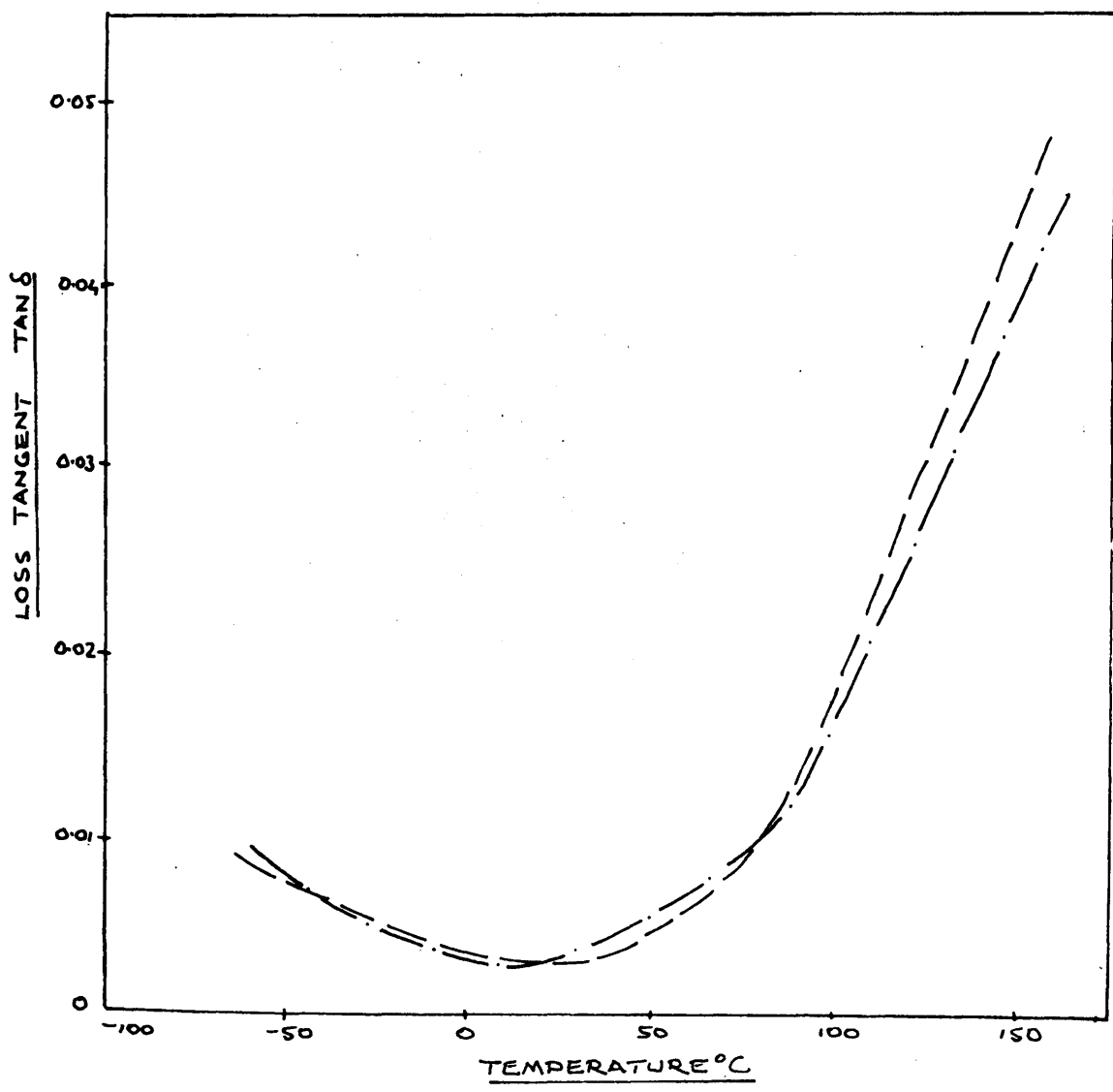


FIG. 14

ACETATE FIBRE

FIBRE 1 ———
2 - - - -
3 ······
4 - · - ·

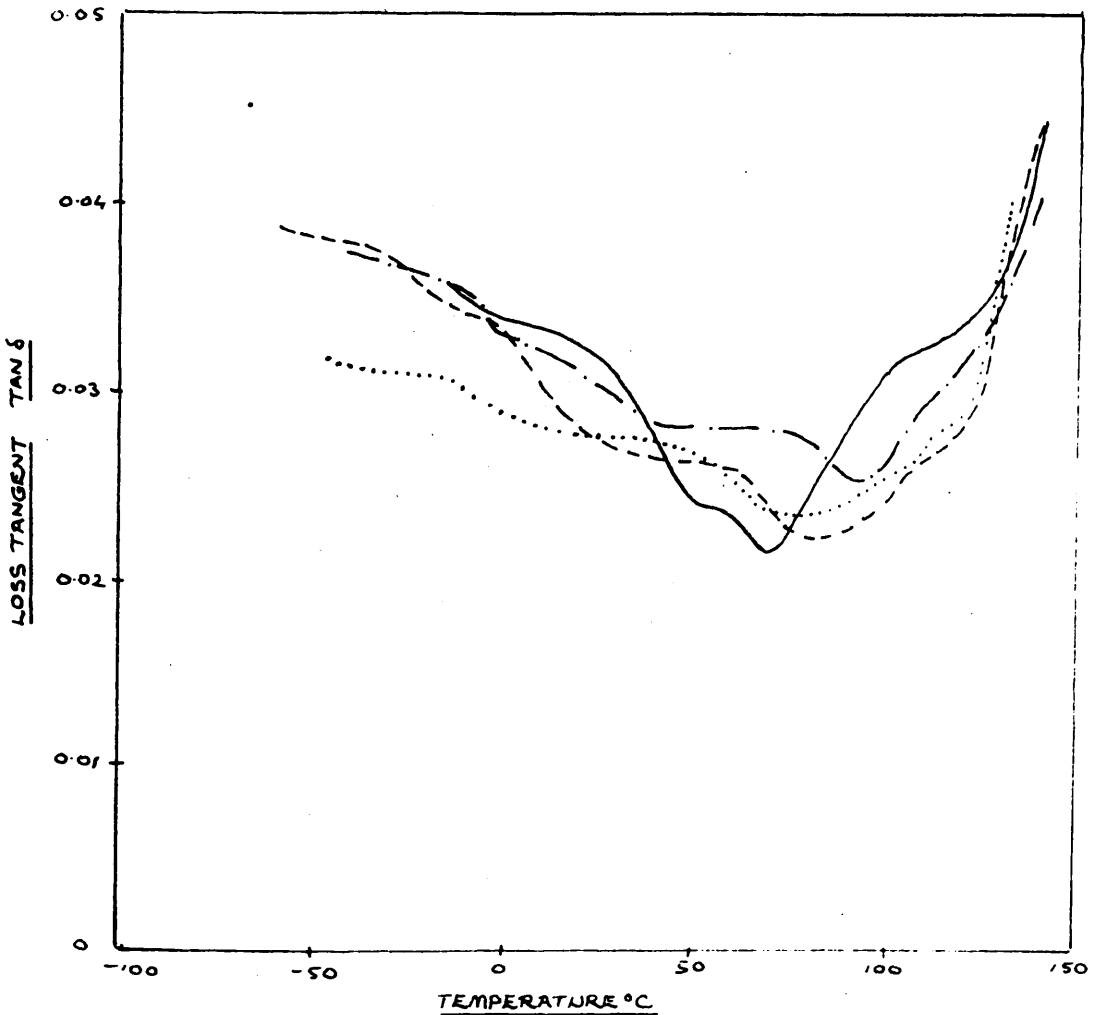


FIG. 15

TRICEL

FIBRE 1 —————
2 - - - - -
3
4 - . - . -

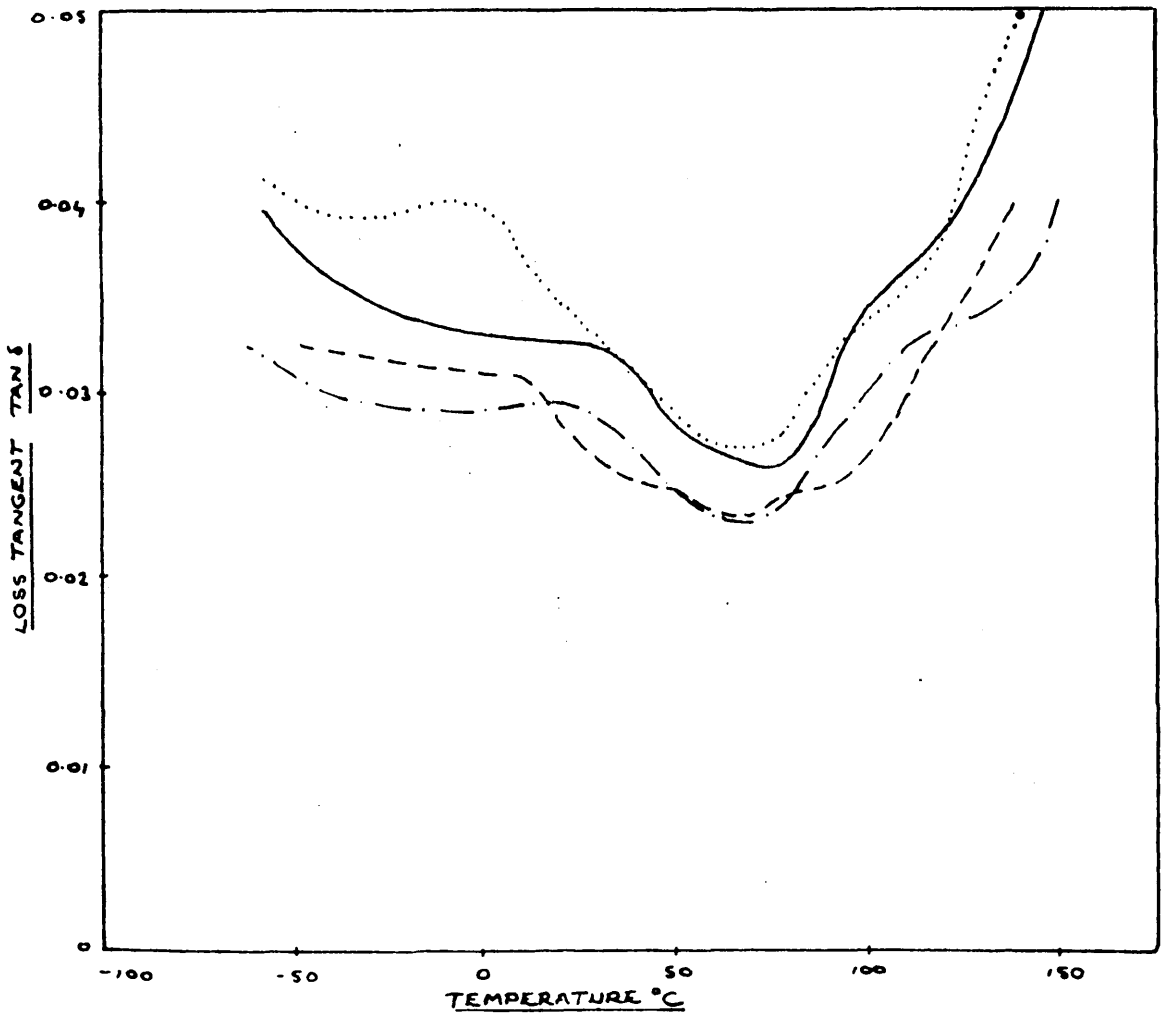


FIG. 16

ACRILAN A

FIBRE 1 ———
2 - - - -
3 ······

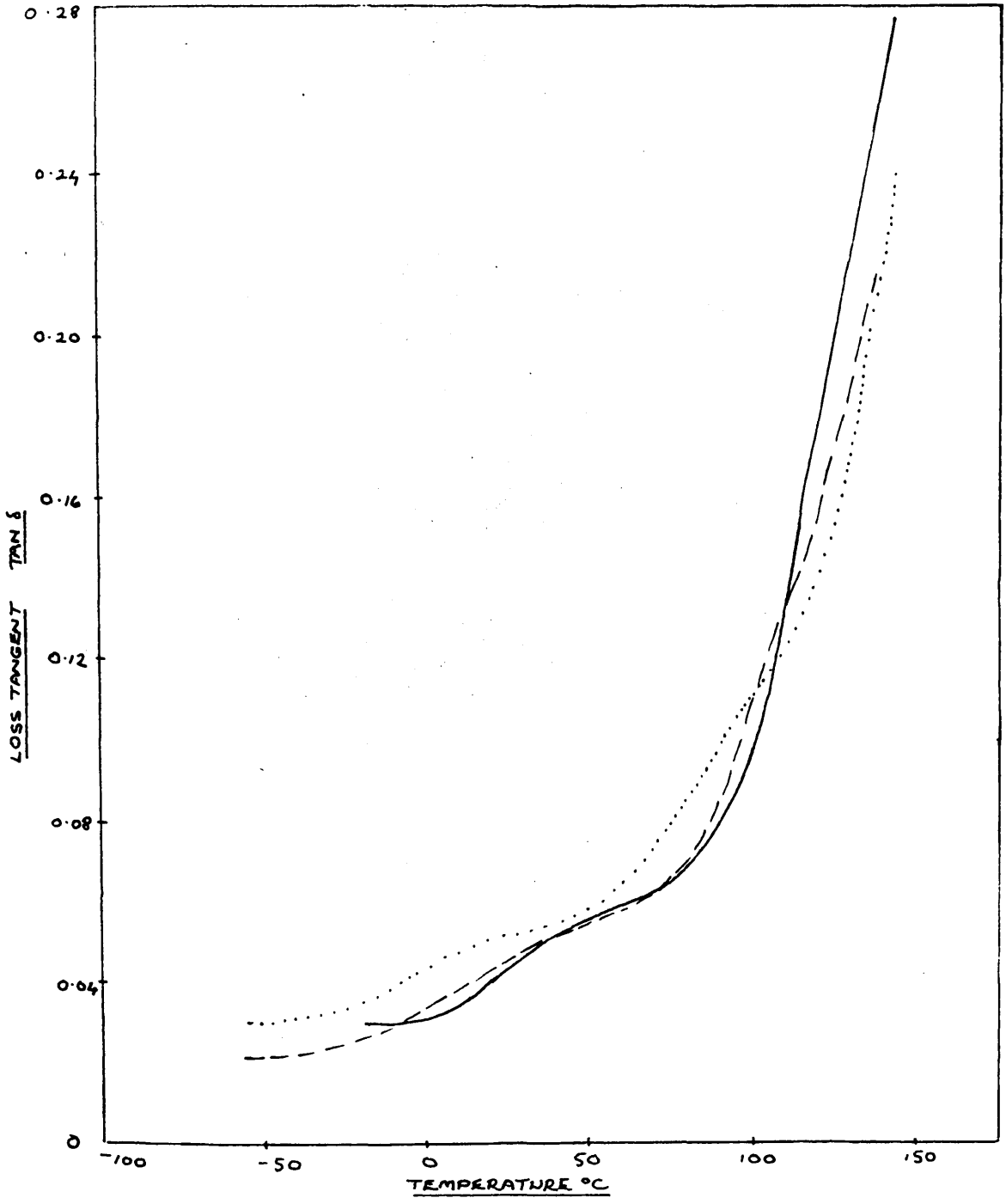
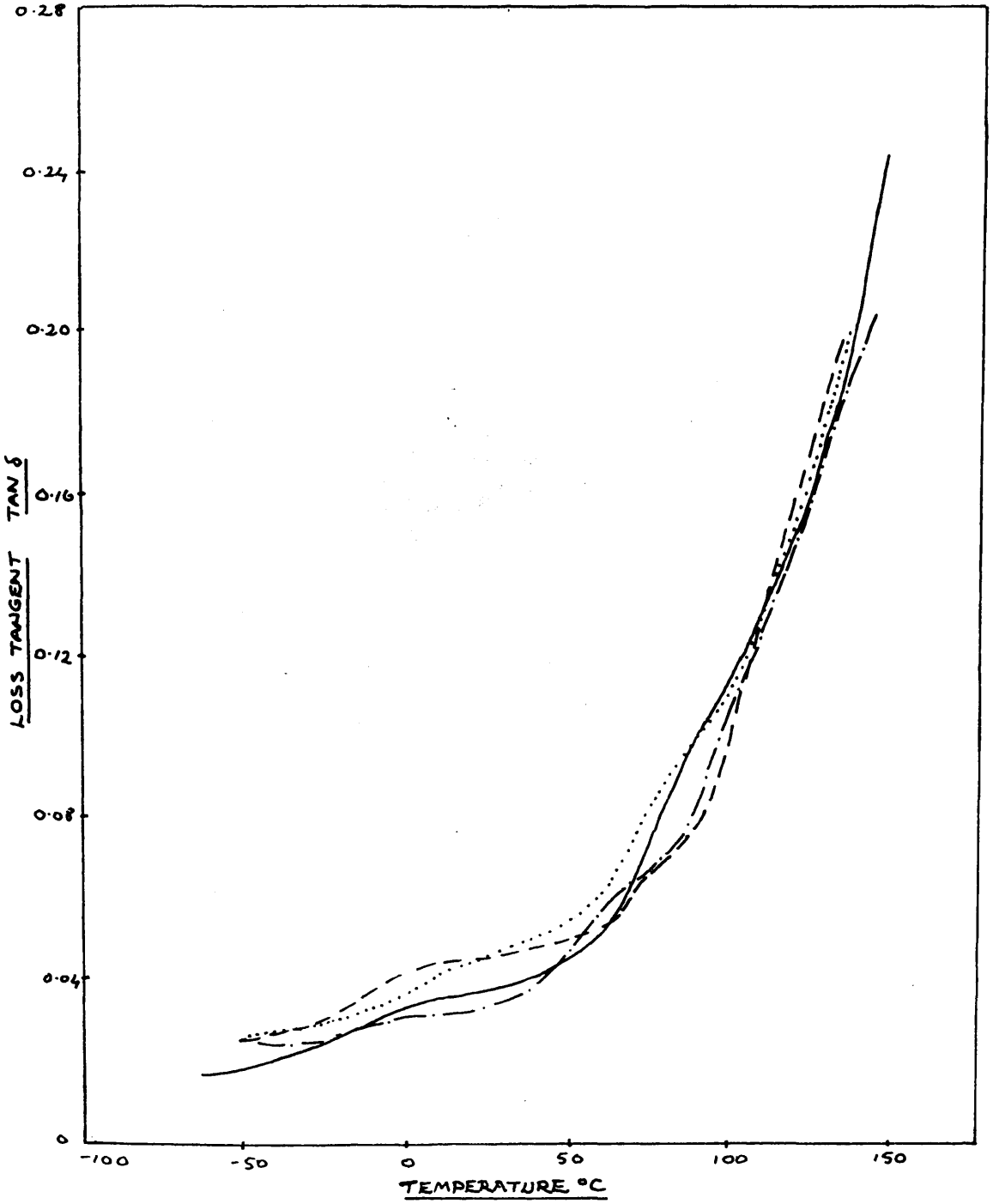


FIG. 17

ACRILAN B

FIBRE 1 ———
2 - - - -
3 ······
4 — · — ·



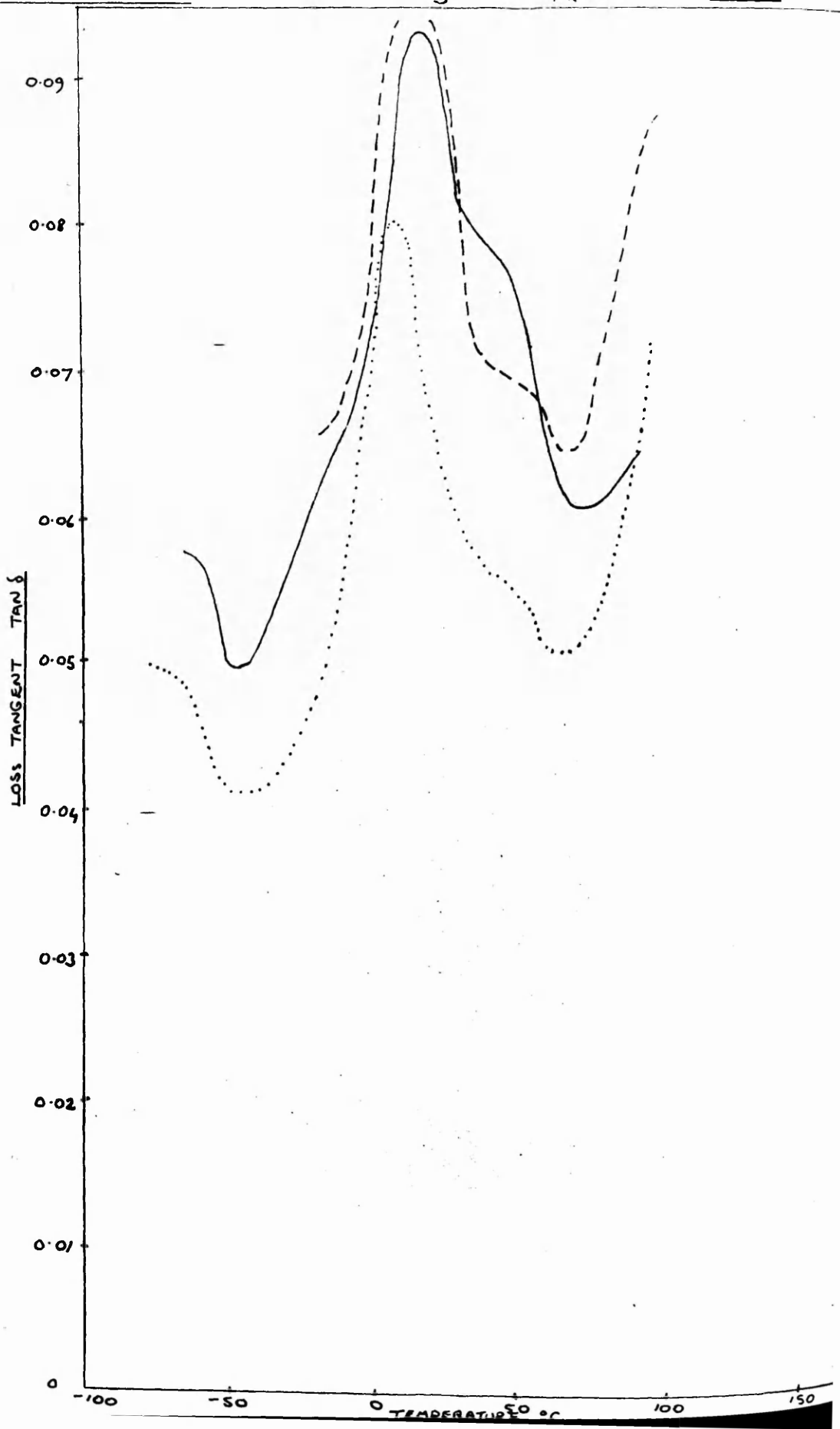


FIG. 19

WOOL

FIBRE 1 —————
2 - - - - -
3
4 - - - - -
5 - - - - -

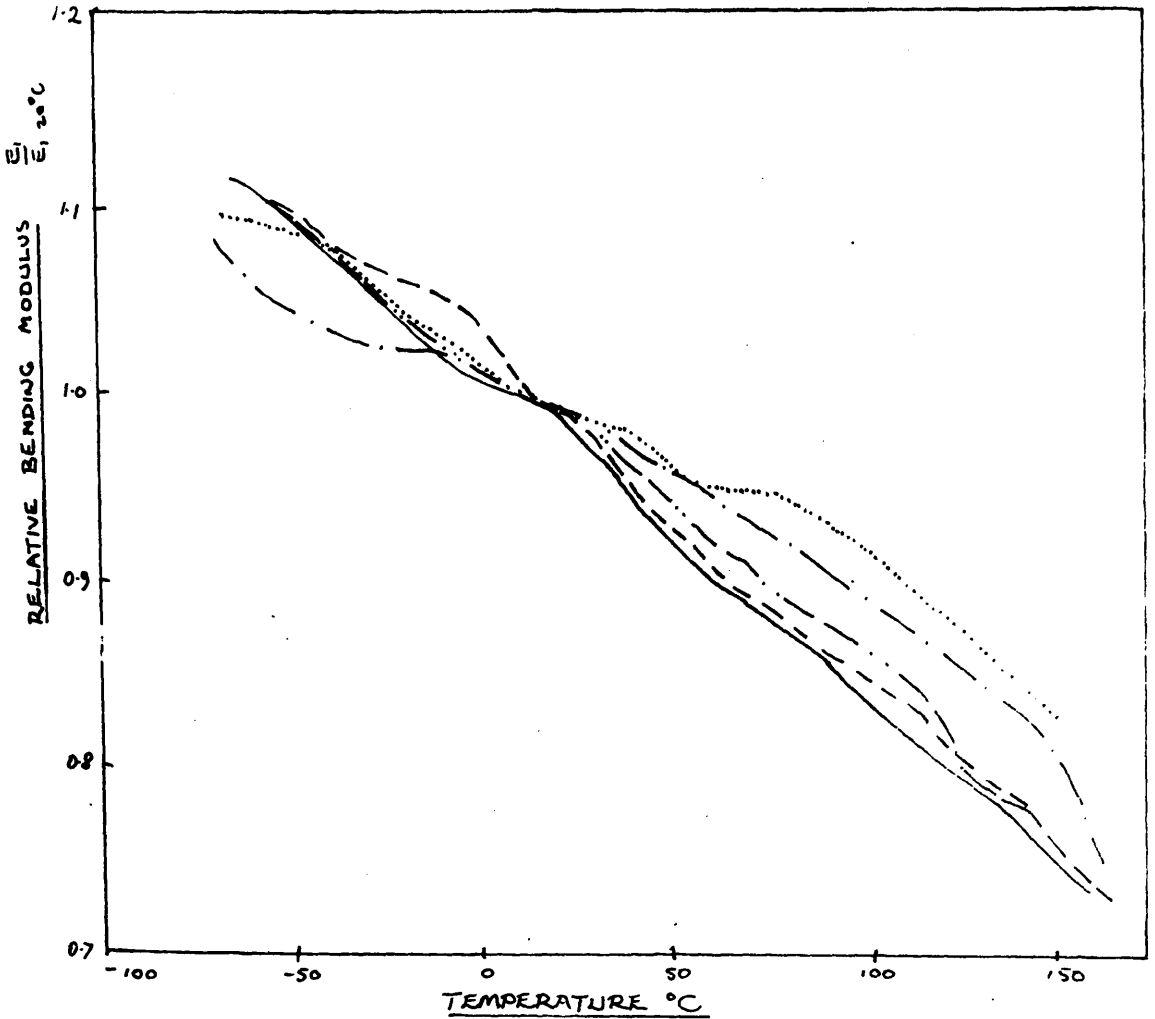
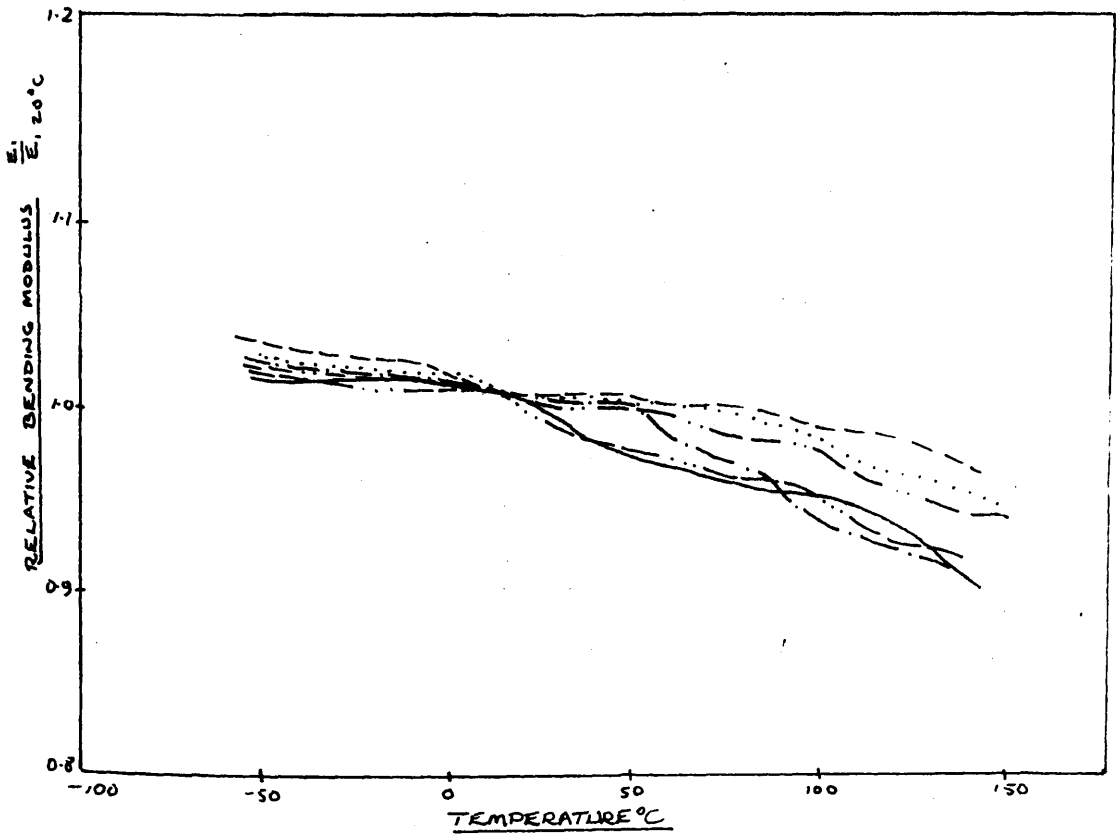


FIG. 20

SILK

- FIBRE 1 _____
2 - - - - -
3
4 - - - - -
5 - · - · -
6 - - - - -



FIBROLANE

FIBRE 1 ———
2 - - - -
3 ·····

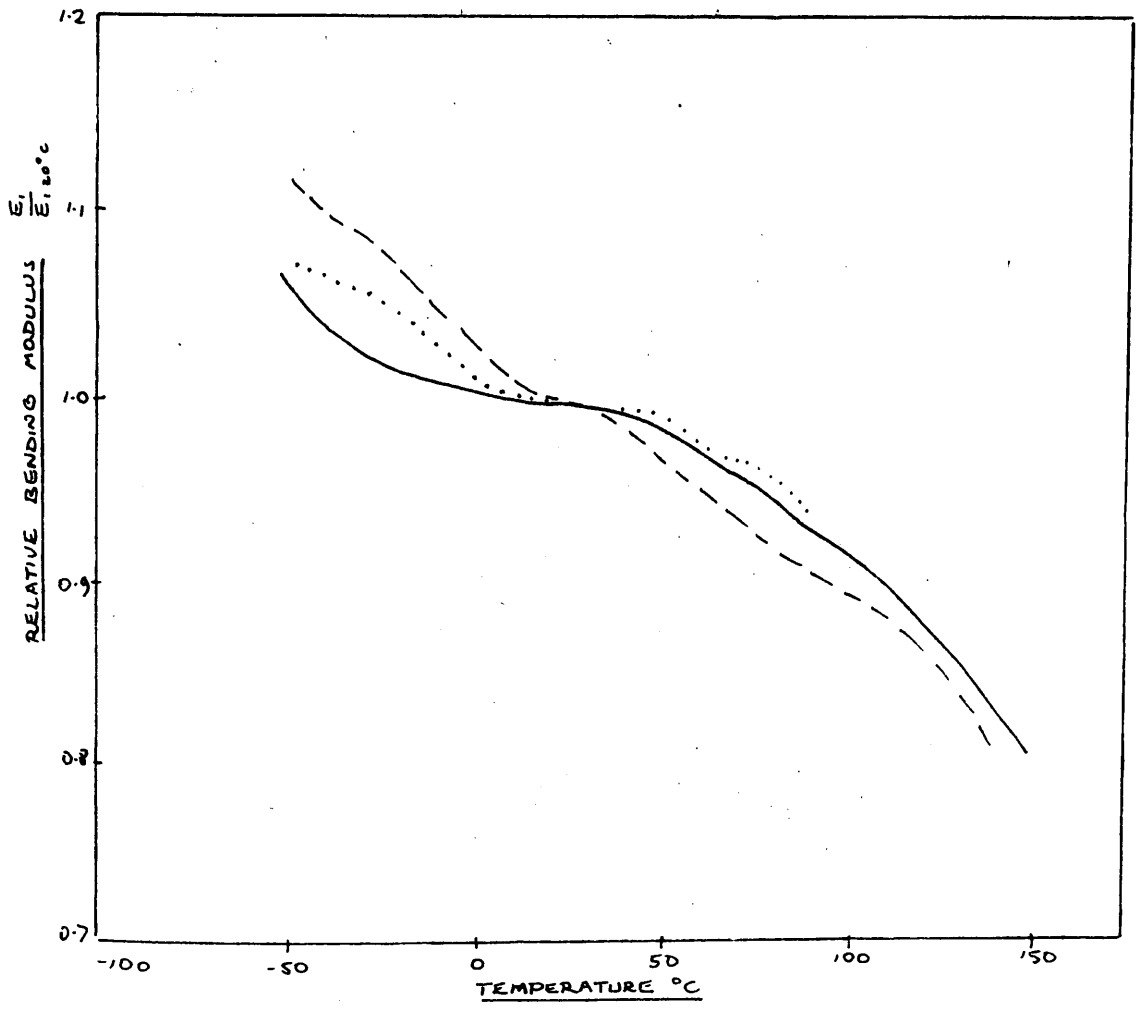
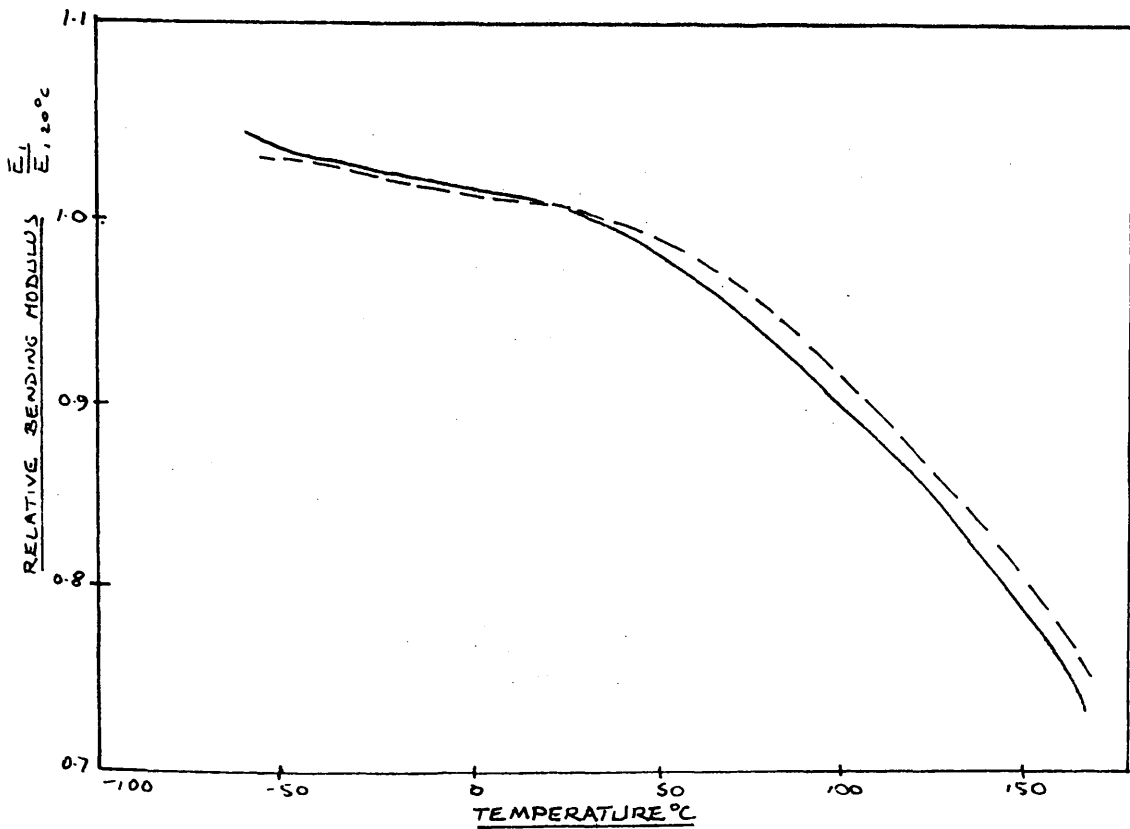


FIG. 22

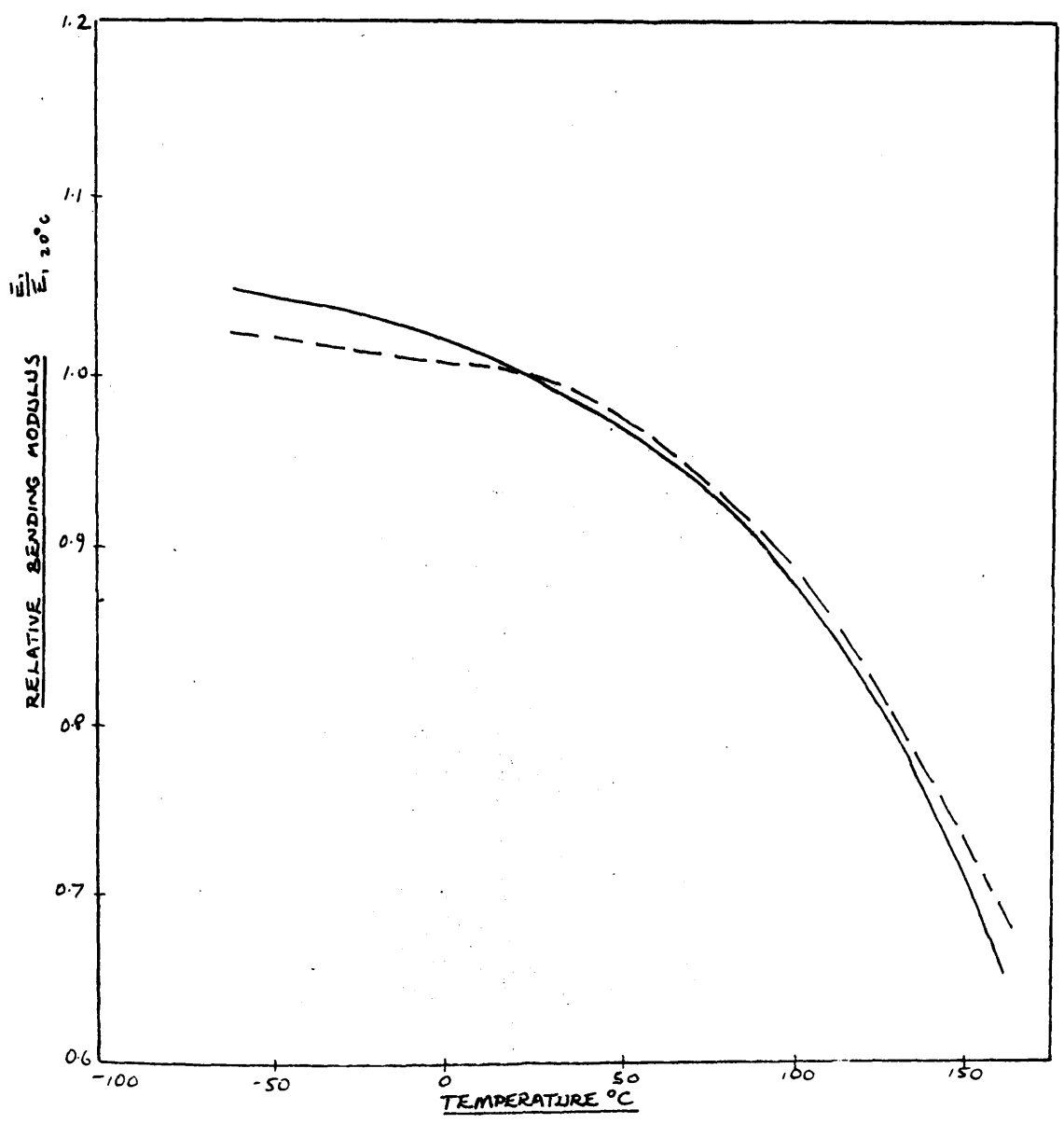
RAMIE

FIBRE 1 ———
2 - - - -



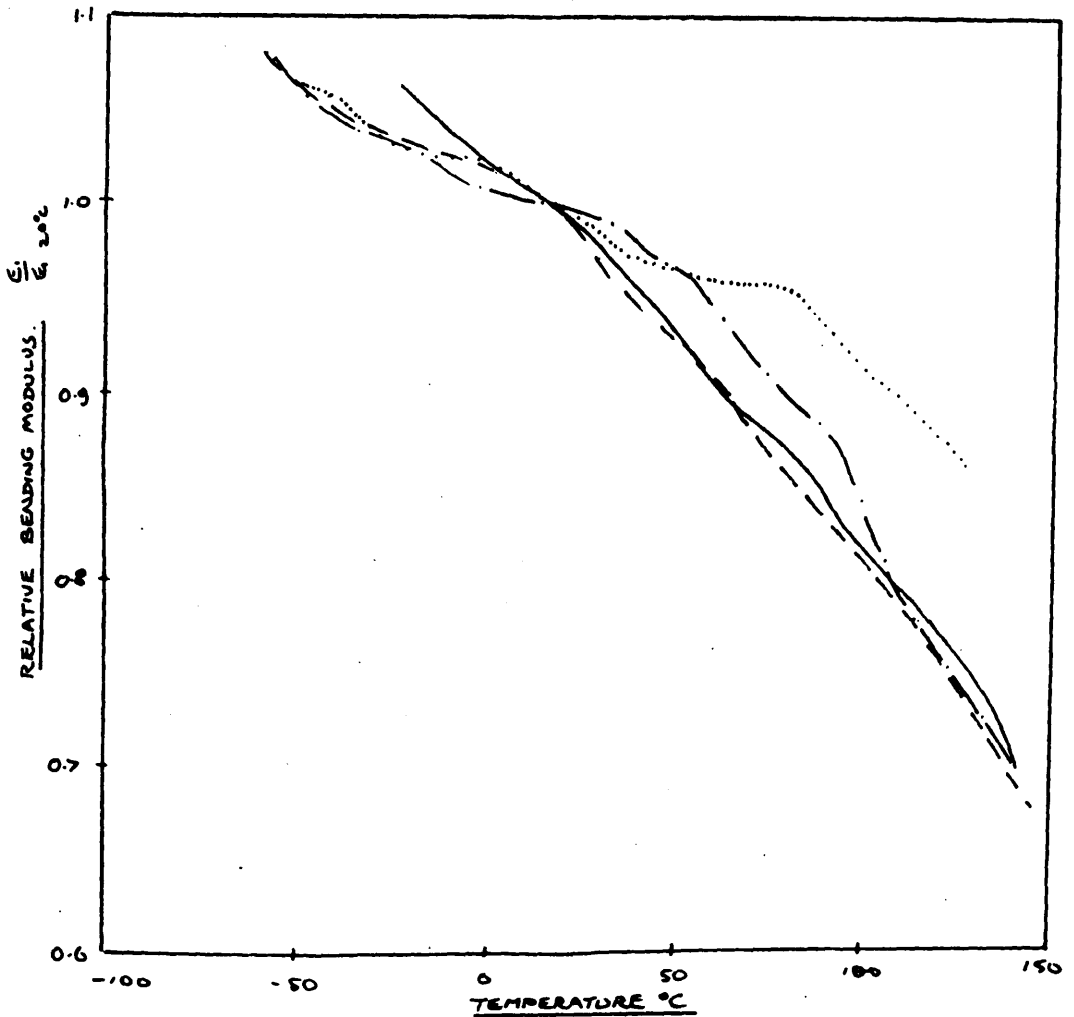
FORTISAN

FIBRE 1 —————
2 - - - - -



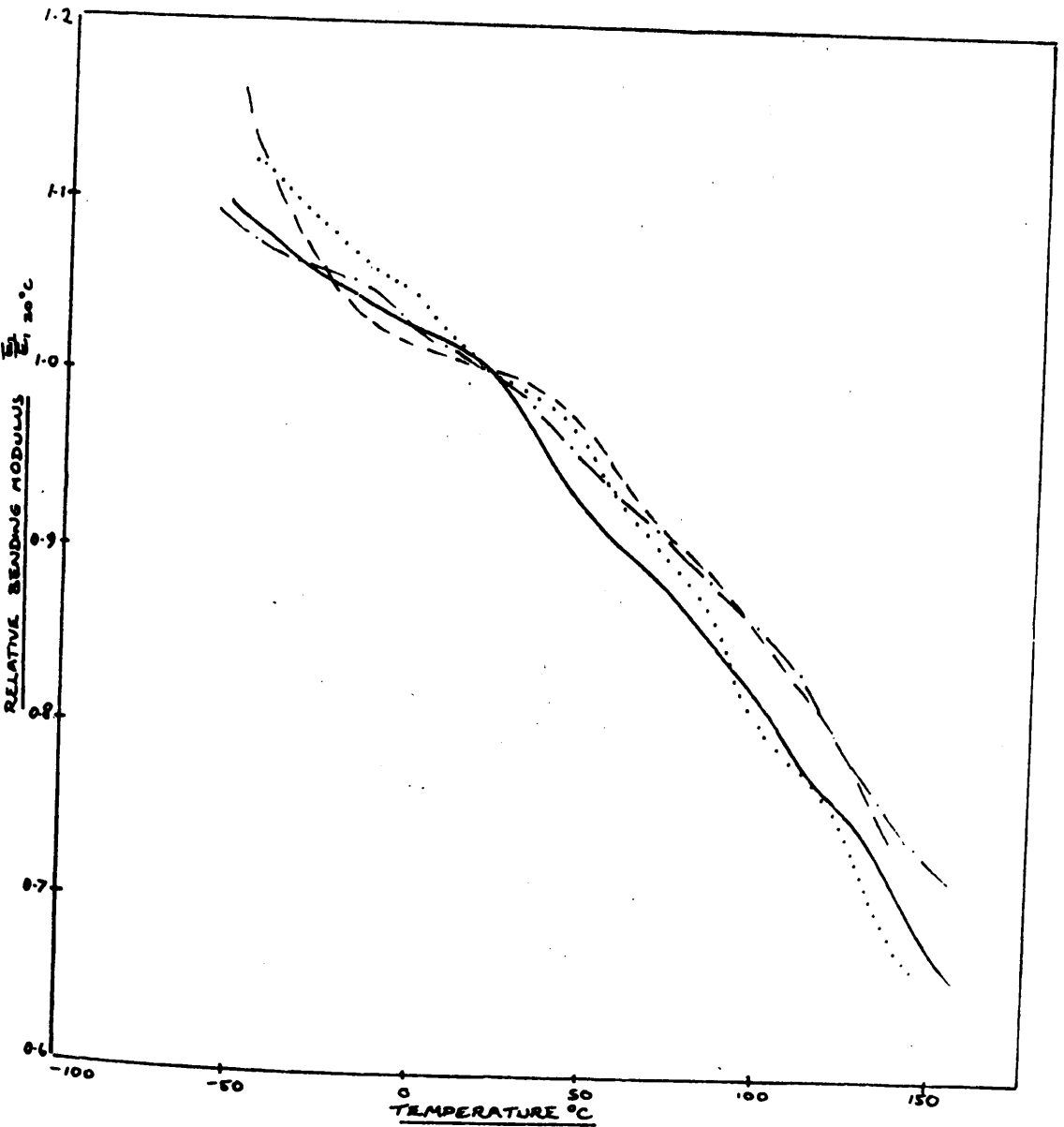
ACETATE FIBRE

FIBRE 1 —————
2 - - - - -
3
4 - · - · -



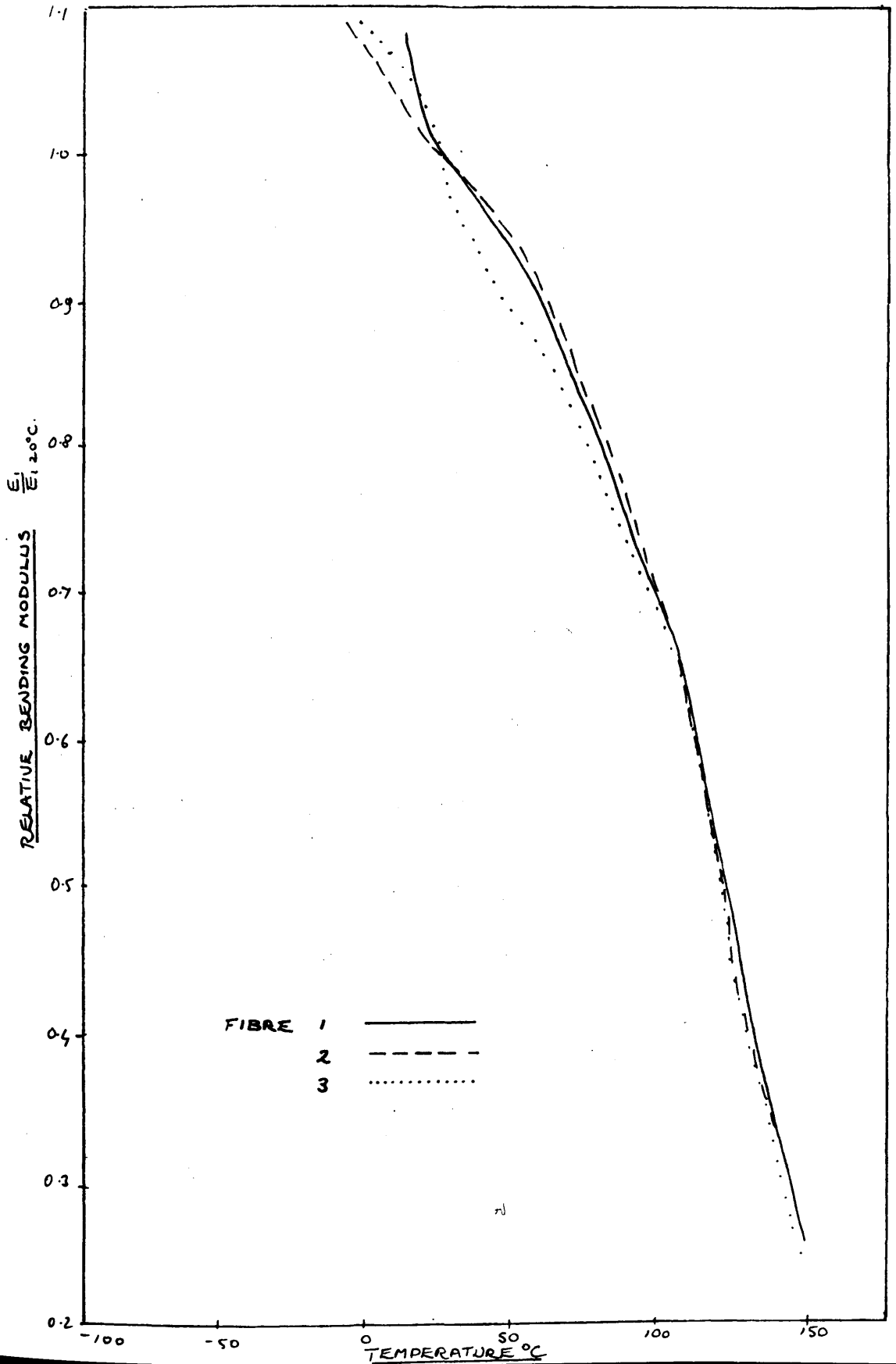
TRICEL

- FIBRE 1 —————
 2 - - - - -
 3 ······
 4 - · - · - ·



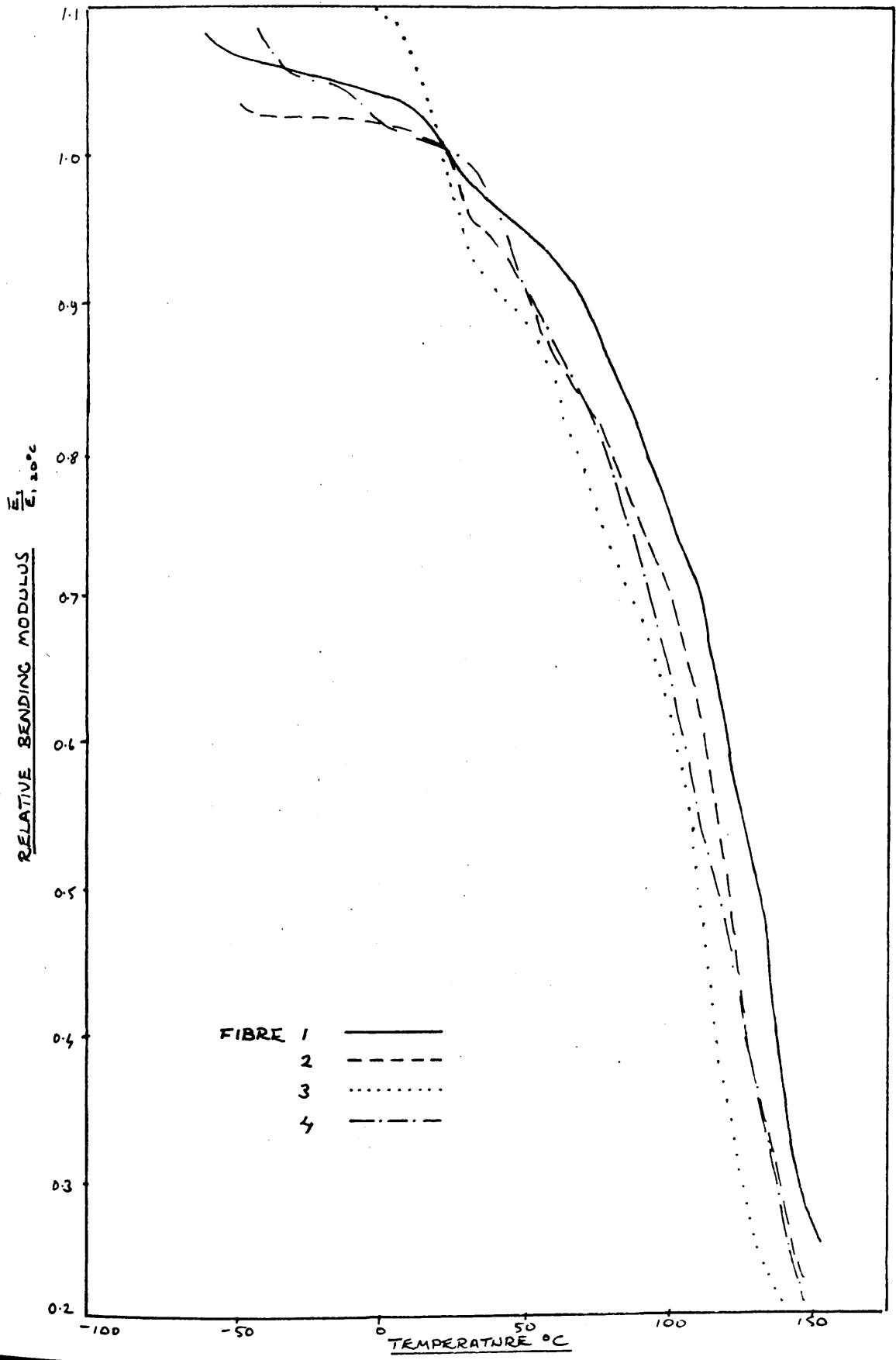
ACRILAN A

FIG. 26



ACRILAN B

FIG. 27



POLYPROPYLENE

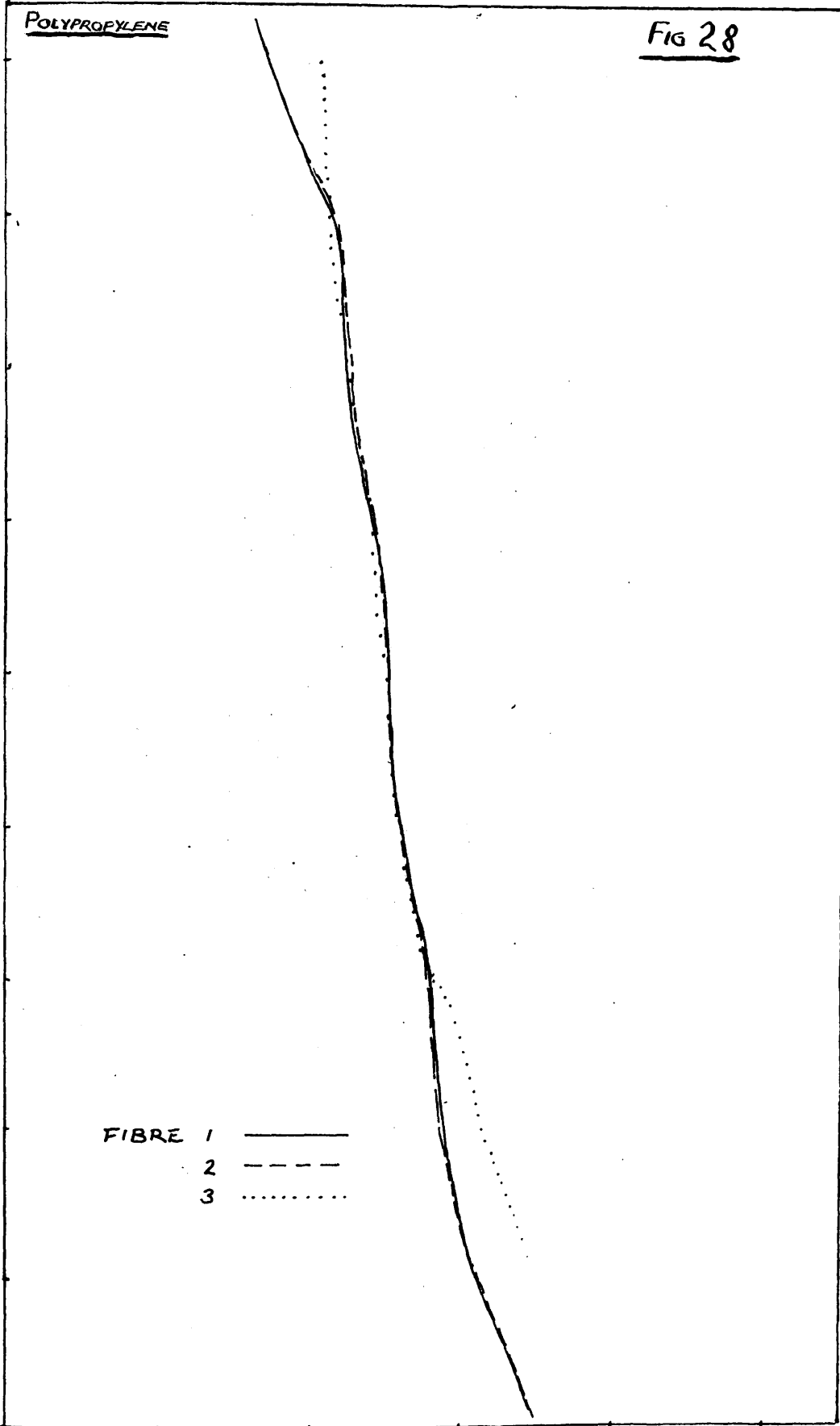
FIG 28

$\frac{E'_{130^{\circ}C}}{E'_{20^{\circ}C}}$
RELATIVE BENDING MODULUS

1.3
1.2
1.1
1.0
0.9
0.8
0.7
0.6
0.5
0.4

FIBRE 1 ———
2 - - - -
3 ·····

-100 -50 0 50 100 150
TEMPERATURE °C

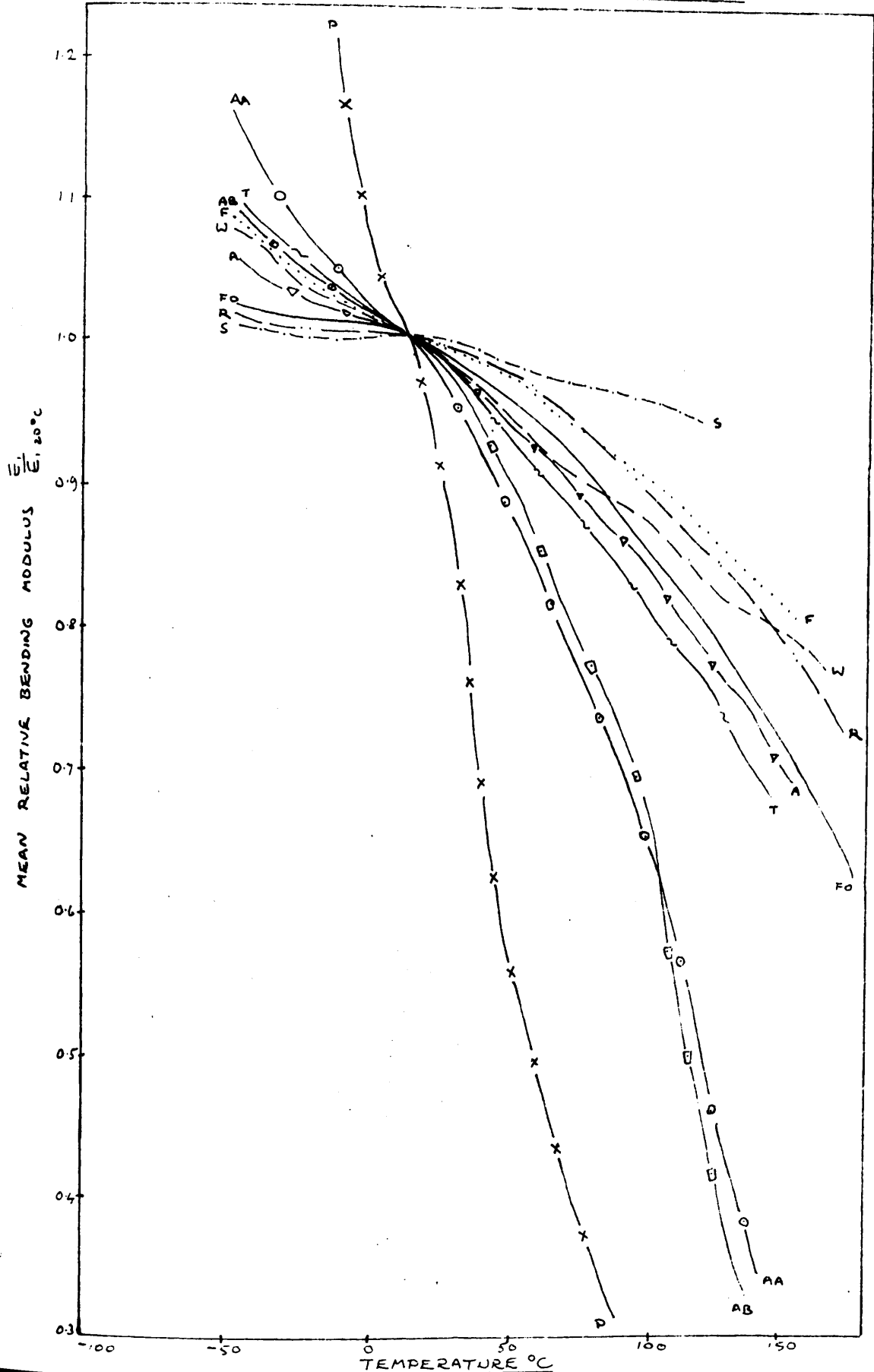


KEY TO FIG. 29

ACETATE FIBRE	A	— ▽ — ▽ —
ACRILAN A	AA	— ○ — ○ —
ACRILAN B	AB	— □ — □ —
FIBROLANE	F
FORTISAN	FO	— . — . —
POLYPROPYLENE	P	— X — X —
TRAME	R	— — — — —
SILK	S	— — — — —
TRICEL	T	— ~ — ~ —
WOOL	W.	—————

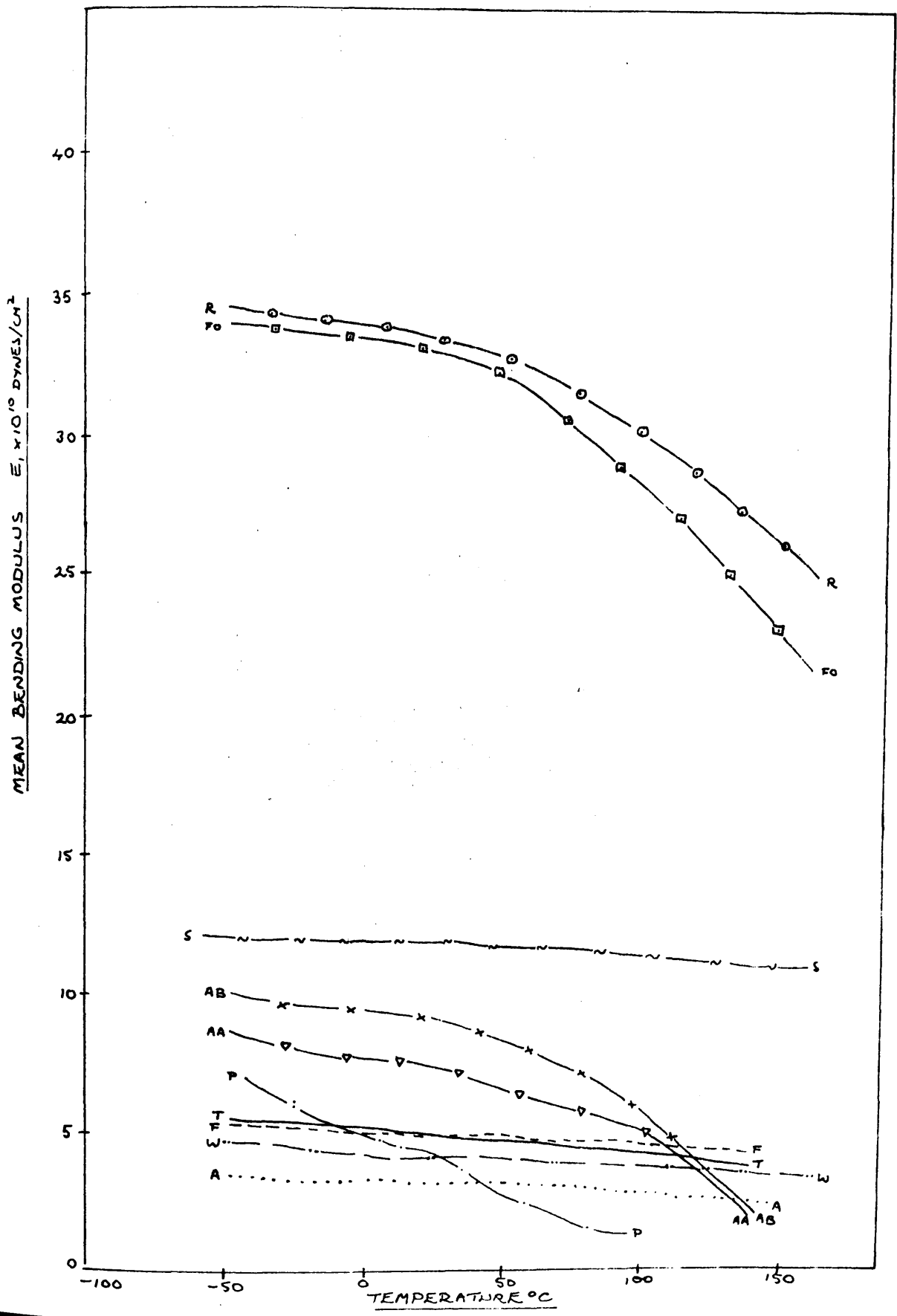
KEY TO FIG. 30

ACETATE FIBRE	A	— ▽ — ▽ —
ACRILAN A	AA	— ○ — ○ —
ACRILAN B	AB	— □ — □ —
FIBROLANE	F
FORTISAN	FO	—————
POLYPROPYLENE	P	— × — × —
RAMIE	R	— · · · —
SILK	S	— · · · · · —
TRICEL	T	— ~ — ~ —
WOOL	W	— - - - - -



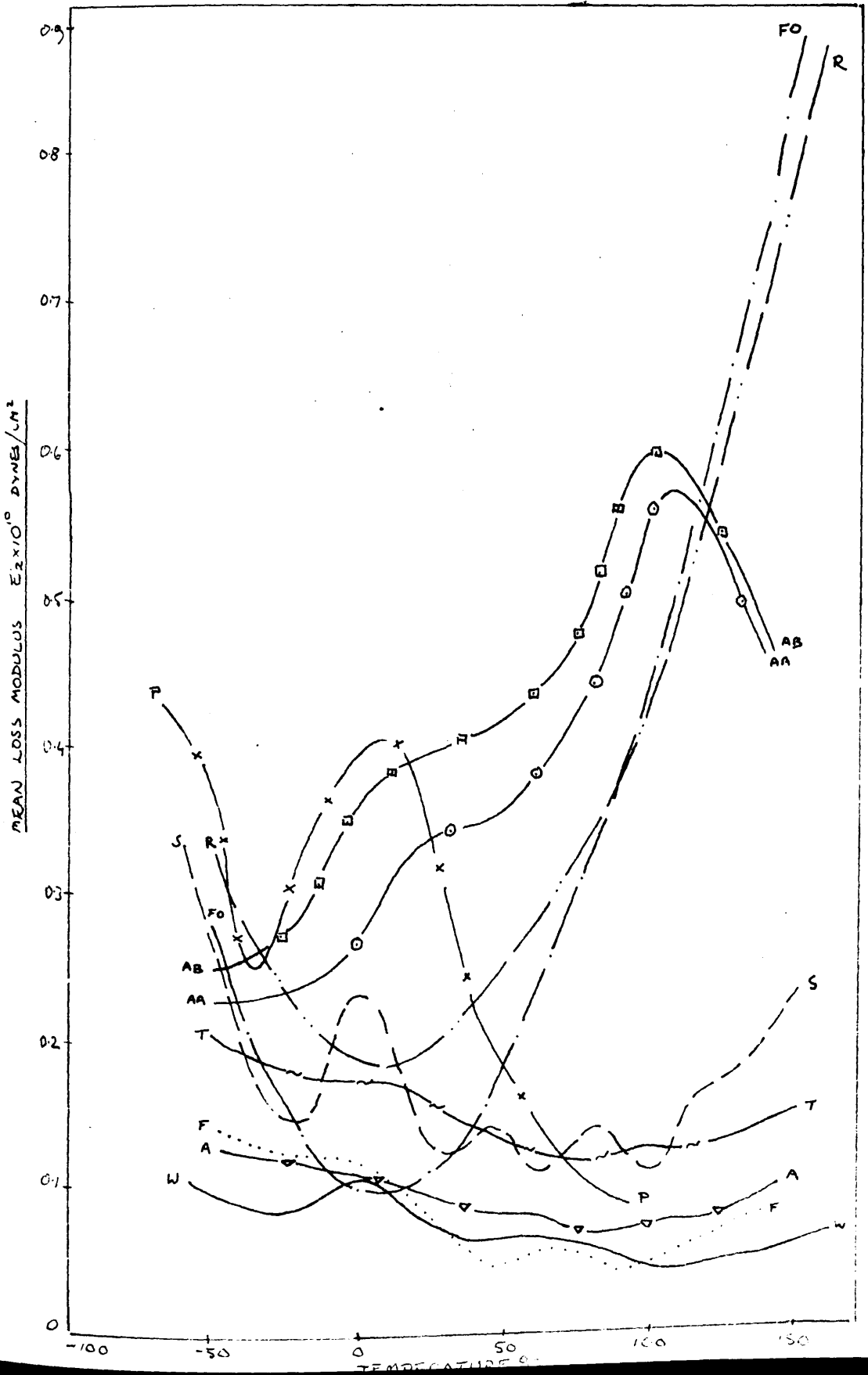
KEY TO FIG. 31

ACETATE FIBRE	A
ACRILAN A	AA	—▽—▽—▽—
ACRILAN B	AB	—x—x—x—
FIBROLAN	F	-----
FORTISAN	FO	—□—□—□—□—
POLYPROPYLENE	P	—
RAMIE	R	—○—○—○—
SILK	S	—~—~—~—
TRICEL	T	—————
WOOL	W	—



KEY TO FIG. 32

ACETATE FIBRE	A	— ▽ — ▽ —
ACRILAN A	AA	— ○ — ○ —
ACRILAN B	AB	— □ — □ —
FIBROLANE	F
FORTISAN	FO	— — — — —
POLYPROPYLENE	P	— x — x —
RAMIE	R	— — — — —
SILK	S	— — — — —
TRICEL	T	— ~ — ~ — ~ —
WOOL	W	— — — — —



Effect of Temperature on Dynamic Properties

Table 6.

WOOL. FIBRE 1.

Temperature °C	Resonant Frequency, c/s	Bending Modulus, dynes/ cm ² x 10 ¹⁰	Loss Tangent	Loss Modulus, dynes/ cm x 10 ¹⁰	Relative Bending Modulus
170	187.5	2.91	0.0204	0.0595	0.730
162	189.1	2.96	0.0172	0.0518	0.736
151	191.8	3.06	0.0161	0.0494	0.764
142	194.6	3.20	0.0136	0.0435	0.789
133	196.4	3.25	0.0131	0.0425	0.801
126	198.4	3.27	0.0120	0.0393	0.806
119	199.9	3.33	0.0109	0.0370	0.820
108	201.3	3.37	0.0087	0.0292	0.831
101	202.7	3.46	0.0092	0.0318	0.853
94	203.6	3.51	0.0112	0.0392	0.865
88	204.9	3.54	0.0124	0.0439	0.874
77	206.4	3.59	0.0124	0.0446	0.885
69	207.7	3.63	0.0129	0.0465	0.896
60	208.9	3.69	0.0142	0.0525	0.910
50	211.7	3.78	0.0147	0.0556	0.934
40	214.2	3.87	0.0140	0.0543	0.955
34	214.8	3.91	0.0159	0.0622	0.965
30	215.4	3.94	0.0172	0.0678	0.973
27	216.0	3.96	0.0172	0.0681	0.975
22	218.5	4.05	0.0183	0.0740	0.999
11	221.0	4.06	0.0222	0.0831	1.002
1/2	221.0	4.06	0.0230	0.0935	1.002
- 5	222.6	4.11	0.0210	0.0862	1.018
-16	224.5	4.20	0.0200	0.0840	1.040
-27	227.0	4.28	0.0199	0.0850	1.060
-35	228.2	4.37	0.0210	0.0919	1.080
-42	228.6	4.43	0.0223	0.0988	1.095
-55	231.1	4.47	0.0215	0.0962	1.104
-65	233.0	4.52	0.0215	0.0968	1.116

Fibre Dimensions: Length = 0.76 cm. Mass/unit length = 23.2 microgrammes/cm.

Density = 1.305 gm/cc. Shape  14.5

Shape factor (minor axis) = 1.104 ¹⁶

$$E_b \text{ at } 20^\circ\text{C} = 4.05 \times 10^{10} \text{ dynes/cm.}^2$$

Footnote: The numbers against cross-sectional shapes give the dimensions in arbitrary units for all fibres in temperature experiments.

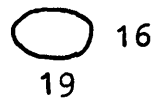
WOOL
FIBRE 2

Table 7

Temperature °C	Resonant Frequency, c/s	Bending Modulus, dynes/ cm ² x10 ¹⁰	Loss Tangent	Loss Modulus, dynes/ cm ² x10 ¹⁰	Relative Bending Modulus
170	162.7	3.37	0.0293	0.0985	0.716
166	164.7	3.44	0.0248	0.0852	0.730
154	167.15	3.53	0.0232	0.0815	0.749
151	167.7	3.54	0.0230	0.0815	0.749
146	169.4	3.65	0.0211	0.0771	0.775
138	170.4	3.70	0.0197	0.0729	0.786
128	173.3	3.78	0.0190	0.0718	0.803
116	175.7	3.92	0.0187	0.0732	0.832
113	175.9	3.97	0.0179	0.0711	0.842
105	176.3	4.01	0.0155	0.0621	0.850
97	177.8	4.04	0.0176	0.0712	0.856
88	179.3	4.09	0.0178	0.0730	0.865
79	180.3	4.16	0.0197	0.0819	0.884
69	181.6	4.21	0.0208	0.0875	0.892
61	183.2	4.28	0.0220	0.0950	0.908
52	185.0	4.35	0.0230	0.1000	0.922
38	188.1	4.49	0.0253	0.1135	0.953
32	189.2	4.59	0.0256	0.1175	0.975
22	192.6	4.69	0.0305	0.1240	0.995
16	193.3	4.72	0.0328	0.1590	1.002
10	193.8	4.74	0.0322	0.1550	1.004
4	195.8	4.80	0.0296	0.1420	1.040
-5	197.1	4.90	0.0256	0.1251	1.062
-21	199.5	4.96	0.0233	0.1152	1.064
-30	199.8	4.97	0.0212	0.1052	1.068
-36	202.4	5.10	0.0212	0.1069	1.084
-46	202.8	5.22	0.0260	0.1355	1.110
-51	203.4	5.23	0.0290	0.1514	1.112
-57	203.5	5.24	0.0314	0.1648	1.113
-63	203.5	5.24	0.0314	0.1648	1.113

Fibre Dimensions: Length = 0.92 cm. Mass/unit length = 31.8 microgrammes/cm.

Density = 1.305 gm/cc. Shape



Shape factor (minor axis) = 1.19

$$E_b \text{ at } 20^\circ\text{C} = 4.71 \times 10^{10} \text{ dynes/cm.}^2$$

WOOL
FIBRE 3

Table 8

Temperature °C	Resonant Frequency, c/s	Bending Modulus, dynes/ cm ² x 10 ¹⁰	Loss Tangent	Loss Modulus, dynes/ cm ² x 10 ¹⁰	Relative Bending Modulus
155	250.6	3.53	0.0200	0.0706	0.826
148	254.3	3.57	0.0180	0.0643	0.835
138	257.4	3.64	0.0153	0.0560	0.850
131	259.3	3.67	0.0128	0.0471	0.858
126	261.8	3.75	0.0115	0.0431	0.878
119	264.7	3.86	0.0101	0.0390	0.902
105	266.8	3.91	0.0094	0.0366	0.916
97	268.1	3.97	0.0093	0.0370	0.927
92	269.0	3.98	0.0099	0.0394	0.929
87	269.5	4.01	0.0095	0.0381	0.936
81	270.2	4.03	0.0092	0.0371	0.945
77	270.8	4.04	0.0099	0.0400	0.946
70	271.1	4.05	0.0101	0.0409	0.948
63	272.3	4.06	0.0106	0.0431	0.950
57	273.0	4.08	0.0123	0.0503	0.954
51	273.6	4.13	0.0138	0.0571	0.965
46	275.4	4.17	0.0121	0.0505	0.973
41	277.9	4.22	0.0112	0.0472	0.985
36	278.0	4.22	0.0112	0.0472	0.985
30	278.8	4.24	0.0110	0.0466	0.991
26	279.2	4.26	0.0114	0.0485	0.997
19	280.0	4.27	0.0120	0.0512	1.000
11	281.0	4.29	0.0132	0.0566	1.004
1	282.4	4.36	0.0135	0.0588	1.020
-4	284.0	4.40	0.0133	0.0585	1.030
-11	285.7	4.44	0.0128	0.0570	1.040
-18	287.3	4.44	0.0120	0.0530	1.041
-26	288.3	4.53	0.0129	0.0583	1.060
-33	289.5	4.59	0.0138	0.0634	1.075
-40	290.6	4.61	0.0148	0.0682	1.078
-46	291.7	4.64	0.0156	0.0724	1.085
-52	292.2	4.66	0.0155	0.0721	1.090
-59	293.9	4.68	0.0154	0.0721	1.095
-64	294.5	4.70	0.0158	0.0745	1.110
-69	295.6	4.70	0.0157	0.0738	1.110

Fibre Dimensions: Length = 0.70 cm. Mass/unit length = 24.2 microgrammes/cm.

Density = 1.305 gm/cc.

Shape



16

Shape factor = 1.232
(minor axis)

$$E_b \text{ at } 20^\circ\text{C} = 4.27 \times 10^{10} \text{ dynes/cm.}^2$$

WOOL
FIBRE 4

Table 9

Temperature °C	Resonant Frequency, c/s	Bending Modulus, dynes/ cm ² x10 ¹⁰	Loss Tangent	Loss Modulus, dynes/ cm ² x10 ¹⁰	Relative Bending Modulus
164	228.2	3.34	0.0221	0.0736	0.748
154	231.3	3.66	0.0181	0.0663	0.820
147	232.0	3.72	0.0165	0.0615	0.832
138	234.4	3.76	0.0146	0.0549	0.842
131	235.5	3.82	0.0137	0.0524	0.855
125	237.0	3.87	0.0135	0.0522	0.868
120	238.1	3.89	0.0126	0.0490	0.870
113	239.2	3.94	0.0125	0.0493	0.883
104	241.1	3.98	0.0123	0.0490	0.891
98	241.9	4.03	0.0117	0.0471	0.902
90	243.0	4.07	0.0148	0.0603	0.912
85	244.5	4.11	0.0164	0.0674	0.921
78	245.1	4.14	0.0183	0.0759	0.927
68	247.6	4.20	0.0191	0.0802	0.941
56	249.5	4.26	0.0204	0.0855	0.955
50	250.0	4.31	0.0232	0.0998	0.965
44	250.8	4.33	0.0166	0.0720	0.968
37	251.5	4.36	0.0149	0.0650	0.978
31	252.8	4.40	0.0147	0.0647	0.985
27	253.3	4.44	0.0179	0.0795	0.995
21	254.8	4.46	0.0196	0.0874	1.000
18	255.2	4.46	0.0204	0.0910	1.000
11	256.0	4.47	0.0228	0.1038	1.002
1	256.8	4.51	0.0246	0.1108	1.012
- 5	257.5	4.55	0.0188	0.0855	1.020
- 8	258.1	4.37	0.0172	0.0786	1.023
-14	258.1	4.37	0.0165	0.0755	1.023
-25	259.8	4.59	0.0190	0.0873	1.031
-33	260.5	4.61	0.0232	0.1070	1.033
-43	261.3	4.63	0.0242	0.1118	1.040
-51	262.8	4.69	0.0240	0.1125	1.052
-57	263.5	4.70	0.0240	0.1126	1.054
-63	265.8	4.82	0.0241	0.1168	1.080
-68	266.3	4.96	0.0241	0.1191	1.092

Fibre Dimensions: Length = 0.75 cm. Mass/unit length = 26.0 microgrammes/cm.

Density = 1.305 gm/cc. Shape  13.5

16

Shape factor (minor axis) = 1.19

E_b 20°C = 4.46 x 10¹⁰ dynes/cm.²

WOOL
FIBRE 5

Table 10.

Temperature °C	Resonant Frequency, c/s	Bending Modulus, dynes/ cm ² x 10 ¹⁰	Loss Tangent	Loss Modulus, dynes/ cm ² x 10 ¹⁰	Relative Bending Modulus
140	274.8	3.10	0.0160	0.0497	0.780
132	277.4	3.22	0.0125	0.0403	0.811
125	280.8	3.28	0.0120	0.0394	0.825
115	282.7	3.32	0.0117	0.0389	0.835
106	285.6	3.40	0.0118	0.0401	0.856
96	288.5	3.48	0.0128	0.0446	0.874
87	290.4	3.52	0.0132	0.0465	0.885
78	292.2	3.56	0.0139	0.0495	0.895
68	294.9	3.63	0.0139	0.0505	0.914
60	297.1	3.69	0.0135	0.0500	0.927
50	300.3	3.76	0.0126	0.0474	0.945
43	302.5	3.82	0.0155	0.0592	0.960
34	304.7	3.88	0.0160	0.0621	0.975
29	306.2	3.94	0.0161	0.0635	0.990
24	307.3	3.95	0.0170	0.0671	0.993
20	309.1	3.97	0.0210	0.0835	1.000
110	311.3	4.01	0.0246	0.0986	1.005
0	313.5	4.05	0.0262	0.1061	1.015
-10	313.7	4.11	0.0260	0.1075	1.030
-20	317.9	4.17	0.0258	0.1075	1.042
-30	321.5	4.30	0.0232	0.0996	1.078
-40	324.2	4.35	0.0219	0.0955	1.090
-50	325.8	4.48	0.0226	0.1012	1.111
-60	328.0	4.62	0.0232	0.1071	1.116

Fibre Dimensions: Length = 0.64 cm. Mass/unit length = 23.6 microgrammes/cm.

Density = 1.305 gm/cc. Shape  13

15

Shape factor (minor axis) = 1.23

E_b 20°C = 3.97 x 10¹⁰ dynes/cm.²

Table 11WOOLMean Values

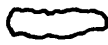
Temperature °C	Bending Modulus, $\times 10^{10}$ dynes/cm ²	Loss Modulus, $\times 10^{10}$ dynes/cm ²
160	3.29	0.0708
150	3.39	0.0631
140	3.48	0.0575
130	3.51	0.0530
120	3.59	0.0468
110	3.67	0.0431
100	3.74	0.0438
90	3.77	0.0486
80	3.82	0.0600
70	3.88	0.0661
60	3.97	0.0675
50	4.05	0.0649
40	4.10	0.0639
30	4.18	0.0690
20	4.29	0.0818
10	4.33	0.1005
0	4.38	0.1055
-10	4.43	0.0980
-20	4.48	0.0842
-30	4.54	0.0831
-40	4.56	0.0870
-50	4.61	0.0935
-60	4.67	0.1098

Table 12.

SILK. FIBRE 1

Temperature °C	Resonant Frequency, c/s	Bending Modulus, dynes/ cm ² x10 ¹⁰	Loss Tangent	Loss Modulus, dynes/ cm ² x10 ¹⁰	Relative Bending Modulus
135	117.1	10.75	0.0280	0.3015	0.893
127	117.4	11.05	0.0251	0.2781	0.919
115	118.0	11.18	0.0214	0.2391	0.930
107	118.4	11.24	0.0201	0.2256	0.935
98	118.9	11.36	0.0192	0.2180	0.944
92	119.0	11.36	0.0186	0.2110	0.944
86	119.3	11.40	0.0182	0.2076	0.948
77	119.8	11.42	0.0180	0.2060	0.951
69	120.1	11.53	0.0181	0.2090	0.956
63	120.3	11.57	0.0182	0.2110	0.958
57	120.3	11.57	0.0180	0.2085	0.958
50	120.6	11.59	0.0173	0.2010	0.960
43	120.9	11.65	0.0164	0.1911	0.970
36	121.3	11.81	0.0164	0.1939	0.982
30	121.6	11.84	0.0176	0.2086	0.985
22	122.5	11.92	0.0183	0.2184	0.992
19	123.0	12.04	0.0189	0.2280	1.004
10	123.3	12.10	0.0286	0.3462	1.010
0	122.3	12.10	0.0286	0.3462	1.010
-10	122.2	12.06	0.0295	0.3560	1.005
-20	123.3	12.10	0.0281	0.3400	1.010
-30	123.3	12.10	0.0256	0.3100	1.010
-40	123.8	12.12	0.0285	0.3461	1.012
-50	123.9	12.12	0.0292	0.3542	1.012
-60	124.1	12.20	0.0290	0.3540	1.020

Fibre Dimensions: Length = 0.44 cm. Mass/unit length = 1.1 microgrammes/cm.

Density = 1.353 gm/cc. Shape  2½
8

Shape factor (major axis) = 0.312

E_b 20°C = 12.0 x 10¹⁰ dynes/cm.²

Table 13.

SILK

FIBRE 2

Temperature °C	Resonant Frequency, c/s	Relative Bending Modulus	Loss Tangent
138	214.1	0.950	0.0122
131	214.7	0.955	0.0099
125	215.4	0.962	0.0083
119	215.9	0.965	0.0081
111	216.6	0.970	0.0072
105	217.0	0.971	0.0063
99	217.5	0.974	0.0041
95	217.7	0.977	0.0055
89	218.0	0.983	0.0057
82	218.2	0.986	0.0061
76	219.0	0.991	0.0058
67	219.3	0.995	0.0054
60	219.3	0.995	0.0050
54	219.5	0.996	0.0049
45	219.7	0.999	0.0054
37	219.7	0.999	0.0054
29	220.0	1.000	0.0054
18	220.0	1.000	0.0082
10	220.6	1.008	0.0121
0	220.9	1.010	0.0128
-12	221.2	1.020	0.0127
-22	221.2	1.020	0.0133
-30	222.4	1.025	0.0141
-40	223.0	1.027	0.0147
-50	223.0	1.027	0.0147
-57	223.2	1.039	0.0152
-62	221.2	1.020	0.0181

Table 14.

SILK
FIBRE 3.

Temperature °C	Resonant Frequency, c/s	Relative Bending Modulus	Loss Tangent
150	118.2	0.935	0.0140
140	118.6	0.943	0.0110
132	118.9	0.950	0.0098
122	119.4	0.955	0.0076
112	119.8	0.961	0.0057
104	120.1	0.970	0.0057
100	120.3	0.972	0.0057
92	120.6	0.977	0.0049
86	120.9	0.980	0.0053
76	121.4	0.990	0.0055
68	121.5	0.991	0.0056
61	121.7	0.992	0.0053
48	121.9	0.996	0.0049
39	122.0	0.998	0.0050
29	122.0	0.998	0.0050
17	122.4	1.010	0.0090
4	122.9	1.015	0.0107
- 5	123.2	1.017	0.0110
-17 $\frac{1}{2}$	123.5	1.020	0.0118
-24	123.2	1.017	0.0125
-37	123.7	1.021	0.0147
-47	124.3	1.024	0.0158
-59	124.3	1.024	0.0158

Table 15.

SILK
FIBRE 4.

Temperature °C	Resonant Frequency, c/s	Relative Bending Modulus	Loss Tangent
140	208.8	0.895	0.0245
130	211.5	0.902	0.0202
123	212.1	0.910	0.0196
113	212.8	0.912	0.0160
108	213.3	0.920	0.0157
102	214.2	0.924	0.0176
96	214.7	0.929	0.0187
89	215.3	0.942	0.0175
83	216.0	0.951	0.0174
79	216.4	0.953	0.0165
74	216.8	0.957	0.0159
70	217.4	0.964	0.0158
65	218.0	0.970	0.0168
60	218.8	0.980	0.0177
55	219.3	0.985	0.0181
50	220.2	0.990	0.0195
44	220.5	0.995	0.0192
37	221.1	0.998	0.0175
31	221.5	0.999	0.0167
22	221.7	0.999	0.0161
16	222.0	1.002	0.0170
7	222.6	1.007	0.0197
0	223.0	1.010	0.0198
- 8	222.7	1.009	0.0205
-18	222.7	1.009	0.0215
-28	223.0	1.010	0.0215
-34	223.0	1.010	0.0220
-44	223.8	1.024	0.0225
-54	223.8	1.024	0.0228

Table 16.

SILK
FIBRE 5.

Temperature °C	Resonant Frequency, c/s	Relative Bending Modulus	Loss Tangent
152	114.4	0.930	0.0223
147	114.7	0.932	0.0216
140	114.9	0.934	0.0202
130	115.5	0.940	0.0176
125	115.7	0.945	0.0163
115	116.4	0.957	0.0159
106	116.9	0.962	0.0161
98	117.2	0.972	0.0164
90	117.6	0.978	0.0158
81	117.7	0.979	0.0155
72	118.0	0.982	0.0158
65	118.2	0.990	0.0162
58	118.4	0.992	0.0170
51	118.5	0.994	0.0170
42	118.6	0.996	0.0176
34	119.0	0.998	0.0183
26	119.1	0.999	0.0189
16	119.2	1.000	0.0206
8	120.0	1.004	0.0212
5	120.2	1.008	0.0232
- 5	120.4	1.012	0.0274
-15	120.6	1.015	0.0287
-25	120.8	1.020	0.0298
-35	120.8	1.020	0.0314
-45	121.0	1.024	0.0385
-60	121.0	1.024	0.0385

Table 17.

SILK
FIBRE 6.

Temperature °C	Resonant Frequency, c/s	Relative Bending Modulus	Loss Tangent
134	135.6	0.910	0.0184
128	134.8	0.912	0.0175
119	135.0	0.914	0.0145
109	135.9	0.924	0.0129
102	136.7	0.939	0.0112
94	137.1	0.948	0.0111
86	137.3	0.950	0.0117
81	137.6	0.952	0.0110
75	137.9	0.954	0.0101
67	138.2	0.960	0.0096
60	138.5	0.962	0.0088
50	138.9	0.970	0.0100
43	139.3	0.975	0.0102
36	139.6	0.980	0.0101
30	139.7	0.982	0.0100
24	140.1	0.990	0.0100
17	141.3	1.002	0.0132
8	141.7	1.004	0.0148
0	141.9	1.006	0.0156
-10	142.0	1.008	0.0156
-20	142.0	1.008	0.0162
-30	142.2	1.010	0.0169
-40	142.4	1.012	0.0175
-50	142.7	1.015	0.0186
-60	144.0	1.040	0.0191

Table 17A

SILK
FIBRE 7

Bending Modulus_{20°C} only.

Fibre Dimensions:

Mass/unit length = 1.54 microgrammes/cm. Shape  3½
Shape factor = 0.439 DENSITY = 1.353 GM./CC. 8
(major axis)

Length, cm.	Resonant frequency, c/s (major axis)	$E_b \times 10^{10}$ dynes/cm. ²
0.49	138.7	11.9
0.38	229.8	12.0
0.30	363.0	11.7

Table 18SILKMean Values

Temperature °C	Bending Modulus, $\times 10^{10}$ dynes/cm ²	Loss Modulus, $\times 10^{10}$ dynes/cm ²
150	10.82	0.2332
140	10.93	0.2051
130	11.08	0.1829
120	11.16	0.1692
110	11.30	0.1520
100	11.41	0.1162
90	11.48	0.1295
80	11.60	0.1450
70	11.65	0.1311
60	11.71	0.1079
50	11.78	0.1360
40	11.86	0.1400
30	11.92	0.1242
20	11.95	0.1591
10	11.99	0.2034
0	12.09	0.2320
-10	12.10	0.2005
-20	12.11	0.1521
-30	12.13	0.1560
-40	12.16	0.2486
-50	12.19	0.2905
-60	12.27	0.3380

Table 19

FIBROLANE. FIBRE 1

Temperature °C	Resonant Frequency,	Bending Modulus, dynes/ cm ² x10 ¹⁰	Loss Tangent	Loss Modulus, dynes/ cm ² x10 ¹⁰	Relative Bending Modulus
150	262.5	4.02	0.0233	0.0940	0.795
143	270.8	4.24	0.0232	0.0980	0.839
138	272.8	4.27	0.0215	0.0916	0.846
130	276.0	4.42	0.0203	0.0896	0.874
122	276.6	4.44	0.0196	0.0870	0.876
111	279.85	4.52	0.0136	0.0615	0.895
103	282.85	4.61	0.0129	0.0595	0.914
95	283.8	4.65	0.0120	0.0559	0.922
87	286.8	4.73	0.0111	0.0526	0.935
80	287.7	4.76	0.0119	0.0567	0.943
74	288.7	4.80	0.0136	0.0654	0.950
67	289.6	4.85	0.0121	0.0586	0.960
58	290.3	4.89	0.0112	0.0548	0.969
50	292.6	4.95	0.0127	0.0679	0.980
42	293.2	4.98	0.0132	0.0658	0.985
32	294.8	5.01	0.0140	0.0701	0.992
27	295.3	5.05	0.0146	0.0736	1.000
19	295.5	5.07	0.0260	0.1320	1.004
8	296.6	5.08	0.0304	0.1541	1.007
-2	297.7	5.09	0.0303	0.1541	1.008
-13	298.8	5.10	0.0302	0.1531	1.010
-23	299.4	5.10	0.0295	0.1502	1.012
-36	300.5	5.17	0.0273	0.1410	1.025
-46	305.5	5.31	0.0287	0.1540	1.052
-56	307.1	5.42	0.0311	0.1685	1.072

Fibre Dimensions: Length = 0.47 cm. Mass/unit length = 5.6 microgrammes/cm.

Density = 1.29 gm/cc. Shape CIRCULAR

Shape factor = 1

$$E_b \text{ at } 20^\circ\text{C} = 5.05 \times 10^{10} \text{ dynes/cm.}^2$$

FIBROLANE
FIBRE 2

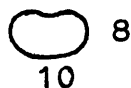
Table 20.

Temperature °C	Resonant Frequency,	Bending Modulus, dynes/ cm ² x10 ¹⁰	Loss Tangent	Loss Modulus, dynes/ cm ² x10 ¹⁰	Relative Bending Modulus
139	126.6	4.00	0.0205	0.0820	0.824
129	128.0	4.04	0.0153	0.0619	0.832
119	129.7	4.21	0.0133	0.0560	0.866
109	130.8	4.26	0.0119	0.0517	0.876
101	131.5	4.33	0.0110	0.0476	0.890
93	132.5	4.39	0.0109	0.0486	0.904
85	133.9	4.44	0.0120	0.0534	0.916
75	134.6	4.52	0.0126	0.0569	0.931
65	135.8	4.59	0.0119	0.0546	0.945
57	136.3	4.64	0.0106	0.0492	0.955
48	137.3	4.70	0.0099	0.0466	0.969
38	138.2	4.78	0.0099	0.0474	0.984
30	138.9	4.84	0.0104	0.0504	0.996
21	139.2	4.86	0.0134	0.0651	1.000
12	139.4	4.87	0.0183	0.0910	1.002
0	141.8	4.95	0.0215	0.1062	1.020
+10	143.5	5.05	0.0237	0.1193	1.042
-20	144.4	5.20	0.0236	0.1225	1.070
-30	145.3	5.28	0.0246	0.1300	1.090
-40	146.0	5.34	0.0269	0.1435	1.100
-50	147.3	5.44	0.0277	0.1505	1.120

Fibre Dimensions: Length = 0.67 cm. Mass/unit length = 6.7 microgrammes/ cm.

Density = 1.29 gm/cc.

Shape



Shape factor (minor axis) = 1.25

$$E_b \text{ at } 20^\circ\text{C} = 4.86 \times 10^{10} \text{ dynes/cm.}^2$$

Table 21

FIBROLANE
FIBRE 3

Temperature °C	Resonant Frequency, c/s	Bending Modulus, dynes/ cm ² x 10 ¹⁰	Loss Tangent	Loss Modulus, dynes/ cm ² x 10 ¹⁰	Relative Bending Modulus
106	127.2	4.40	0.0120	0.0528	0.895
99	128.6	4.53	0.0100	0.0453	0.921
90	129.6	4.57	0.0092	0.0421	0.932
80	131.0	4.69	0.0091	0.0429	0.955
70	131.5	4.74	0.0092	0.0438	0.965
62	132.4	4.79	0.0096	0.0463	0.975
52	132.9	4.83	0.0120	0.0580	0.983
44	133.8	4.86	0.0089	0.0435	0.990
37	134.1	4.90	0.0089	0.0435	0.998
29	134.4	4.91	0.0090	0.4460	1.000
20	134.4	4.91	0.0132	0.0648	1.000
9	134.9	4.92	0.0168	0.0826	1.002
0	135.2	4.95	0.0194	0.0560	1.010
-10	136.2	5.06	0.0200	0.1012	1.032
-21	137.2	5.12	0.0203	0.1080	1.044
-30	137.9	5.18	0.0210	0.1090	1.058
-41	138.3	5.21	0.0209	0.1085	1.062
-51	139.3	5.26	0.0210	0.1100	1.075

Dimensions of fibre unavailable.

frequency, = 134.4

frequency₂ = 172.6

Table 21A

FIBROLANE
FIBRE 4. Bending Modulus 20°C only.

Fibre Dimensions: Length = 0.56 cm. Mass/unit length = 6.32
microgrammes/cm.

Density = 1.29 gm/cc. Shape $\overset{8}{\circ} 9$

Shape factor = 1.125 Resonant frequency = 213.5 c/s.
(minor axis) (minor axis)

$$E_b = 5.33 \times 10^{10} \text{ dynes/cm.}^2$$

Table 21B

FIBROLANE
FIBRE 5. Bending Modulus 20°C only

Fibre Dimensions: Length = 0.58 cm. Mass/unit length = 4.70
microgrammes/cm.

Density = 1.29 gm/cc. Shape $\overset{6\frac{1}{2}}{\circ} 7$

Shape factor (major axis)₁ = 0.955

Shape factor (minor axis)₂ = 1.075

Resonant frequency₁ = 164.4 E_b ₁ = 4.65×10^{10} dynes/cm.²

Resonant frequency₂ = 172.6 E_b ₂ = 4.42×10^{10} dynes/cm.²

Table 22.

FIBROLANE

Mean Values

<u>Temperature</u> °C	<u>Bending Modulus,</u> x 10 ¹⁰ dynes/cm. ²	<u>Loss Modulus,</u> x 10 ¹⁰ dynes/cm. ²
140	4.04	0.0889
130	4.15	0.0781
120	4.26	0.0684
110	4.34	0.0600
100	4.43	0.0512
90	4.52	0.0466
80	4.57	0.0491
70	4.63	0.0541
60	4.71	0.0518
50	4.78	0.0483
40	4.83	0.0512
30	4.87	0.0662
20	4.91	0.0845
10	4.94	0.1064
0	4.97	0.1198
-10	5.04	0.1221
-20	5.10	0.1234
-30	5.18	0.1247
-40	5.22	0.1317
-50	5.31	0.1405

Table 23.

RAMIE. FIBRE 1.

Temperature °C	Resonant Frequency, c/s	Relative Bending Modulus	Loss Tangent
172	267.7	0.700	0.0450
164	272.4	0.723	0.0436
154	279.3	0.760	0.0384
143	287.4	0.805	0.0363
132	290.9	0.828	0.0298
122	294.5	0.846	0.0272
113	298.5	0.874	0.0240
101	301.0	0.888	0.0221
92	302.9	0.898	0.0182
82	305.7	0.910	0.0153
71	308.5	0.930	0.0133
60	313.3	0.960	0.0124
42	318.1	0.990	0.0108
34	319.5	0.997	0.0103
24	320.0	1.000	0.0105
13	321.5	1.003	0.0108
5	322.0	1.005	0.0110
-5	322.0	1.005	0.0111
-24	323.6	1.012	0.0120
-35	324.7	1.024	0.0130
-45	325.2	1.030	0.0132
-55	325.9	1.032	0.0145
-65	326.0	1.032	0.0150

Table 24.

RAMIE

FIBRE 2

Temperature °C	Resonant Frequency, c/s.	Relative Bending Modulus	Loss Tangent
170	285.0	0.745	0.0295
154	290.9	0.780	0.0281
147	293.4	0.801	0.0216
138	297.9	0.820	0.0201
128	302.5	0.839	0.0159
120	307.1	0.866	0.0128
111	310.5	0.886	0.0106
98	313.5	0.896	0.0086
86	317.4	0.926	0.0066
72	321.4	0.950	0.0047
56	324.5	0.966	0.0028
43	326.8	0.988	0.0027
30	329.0	0.995	0.0027
25	329.9	0.998	0.0027
20	330.2	1.000	0.0036
11	331.0	1.002	0.0026
0	331.5	1.004	0.0027
- 8	332.2	1.010	0.0033
-18	332.5	1.012	0.0040
-28	333.0	1.014	0.0042
-35	333.3	1.017	0.0054
-45	333.3	1.017	0.0053
-55	333.6	1.020	0.0072
-65	333.8	1.021	0.0074

RAMIE
FIBRE 3.

Table 24A

Bending Modulus_{20°C} only.

Length = 0.68 cm. Mass/unit length = 3.1 microgrammes / cm.

Density = 1.553 gm/cc. Shape  4.02

Shape factor (major axis)₁ = 0.574

Shape factor (minor axis)₂ = 1.750

Resonant frequency₁ = 180.0 c/s.

Resonant frequency₂ = 362.0 c/s.

$$E_{b1} = 34.0 \times 10^{10} \text{ dynes/cm.}^2$$

$$E_{b2} = 27.5 \times 10^{10} \text{ dynes/cm.}^2$$

RAMIE

Table 24B

FIBRE 4. Bending Modulus_{20°C} and Loss Tangent_{20°C} only.

Length = 0.93 cm. Mass/unit length = 11.05 microgrammes / cm.

Density = 1.553 gm/cc. Shape  5.5
10.0

Shape factor (major axis)₁ = 0.55

Shape factor (minor axis)₂ = 1.82

Resonant frequency₁ = 253.5 c/s

Resonant frequency₂ = 318 c/s.

$$E_{b1} = 36.5 \times 10^{10} \text{ dynes/cm.}^2$$

$$E_{b2} = 75.6 \times 10^{10} \text{ dynes/cm.}^2$$

$$\text{Loss Tangent}_1 = 0.0075$$

$$\text{Loss Tangent}_2 = 0.0076$$

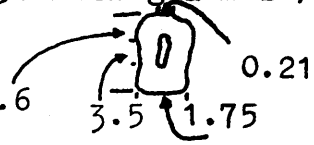
RAMIE

Table 24C

FIBRE 5.

Bending Modulus_{20°C} only

Length = 1.06 cm. Mass/unit length = 11.50 microgrammes / cm.

Density = 1.553 gm/cc. Shape  0.21

Shape factor (major axis) = 0.31

Resonant frequency (major axis) = 114.0 c/s.

$$E_{b20°C} = 44.3 \times 10^{10} \text{ dynes/cm.}^2$$

Table 25

RAMIS

Mean Values

Temperature °C	Bending Modulus $\times 10^{10}$ dynes/cm. ²	Loss Modulus $\times 10^{10}$ dynes/cm. ²
160	25.30	0.8850
150	25.92	0.7951
140	26.72	0.7030
130	27.55	0.6238
120	28.25	0.5600
110	29.04	0.4882
100	29.90	0.4335
90	30.51	0.3845
80	31.12	0.3434
70	31.82	0.3091
60	32.35	0.2799
50	32.80	0.2785
40	33.10	0.2310
30	33.36	0.2200
20	33.70	0.1851
10	33.78	0.1900
0	33.90	0.1910
-10	34.08	0.2080
-20	34.20	0.2248
-30	34.35	0.2580
-40	34.40	0.2908
-50	34.50	0.3380

Table 27.

FORTISAN
FIBRE 2.

Temperature °C	Resonant Frequency, c/s	Relative Bending Modulus	Loss Tangent
162	195.1	0.665	0.0510
145	206.6	0.741	0.0381
130	213.6	0.796	0.0341
114	220.5	0.846	0.0218
104	225.3	0.883	0.0160
89	228.1	0.904	0.0115
71	231.8	0.938	0.0065
58	233.5	0.950	0.0058
48	235.4	0.962	0.0048
39	236.1	0.969	0.0040
30	237.0	0.978	0.0048
25	238.0	0.985	0.0048
19	240.6	1.002	0.0039
6	241.0	1.009	0.0031
- 6	241.5	1.006	0.0047
-15	241.9	1.008	0.0047
-27	242.3	1.010	0.0055
-33	242.7	1.013	0.0054
-40	242.9	1.015	0.0070
-53	243.0	1.018	0.0078
-61	243.0	1.018	0.0069
-65	244.0	1.025	0.0090

Frequency₁ = 176.6 c/s.

Frequency₂ = 148.2 c/s.

$k = 27.8 \times 10^{10}$ dynes/cm²

Table 27A

FORTISAN

FIBRE 3. Bending Modulus_{20°C} and Loss Tangent_{20°C} only.

Length = 0.80 cm. Mass/unit length = 1.50 microgrammes/cm.

Density = 1.52 gm/cc. Shape  1.47

Shape factor (minor axis) = 1.47

Resonant frequency (minor axis) = 133.2 c/s.

$$E_b = 30.3 \times 10^{10} \text{ dynes/cm.}^2$$

$$\text{Loss Tangent} = 0.0101$$

Table 27B

FORTISAN

FIBRE 4.

Bending Modulus_{20°C} only.

Length = 0.76 cm. Mass/unit length = 1.80 microgrammes/cm.

Density = 1.52 gm/cc. Shape  6

Shape factor (major axis)₁ = 0.856

Shape factor (minor axis)₂ = 1.160

Resonant frequency₁ = 136.6 c/s.

Resonant frequency₂ = 148.2 c/s

$$E_{b1} = 37.0 \times 10^{10} \text{ dynes/cm.}^2$$

$$E_{b2} = 33.0 \times 10^{10} \text{ dynes/cm.}^2$$

Table 28FORTISANMean Values

Temperature °C	Bending Modulus, $\times 10^{10}$ dynes/cm ²	Loss Modulus, $\times 10^{10}$ dynes/cm ²
160	21.91	1.0290
150	23.02	0.8810
140	24.18	0.7649
130	25.29	0.6709
120	26.31	0.5878
110	27.20	0.5161
100	28.21	0.4515
90	29.08	0.3900
80	29.84	0.3308
70	30.61	0.2790
60	31.40	0.2260
50	32.08	0.1681
40	32.43	0.1510
30	32.80	0.1208
20	33.20	0.1080
10	33.39	0.1080
0	33.45	0.1090
-10	33.60	0.1148
-20	33.67	0.1392
-30	33.72	0.1763
-40	33.77	0.2210
-50	33.81	0.2705

Table 29

ACETATE FIBRE. FIBRE 1.

Temperature °C	Resonant Frequency, c/s	Bending Modulus, dynes/ cm ² x10 ¹⁰	Loss Tangent	Loss Modulus, dynes/ cm ² x10 ¹⁰	Relative Bending Modulus
141	237.0	2.39	0.0445	0.1065	0.704
132	242.8	2.48	0.0359	0.0891	0.732
123	247.2	2.59	0.0348	0.0900	0.765
112	251.5	2.68	0.0328	0.0878	0.790
100	261.1	2.81	0.0303	0.0853	0.828
90	261.8	2.91	0.0276	0.0804	0.855
78	263.8	2.97	0.0246	0.0730	0.874
69	266.7	3.03	0.0208	0.0630	0.892
59	269.2	3.09	0.0232	0.0717	0.910
49	272.5	3.17	0.0237	0.0750	0.930
39	276.5	3.29	0.0271	0.0892	0.960
29	279.0	3.32	0.0315	0.1045	0.976
23	280.7	3.36	0.0317	0.1061	0.990
20	282.6	3.39	0.0320	0.1085	1.000
4	285.5	3.46	0.0336	0.1160	1.020
-4	287.3	3.50	0.0340	0.1190	1.030
-14	290.6	3.51	0.0352	0.1232	1.052
-25	292.8	3.61	0.0352	0.1269	1.064

Fibre Dimensions: Length = 0.53 cm. Mass/unit length = 7.6 microgrammes/cm.

Density = 1.330 gm/cc.

Shape



Shape factor = 1.57

$$E_b \text{ at } 20^\circ\text{C} = 3.39 \times 10^{10} \text{ dynes/cm.}^2$$

Table 30.ACETATE FIBRE
FIBRE 2.

Temperature °C	Resonant Frequency, c/s	Relative Bending Modulus	Loss Tangent
145	211.5	0.680	0.0449
138	216.0	0.713	0.0402
128	220.7	0.740	0.0302
119	225.0	0.769	0.0278
109	227.9	0.796	0.0260
103	229.3	0.803	0.0247
99	231.2	0.815	0.0240
91	233.1	0.833	0.0228
84	235.7	0.846	0.0225
78	236.8	0.859	0.0227
71	239.2	0.875	0.0240
65	243.5	0.906	0.0257
54	245.9	0.924	0.0261
47	246.9	0.930	0.0256
39	247.7	0.940	0.0269
30	251.7	0.966	0.0277
25	253.5	0.984	0.0280
20	256.2	1.000	0.0282
10	257.5	1.004	0.0320
2	258.9	1.017	0.0342
-10	260.7	1.038	0.0340
-20	261.8	1.042	0.0355
-30	262.2	1.045	0.0376
-40	262.9	1.048	0.0378
-50	264.0	1.062	0.0380
-60	266.0	1.090	0.0380

Table 31

ACETATE FIBRE
FIBRE 3.

Temperature °C	Resonant Frequency, c/s	Relative Bending Modulus	Loss Tangent
134	114.0	0.849	0.0400
123	115.5	0.866	0.0296
116	116.7	0.885	0.0280
108	117.3	0.900	0.0264
100	118.1	0.914	0.0256
91	119.3	0.930	0.0246
84	119.8	0.945	0.0236
76	120.2	0.950	0.0232
68	120.4	0.952	0.0239
60	120.6	0.954	0.0257
51	121.3	0.965	0.0263
41	121.6	0.970	0.0272
31	122.6	0.982	0.0273
24	123.2	0.995	0.0273
15	124.4	1.004	0.0277
6	125.0	1.014	0.0286
-3	125.6	1.023	0.0285
-12	125.6	1.023	0.0302
-22	125.9	1.025	0.0308
-32	126.3	1.042	0.0308
-41	127.1	1.058	0.0317
-51	127.4	1.062	0.0317

Table 32

ACETATE FIBRE
FIBRE 4.

Temperature °C	Resonant Frequency, c/s	Relative Bending Modulus	Loss Tangent
140	128.6	0.690	0.0400
131	132.2	0.730	0.0342
118	135.2	0.763	0.0302
107	137.6	0.793	0.0281
99	143.0	0.855	0.0256
91	145.2	0.879	0.0252
81	146.3	0.898	0.0271
73	147.7	0.912	0.0275
63	150.6	0.940	0.0278
52	151.7	0.961	0.0278
42	152.9	0.975	0.0280
32	154.2	0.995	0.0292
25	154.8	0.997	0.0304
17	155.0	1.000	0.0317
8	155.4	1.004	0.0328
-2	155.8	1.009	0.0340
-12	156.2	1.021	0.0358
-22	157.5	1.032	0.0360
-32	158.6	1.042	0.0370
-42	159.0	1.045	0.0372
-52	161.0	1.071	0.0373

Bending Modulus only

$\rho = 0.85$ gm. Mass/unit length = 6.7 microgrammes/c

$\rho = 1.330$ gm/cc. Shape

□ 10

d (minor axis) = 1.45

ACETATE FIBRE
FIBRE 5.

Table 32A

Bending Modulus_{20°C} only

Length = 0.48 cm. Mass/unit length = 5.7 microgrammes/cm.

Density = 1.330 gm/cc.

Shape

 10
5

Shape factor (major axis)₁ = 0.50

Shape factor (minor axis)₂ = 2.00

Resonant frequency₁ = 164.0 c/s

Resonant frequency₂ = 330.0 c/s.

$$E_{b1} = 3.42 \times 10^{10} \text{ dynes/cm.}^2$$

$$E_{b2} = 3.40 \times 10^{10} \text{ dynes/cm.}^2$$

ACETATE FIBRE
FIBRE 6.

Table 32B

Bending Modulus_{20°C} only

Length = 0.54 cm. Mass/unit length = 6.08 microgrammes/cm.

Density = 1.330 gm/cc.

Shape

6  12

Shape factor (major axis)₁ = 0.50

Shape factor (minor axis)₂ = 2.00

Resonant frequency₁ = 127.1 c/s.

Resonant frequency = 252.6 c/s

$$E_{b1} = 2.94 \times 10^{10} \text{ dynes/cm.}^2$$

$$E_{b2} = 2.98 \times 10^{10} \text{ dynes/cm.}^2$$

ACETATE FIBRE
FIBRE 7.

Table 32C

Bending Modulus_{20°C} only

Length = 0.53 cm. Mass/unit length = 6.7 microgrammes/cm.

Density = 1.330 gm/cc.

Shape

 10
7

Shape factor (minor axis) = 1.43

Resonant frequency (minor axis) = 269.0 c/s.

$$E_b = 3.98 \times 10^{10} \text{ dynes/cm.}^2$$

Table 33ACETATE FIBREMean Values

Temperature °C	Bending Modulus, $\times 10^{10}$ dynes/cm ²	Loss Modulus, $\times 10^{10}$ dynes/cm ²
145	2.35	0.1074
140	2.38	0.1020
130	2.48	0.0920
120	2.58	0.0834
110	2.69	0.0789
100	2.76	0.0750
90	2.84	0.0708
80	2.97	0.0680
70	3.02	0.0692
60	3.08	0.0802
50	3.14	0.0831
40	3.22	0.0864
30	3.29	0.0900
20	3.36	0.0975
10	3.39	0.1062
0	3.42	0.1104
-10	3.44	0.1152
-20	3.46	0.1195
-30	3.49	0.1219
-40	3.52	0.1240
-50	3.56	0.1263

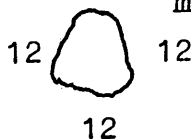
Table 34.

<u>TRICEL</u>	<u>FIBRE 1</u>				
Temperature °C	Resonant Frequency, c/s	Bending Modulus, dynes/ cm ² x10 ¹⁰	Loss Tangent	Loss Modulus, dynes/ cm ² x10 ¹⁰	Relative Bending Modulus
145	124.8	3.10	0.0500	0.1550	0.635
135	129.6	3.32	0.0444	0.1472	0.680
127	133.9	3.57	0.0405	0.1445	0.730
117	136.0	3.70	0.0376	0.1389	0.756
107	138.5	3.83	0.0361	0.1388	0.783
97	140.6	3.93	0.0335	0.1312	0.803
87	143.3	4.09	0.0283	0.1155	0.836
79	144.8	4.17	0.0258	0.1075	0.853
68	145.7	4.31	0.0268	0.1152	0.881
57	149.0	4.41	0.0270	0.1190	0.902
47	150.7	4.50	0.0314	0.1411	0.920
37	152.0	4.60	0.0330	0.1516	0.940
29	153.3	4.69	0.0332	0.1558	0.958
20	157.1	4.90	0.0328	0.1605	1.000
10	158.7	4.98	0.0328	0.1630	1.020
- 1	159.1	5.00	0.0328	0.1640	1.025
-11	160.0	5.07	0.0331	0.1680	1.040
-20	161.0	5.07	0.0336	0.1702	1.040
-30	161.5	5.12	0.0352	0.1800	1.050
-40	163.0	5.25	0.0357	0.1875	1.075
-50	163.8	5.28	0.0385	0.2038	1.081
-60	164.9	5.36	0.0403	0.2160	1.098

Fibre Dimensions: Length = 0.83 cm. Mass/unit length = 13.2 microgrammes/cm.

Density = 1.30 gm/cc.

Shape



Shape factor = 1.2

$$E_b \text{ at } 20^\circ\text{C} = 4.9 \times 10^{10} \text{ dynes/cm.}^2$$

Table 35

TRICEL
FIBRE 2.

Temperature °C	Resonant Frequency, c/s	Bending Modulus, dynes/ cm ² x 10 ¹⁰	Loss Tangent	Loss Modulus, dynes/ cm ² x 10 ¹⁰	Relative Bending Modulus
138	116.8	3.31	0.0402	0.1330	0.736
128	118.6	3.45	0.0367	0.1263	0.765
118	121.1	3.61	0.0320	0.1153	0.800
110	123.3	3.68	0.0291	0.1070	0.815
100	124.5	3.80	0.0262	0.0998	0.844
91	126.0	3.88	0.0246	0.0954	0.861
81	128.2	4.04	0.0242	0.0976	0.896
73	129.4	4.10	0.0238	0.0975	0.910
63	130.6	4.15	0.0232	0.0963	0.920
57	131.8	4.26	0.0247	0.1050	0.946
47	133.1	4.35	0.0247	0.1072	0.965
37	134.6	4.44	0.0250	0.1108	0.985
30	135.2	4.49	0.0262	0.1178	0.996
20	136.0	4.50	0.0274	0.1230	1.000
10	136.6	4.52	0.0308	0.1390	1.005
0	142.2	4.54	0.0317	0.1438	1.009
-11	143.7	4.55	0.0327	0.1488	1.010
-20	144.9	4.56	0.0341	0.1555	1.013
-30	145.8	4.57	0.0350	0.1600	1.015
-40	146.8	4.58	0.0476	0.2170	1.017
-50	148.9	4.59	0.0471	0.2200	1.020

Fibre Dimensions: Length = 0.735 cm. Mass/unit length = 15.0 microgrammes/cm.

Density = 1.30 gm/cc. Shape  9

17

Shape factor (major axis) = 1.88

E_b 20°C = 4.50 x 10¹⁰ dynes/cm².

Table 36.

TRICEL
FIBRE 3.

Temperature °C	Resonant Frequency, c/s	Relative Bending Modulus	Loss Tangent
140	137.0	0.653	0.0506
132	140.6	0.688	0.0465
120	145.1	0.730	0.0380
106	150.2	0.785	0.0347
98	152.0	0.800	0.0340
90	153.2	0.820	0.0322
78	157.8	0.864	0.0274
63	162.4	0.911	0.0272
51	163.9	0.933	0.0284
41	166.5	0.964	0.0312
31	169.5	0.997	0.0314
21	169.9	1.000	0.0350
10	171.4	1.016	0.0378
0	173.2	1.035	0.0398
-10	175.0	1.052	0.0398
-21	176.7	1.070	0.0396
-30	177.6	1.082	0.0392
-40	178.5	1.100	0.0390
-50	181.0	1.120	0.0405
-58	181.5	1.124	0.0418

Table 37A

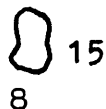
TRICEL
FIBRE 5.

Bending Modulus_{20°C} only

Length = 0.62 cm. Mass/unit length = 12.2 microgrammes /cm.

Density = 1.30 gm/cc.

Shape



Shape factor (major axis)₁ = 0.58

Shape factor (minor axis)₂ = 1.88

Resonant frequency₁ = 183.0 c/s

Resonant frequency₂ = 358.2 c/s

$$E_{b1} = 5.0 \times 10^{10} \text{ dynes/cm.}^2$$

$$E_{b2} = 5.5 \times 10^{10} \text{ dynes/cm.}^2$$

Table 37B

TRICEL
FIBRE 6.

Bending Modulus_{20°C} only

Length = 0.65 cm. Mass/unit length = 13.7 microgrammes /cm.

Density = 1.30 gm/cc.

Shape



Shape factor (major axis)₁ = 0.56

Shape factor (minor axis)₂ = 1.78

Resonant frequency₁ = 178.3 c/s.

Resonant frequency₂ = 350.3 c/s.

$$E_{b1} = 4.85 \times 10^{10} \text{ dynes/cm.}^2$$

$$E_{b2} = 5.90 \times 10^{10} \text{ dynes/cm.}^2$$

Table 37C

TRICEL
FIBRE 7.

Dynamic Bending Modulus_{20°C} and Loss Tangent_{20°C} only.

Length = 0.72 cm. Mass/unit length = 14.00 microgrammes /cm.

Density = 1.30 gm/cc.

Shape



Shape factor (major axis) = 0.59

Resonant frequency (major axis) = 272.5 c/s.

$$E = 5.55 \times 10^{10} \text{ dynes/cm.}^2$$

Loss tangent = 0.0251

Table 38TRICEL FIBREMean Values

Temperature °C	Bending Modulus, $\times 10^{10}$ dynes/cm ²	Loss Modulus, $\times 10^{10}$ dynes/cm ²
150	3.33	0.1582
140	3.50	0.1500
130	3.63	0.1418
120	3.75	0.1335
110	3.07	0.1272
100	4.06	0.1270
90	4.28	0.1277
80	4.39	0.1248
70	4.46	0.1228
60	4.57	0.1240
50	4.67	0.1300
40	4.80	0.1382
30	4.90	0.1461
20	5.05	0.1615
10	5.09	0.1720
0	5.15	0.1734
-10	5.23	0.1740
-20	5.30	0.1749
-30	5.37	0.1779
-40	5.46	0.1850
-50	5.55	0.2059

Table 39ACRILAN A.FIBRE 1.

Temperature °C	Resonant Frequency, c/s	Relative Bending Modulus	Loss Tangent
144	166.0	0.235	0.278
140	185.0	0.292	0.240
131	213.5	0.389	0.210
123	238.0	0.478	0.185
110	265.0	0.596	0.135
105	280.0	0.669	0.095
97	289.0	0.705	0.089
86	304.2	0.784	0.082
67	314.6	0.836	0.060
57	326.5	0.902	0.057
49	331.4	0.930	0.057
40	334.2	0.951	0.053
31	339.9	0.980	0.048
20	343.5	1.000	0.039
10	366.5	1.120	0.036
0	367.6	1.140	0.034
- 9	371.0	1.160	0.031
-19	372.1	1.180	0.030

Table 40.ACRILAN A
FIBRE 2

Temperature °C	Resonant Frequency, c/s	Relative Bending Modulus	Loss Tangent
139	128.0	0.275	0.218
133	137.0	0.314	0.210
121	166.5	0.469	0.147
113	182.0	0.561	0.138
104	190.0	0.610	0.118
98	203.0	0.695	0.096
90	205.8	0.710	0.079
71	222.9	0.836	0.063
58	228.5	0.875	0.058
49	233.8	0.915	0.053
41	237.5	0.951	0.048
33	239.0	0.960	0.045
25	240.5	0.971	0.044
13	248.2	1.020	0.041
1	252.0	1.060	0.036
-10	255.8	1.090	0.032
-22	257.1	1.110	0.026
-37	259.0	1.120	0.023
-46	260.7	1.130	0.022
-55	263.3	1.150	0.021

Table 41.

ACRILAN A
FIBRE 3.

Temperature °C	Resonant Frequency, c/s	Relative Bending	Loss Tangent
144	129.2	0.245	0.240
135	140.3	0.288	0.198
130	159.0	0.372	0.156
121	179.3	0.476	0.136
110	197.6	0.575	0.120
99	214.0	0.672	0.099
87	221.0	0.722	0.093
76	231.0	0.784	0.082
66	235.0	0.810	0.071
57	241.5	0.854	0.061
49	247.0	0.894	0.057
39	249.2	0.910	0.054
29	255.1	0.959	0.053
23	257.3	0.971	0.050
16	265.0	1.020	0.049
8	268.5	1.060	0.048
- 1	271.3	1.080	0.045
- 7	274.2	1.090	0.040
-15	275.0	1.100	0.035
-25	275.5	1.120	0.034
-35	275.5	1.120	0.034
-44	278.6	1.130	0.031
-54	279.5	1.140	0.030

Table 41A

ACRILAN A

FIBRE 4. Bending Modulus_{20°C} and Loss Tangent_{20°C} only

Length = 0.59 cm. Mass/unit length = 3.80 microgrammes /cm.

Density= 1.135 gm/cc. Shape **CIRCULAR**

Shape factor 1.0

Resonant frequency = 204.0 c/s.

$$E_b = 7.95 \times 10^{10} \text{ dynes/cm.}^2$$

Loss tangent = 0.0415.

Table 41B

ACRILAN A

FIBRE 5. Bending Modulus_{20°C} only

Length = 0.65 cm. Mass/unit length = 3.50 microgrammes /cm.

Density= 1.135 gm/cc. Shape **CIRCULAR**

Shape factor 1.0

Resonant frequency = 165.0 c/s

$$E_b = 7.75 \times 10^{10} \text{ dynes/cm.}^2$$

Table 41C

ACRILAN A

FIBRE 6. Bending Modulus_{20°C} only

Length = 0.495 cm. Mass/unit length = 3.4 microgrammes /cm.

Density= 1.135 gm/cc. Shape **CIRCULAR**

Shape factor 1.0

Resonant frequency = 270.0 c/s

$$E_b = 7.20 \times 10^{10} \text{ dynes/cm.}^2$$

Table 42.

ACRILAN A

Mean Values

Temperature °C	Bending Modulus $\times 10^{10}$ dynes/cm ²	Loss Modulus $\times 10^{10}$ dynes/cm ²
140	2.02	0.4651
130	2.63	0.5000
120	3.55	0.5507
110	4.44	0.5710
100	5.10	0.5700
90	5.31	0.5005
80	5.65	0.4370
70	5.91	0.4020
60	6.22	0.3791
50	6.55	0.3660
40	6.91	0.3468
30	7.21	0.3410
20	7.41	0.3400
10	7.58	0.3145
0	7.65	0.2640
-10	7.79	0.2552
-20	7.99	0.2396
-30	8.18	0.2318
-40	8.41	0.2300
-50	8.75	0.2278

Table 43.ACRILAN B.FIBRE 1

Temperature °C	Resonant Frequency, c/s	Relative Bending Modulus	Loss Tangent
144	176.2	0.242	0.2442
140	200.4	0.310	0.2102
130	240.2	0.446	0.1625
122	273.5	0.579	0.1502
114	285.5	0.627	0.1422
107	300.4	0.697	0.1254
98	310.6	0.745	0.1004
90	317.5	0.779	0.0972
81	328.4	0.835	0.0904
75	334.2	0.866	0.0636
64	342.8	0.927	0.0502
57	346.5	0.935	0.0522
49	349.0	0.945	0.0514
40	351.9	0.953	0.0482
34	355.2	0.971	0.0406
26	357.2	0.990	0.0392
20	359.0	1.000	0.0374
14	364.0	1.020	0.0374
6	367.4	1.040	0.0370
2	366.2	1.040	0.0340
- 5	366.4	1.040	0.0300
-12	367.7	1.040	0.0292
-22	368.5	1.044	0.0275
-28	368.5	1.044	0.0236
-34	371.1	1.062	0.0220
-42	372.2	1.064	0.0195
-50	373.1	1.076	0.0167
-58	373.1	1.076	0.0167
-64	374.1	1.080	0.0150

Table 44.

ACRILAN B
FIBRE 2.

Temperature °C	Resonant Frequency, c/s	Relative Bending Modulus	Loss Tangent
144	115.6	0.225	-----
142	120.2	0.245	0.2102
134	135.4	0.313	0.2002
124	159.2	0.430	0.1750
115	177.0	0.536	0.1642
108	190.2	0.616	0.1100
101	200.6	0.688	0.1002
94	205.6	0.716	0.0787
86	211.4	0.765	0.0685
77	217.4	0.805	0.0686
73	220.0	0.828	0.0624
67	222.0	0.840	0.0616
61	223.5	0.855	0.0495
53	227.0	0.885	0.0484
47	231.0	0.921	0.0485
40	234.0	0.935	0.0482
34	236.0	0.951	0.0442
19	243.0	1.000	0.0452
13	261.0	1.014	0.0444
2	264.0	1.018	0.0452
- 8	263.0	1.018	0.0436
-15	266.5	1.020	0.0349
-21	266.0	1.020	0.0292
-31	266.8	1.020	0.0280
-40	268.6	1.022	0.0270
-53	269.5	1.023	0.0265

Table 45.

ACRILAN B

FIBRE 3

Temperature °C	Resonant Frequency, c/s	Relative Bending Modulus	Loss Tangent
142	104.0	0.184	0.2104
132	109.0	0.247	0.1905
124	125.0	0.275	0.1602
108	171.0	0.505	0.1202
93	191.0	0.642	0.0926
67	213.3	0.794	0.0742
57	220.3	0.850	0.0604
47	226.5	0.895	0.0564
35	230.5	0.906	0.0482
24	235.5	0.970	0.0442
16	241.5	1.020	0.0415
7	249.5	1.082	0.0385
-3	252.5	1.104	0.0380
-14	255.5	1.124	0.0355
-21	256.0	1.140	0.0350
-30	256.0	1.140	0.0300
-40	257.5	1.146	0.0280
-50	258.5	1.160	0.0275

Table 46.

ACRILAN B
FIBRE 4

Temperature °C	Resonant Frequency, c/s.	Relative Bending Modulus	Loss Tangent
143	134.0	0.185	0.2052
133	170.2	0.298	0.1754
120	208.2	0.444	0.1652
110	226.0	0.525	0.1136
101	246.1	0.624	0.1094
91	263.6	0.715	0.0847
82	269.6	0.749	0.0732
74	278.4	0.794	0.0635
64	288.0	0.850	0.0594
55	293.7	0.876	0.0550
46	298.6	0.911	0.0422
38	306.9	0.964	0.0385
31	311.1	0.990	0.0370
11	313.2	1.010	0.0286
3	314.3	1.012	0.0296
-7	317.6	1.024	0.0295
-16	319.5	1.040	0.0280
-22	322.7	1.050	0.0270
-31	322.8	1.050	0.0252
-40	324.8	1.080	0.0242
-47	326.0	1.090	0.0241

1.155 ga/cm.

Shape

4

factor 1.18

frequency = 210.8 c/s.

Table 46A

ACRILAN B

FIBRE 5. Bending Modulus_{20°C} and Loss Tangent_{20°C} only.

Length = 0.66cm. Mass/unit length = 3.81 microgrammes / cm.

Density= 1.135 gm/cc. Shape CIRCULAR

Shape factor 1.0

Resonant frequency = 181.0 c/s.

$$E_b = 9.30 \times 10^{10} \text{ dynes/cm.}^2$$

Loss tangent = 0.0435

Table 46B

ACRILAN B

FIBRE 6. Bending Modulus_{20°C} and Loss Tangent_{20°C} only.

Length = 0.535 cm. Mass/unit length = 3.72 microgrammes/cm.

Density= 1.135 gm/cc. Shape CIRCULAR

Shape factor 1.0

Resonant frequency = 279.7 c/s.

$$E_b = 9.45 \times 10 \text{ dynes/cm.}^2$$

Loss tangent = 0.0394

Table 46C

ACRILAN B

FIBRE 7. Bending Modulus_{20°C} only

Length = 0.61 cm. Mass/unit length = 3.72 microgrammes/ cm.

Density= 1.135 gm/cc. Shape  6

Shape factor 1.18

Resonant frequency = 212.2 c/s.

$$E_b = 7.90 \times 10^{10} \text{ dynes/cm.}^2$$

Table 47.

ACRILAN B

Mean Values

Temperature °C	Bending Modulus, $\times 10^{10}$ dynes/cm ²	Loss Modulus, $\times 10^{10}$ dynes/cm ²
140	2.32	0.4710
130	3.19	0.5182
120	4.00	0.5593
110	4.82	0.5790
100	5.85	0.6020
90	6.52	0.5808
80	7.03	0.4982
70	7.41	0.4591
60	7.89	0.4359
50	8.22	0.4190
40	8.63	0.4088
30	9.00	0.3990
20	9.29	0.3910
10	9.37	0.3812
0	9.45	0.3490
-10	9.60	0.3308
-20	9.69	0.2914
-30	9.84	0.2610
-40	9.96	0.2578
-50	10.12	0.2420

Table 48.

POLYPROPYLENE. FIBRE 1

Temperature °C	Resonant Frequency, c/s	Bending Modulus, dynes/ cm ² x10 ¹⁰	Loss Tangent	Loss Modulus, dynes/ cm ² x10 ¹⁰	Relative Bending Modulus
91	143.2	1.59	0.0643	0.1025	0.342
87	145.0	1.64	0.0636	0.1040	0.348
81	150.7	1.75	0.0626	0.1085	0.376
75	155.2	1.86	0.0620	0.1150	0.402
69	160.2	1.97	0.0598	0.1178	0.427
64	167.0	2.20	0.0671	0.1472	0.464
58	173.8	2.33	0.0695	0.1620	0.500
50	183.1	2.58	0.0770	0.1985	0.555
43	199.6	3.05	0.0785	0.2394	0.656
35	213.7	3.50	0.0790	0.2760	0.752
29	226.6	3.61	0.0874	0.3160	0.776
24	235.1	4.25	0.0910	0.3870	0.913
15	261.5	4.85	0.1010	0.4900	1.040
5	270.6	5.68	0.0750	0.4260	1.220
- 4	274.2	5.74	0.0660	0.3782	1.230
-14	285.0	6.06	0.0635	0.3840	1.302
-24	293.8	6.43	0.0580	0.3730	1.382
-33	300.9	6.70	0.0575	0.3850	1.440
-43	304.8	6.90	0.0495	0.3418	1.480
-53	309.9	7.04	0.0556	0.3910	1.520
-63	312.3	7.18	0.0576	0.4140	1.540

Fibre Dimensions: Length = 0.61 cm. Mass/unit length = 5.8 microgrammes/cm.

Density = 0.90 gm/cc. Shape CIRCULAR

Shape factor 1

$$E_b \text{ } 20^\circ\text{C} = 4.65 \times 10^{10} \text{ dynes/cm.}^2$$

Table 49.

POLYPROPYLENE
FIBRE 2.

Temperature °C	Resonant Frequency, c/s	Bending Modulus, dynes/ cm ² x10 ¹⁰	Loss Tangent	Loss Modulus, dynes/ cm ² x10 ¹⁰	Relative Bending Modulus
96	168.7	1.80	0.0875	0.1575	0.410
90	172.8	1.89	0.0850	0.1610	0.429
82	180.5	2.07	0.0723	0.1500	0.470
74	193.5	2.38	0.0655	0.1560	0.541
64	207.9	2.78	0.0640	0.1780	0.632
56	219.7	3.06	0.0685	0.2098	0.696
49	225.2	3.21	0.0695	0.2232	0.729
40	247.1	3.94	0.0702	0.2762	0.884
30	262.4	4.37	0.0700	0.3060	0.993
20	263.3	4.40	0.0950	0.4170	1.000
10	267.0	4.53	0.1020	0.4610	1.030
0	278.0	4.84	0.0890	0.4310	1.110
-10	285.0	5.10	0.0665	0.3390	1.160
-20	298.0	5.55	0.0640	0.3550	1.260

Fibre Dimensions: Length = 0.57 cm. Mass/unit length = 5.5
microgrammes/cm.

Density = 0.90 gm/cc. Shape CIRCULAR

Shape factor = 1.

$$E_b \text{ at } 20^\circ\text{C} = 4.40 \times 10^{10} \text{ dynes/cm.}^2$$

Table 50POLYPROPYLENE
FIBRE 3

Temperature °C	Resonant Frequency, c/s	Relative Bending Modulus	Loss Tangent
96	129.5	0.410	0.0717
90	132.7	0.422	0.0607
84	137.3	0.455	0.0576
77	142.0	0.486	0.0536
70	146.0	0.513	0.0510
57	159.1	0.608	0.0515
52	166.5	0.665	0.0555
41	169.1	0.700	0.0560
17	206.6	1.020	0.0710
9	235.1	1.200	0.0800
1	243.7	1.390	0.0750
- 7	252.1	1.500	0.0630
-15	256.1	1.520	0.0497
-24	258.9	1.540	0.0482
-32	261.5	1.560	0.0440
-40	266.5	1.620	0.0413
-47	269.4	1.630	0.0410
-54	271.8	1.660	0.0424
-60	273.2	1.670	0.0491
-67	273.5	1.680	0.0490

Table 50A

POLYPROPYLENE

FIBRE 4. Bending Modulus_{20°C} only.

Length = 0.52 cm. Mass/unit length = 3.50 microgrammes / cm.

Density = 0.90 gm/cc. Shape CIRCULAR

Shape factor 1.0

Resonant frequency = 258.9 c/s.

$$E_b = 4.55 \times 10^{10} \text{ dynes/cm.}^2$$

Table 50B

POLYPROPYLENE

FIBRE 5. Bending Modulus_{20°C} only.

Length = 0.57 cm. Mass/unit length = 5.6 microgrammes / cm.

Density = 0.90 gm/cc. Shape CIRCULAR

Shape factor 1.0

Resonant frequency = 376.4 c/s.

$$E_b = 4.72 \times 10^{10} \text{ dynes/cm.}^2$$

Table 51.

POLYPROPYLENE

Mean Values

Temperature °C	Bending Modulus, $\times 10^{10}$ dynes/cm ²	Loss Modulus, $\times 10^{10}$ dynes/cm ²
95	1.23	0.0914
90	1.35	0.0931
80	1.60	0.1065
70	1.90	0.1198
60	2.21	0.1442
50	2.62	0.1731
40	3.42	0.2109
30	3.83	0.2730
20	4.55	0.3960
10	4.70	0.4112
0	5.00	0.3900
-10	5.30	0.3578
-20	5.69	0.3301
-30	6.12	0.3306
-40	6.72	0.2620
-50	7.22	0.3720
-60	7.27	0.4006
-70	7.35	0.4361

Table 52.

Bending Moduli, Loss Tangents and Loss Moduli at 20°C.

	E_b dynes/cm ² x 10	Loss Tangent	E_2 dynes/cm ² x 10 ¹⁰
Ramie	33.7	0.0055	0.1851
Fortisan	33.2	0.00325	0.1080
Silk	11.95	0.0134	0.1591
Acrilan B	9.29	0.0420	0.3910
Acrilan A	7.49	0.0464	0.3470
Tricel	5.05	0.0320	0.1615
Fibrolane	4.91	0.0172	0.0845
Polypropylene	4.55	0.0870	0.3960
Wool	4.29	0.0190	0.0818
Acetate Fibre	3.36	0.0290	0.0975

Table 53.

Mean Loss Tangents (Maxima).

Temperature °C	Loss Tangent	Temperature °C	Loss Tangent	Temperature °C	Loss Tangent
<u>Wool</u>		<u>Silk</u>		<u>Fibrolane</u>	
*126	0.0141	*117	0.0145	68	0.0120
106	0.0170	80	0.0125	-3	0.0243
2 $\frac{1}{2}$	0.0241	47	0.0119		
		0	0.0192		
<u>Acetate fibre</u>		<u>Tricel</u>			
*105	0.0282	*98	0.0310		
*60	0.0260	*14	0.0339		
*11	0.0310				
<u>Acrilan A</u>		<u>Acrilan B</u>		<u>Polypropylene</u>	
*102	0.1150	*80	0.0710	*51	0.0662
*20	0.0464	*5	0.0391	12	0.0898

* Shoulder.

relative bending modulus. These curves were derived in a similar manner to those of Fig.29.

Fig.31 shows the effect of temperature on the mean bending modulus. In the case of wool and Fibrolane fibres which had been examined over the complete temperature range, the mean bending modulus at any temperature could be calculated from the observed resonant frequencies and fibre dimensions. (The data for Fibrolane were, however, supplemented to determine the bending modulus at 20°C more accurately, in the same manner as that outlined below). In the case of the other fibres it was not always possible to obtain the fibre dimensions. Separate experiments were therefore conducted to find the bending modulus at 20°C only, which was calculable when the required dimensional data had been obtained. The **mean** bending modulus at any temperature could then be derived from the product of the mean bending modulus at 20°C and the mean relative bending modulus at the required temperatures in the range. To supplement already available data, the loss tangents of fibres in these separate experiments were also determined, whenever possible.

Fig.32 shows the effect of temperature on the mean loss modulus. The **mean** loss modulus at temperatures within the range covered is obtained from the product of the

derived mean bending modulus and the derived mean loss tangent.

The data from which **curves** are produced are recorded in tabular form in the order, wool (Table 6), silk, Fibrolane, ramie, Fortisan, acetate fibre, Tricel, Acrilan A, Acrilan B and polypropylene (Table 51).

The derived data of bending modulus and loss modulus from which bending and loss modulus curves are produced, and which are labelled "mean values", are given for wool in Table 11, silk in Table 18, Fibrolane in Table 22, ramie in Table 25, Fortisan in Table 28, acetate fibre in Table 33, Tricel in Table 38, Acrilan A in Table 42, Acrilan B in Table 47 and polypropylene in Table 51. Where only the bending moduli at 20°C were determined, the necessary data are recorded in sub-tables, e.g. silk, fibre 7, Table 17A, Fibrolane, fibre 4, Table 21A, Fibrolane, fibre 5, Table 21B, etc. In some instances, as stated earlier, the loss tangent was also recorded.

Fibre dimensions: Where available, the fibre dimensions are stated. The length, mass per unit length, resonant frequency and shape of the fibre were determined experimentally. The shape factor was calculated by the method previously described. Shape factor (major axis) or shape factor (major axis)₁ and resonant frequency (major

axis) or resonant frequency₁ refer to the fibre vibrating about its major axis, while by substituting the term "minor axis", the same notation is used for the fibre vibrating about its minor axis. Most fibres will have two principal axes and vibrate at two different resonant frequencies, about these axes. While the resonant frequencies are independent of the polar position of the cross section in relation to the disturbing force (the electrodes) the amplitudes of vibration at the two resonant frequencies are dependent on the polar positioning. The explanation lies in the fact that the disturbing force can be resolved into two components and the fibre vibrates in two different directions according to the two principal axes¹²⁰. It sometimes happens that the two resonant frequencies are so close (e.g. in the case of almost symmetrical cross sections having only a small difference in the lengths of the principal axes) that the bandwidth cannot be measured, and a new specimen must be employed for the dynamic experiments. Fibres whose cross sections are circular or correspond to the shape of an equilateral triangle, will vibrate only in one plane.

The densities quoted are the assumed densities of the dry fibres obtained from literature - wool¹¹⁶, silk¹²¹, Fibrolane¹²², ramie¹²³, Fortisan¹²², acetate fibre¹²⁴,

Tricel¹²², Acrilan A and B¹²⁵, and polypropylene¹²⁶.

The bending modulus is generally denoted by E_1 but the bending modulus of dry fibres at 20°C is denoted more specifically by E_b or $E_{b20°C}$.

Lastly, Table 52 gives the values of bending moduli, loss tangents and loss moduli of all fibres tested, at 20°C, while Table 53 gives data relating to Fig.29 (mean loss tangent - temperature).

Thermal Expansion.

As a fibre is heated or cooled, it will be subject to changes in length and cross-sectional area. It would be expected therefore that the values of dynamic bending moduli and loss moduli of the various fibres, will be in error. Considerable research on the thermal expansion of high polymers has been carried out, including work on the 1,38,127,128,129,130,131. polymers concerned in the present investigation.

Polypropylene is the most deformable fibre, with temperature, having a coefficient of cubical expansion of 9.4×10^{-4} cc./cc./°C below the melting point¹³¹ (this is in fact the value for polyethylene but will give a fair approximation) and a linear expansion of about 1.5×10^{-4} cm./cm./°C.¹³⁰ Preliminary calculations show that at 85°C

the bending modulus will be in error by approximately 5% and at -50°C , by a similar amount. Acrilan exhibits the second largest response to temperature having a coefficient of cross-sectional expansion of 4.1×10^{-4} sq.cm./sq.cm./ $^{\circ}\text{C}$ above 87°C and 1.3×10^{-4} sq.cm./sq.cm./ $^{\circ}\text{C}$ below 87°C ¹. The linear expansions are 0.48×10^{-4} cm./cm./ $^{\circ}\text{C}$ above 87°C and 0.22×10^{-4} cm./cm./ $^{\circ}\text{C}$ below 87°C ¹²⁹. (These in fact are values for pure polyacrylonitrile which would not be expected to differ greatly from the actual values for Acrilan.) Preliminary calculations show that at 150°C , an error of approximately 4% and at -50°C , of about 2% occurs, in the bending modulus. The expansion coefficients of the other fibres are smaller still, and the error further reduces, to within experimental error. Moreover, the closer to room temperature, the smaller the error due to thermal expansion becomes and while for the purposes of this investigation the anomalies are of no consequence, in the case of Acrilan and polypropylene, and within experimental error for the other fibres, should a very accurate value of bending modulus be required at a particular temperature, it would appear that a correction for thermal expansion would only be necessary below a relatively low temperature, and above a relatively high temperature.

Thus, in practice, the shapes and heights of both the bending and loss moduli curves may be regarded as true,

without correction for thermal expansion.

Humidity Experiments

The effect of humidity on the resonant frequency and bandwidth of wool, nylon and viscose rayon is measured according to the procedure previously described. At 0% relative humidity, the vacuum pressure must be maintained at less than 0.02 mm. mercury, as in temperature experiments, and similar precautions regarding the amplitude of vibration are taken as in temperature experiments. At other humidities, the vacuum pressure is dependent on humidity and a correction factor for the damping due to the vapour pressure is applied, in order to determine the energy loss of the fibre alone, while the amplitude of vibration is controlled within the necessary limits throughout.

The technique employed, allowed five fibres to be investigated simultaneously (in temperature experiments, the Townsend and Mercer Bath limited the technique to a single fibre at a time). Since in temperature experiments, wool gave the most variable results, and the "modified" regenerated cellulose fibres were less consistent than the fully synthetics, it was decided to examine two wool and two viscose fibres, and only one of nylon.

The results are recorded in Figs.33 to 35 and Tables 54 to 59B.

Figs.33, 34 and 35 show the effect of relative humidity on the loss tangent, bending modulus and loss modulus respectively, of wool, nylon and viscose rayon.

Table 54 presents the data for the effect of relative humidity on wool (fibre 1).

55 humidity on wool (fibre 2).

56 humidity on nylon.

57 humidity on viscose rayon (fibre 1).

58 humidity on viscose rayon (fibre 2).

Table 59A presents the means of the data in Tables 54 and 55, while Table 59B presents the means of the data in Tables 57 and 58.

Figs.33, 34 and 35 are thus derived from Tables 56, 59A and 59B and represent mean values of the dynamic properties (except in the case of nylon where only one specimen was investigated).

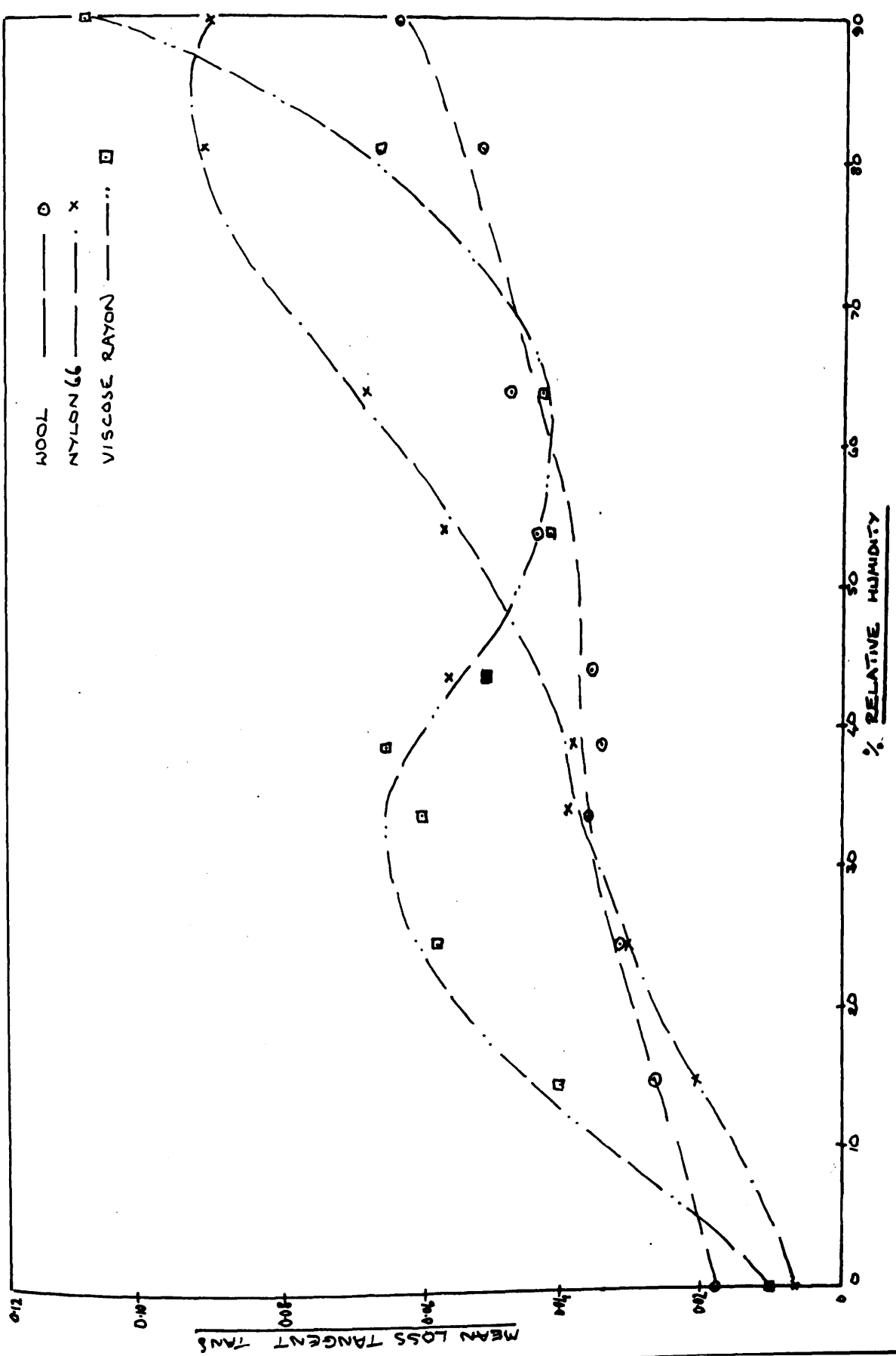
Fibre Dimensions.

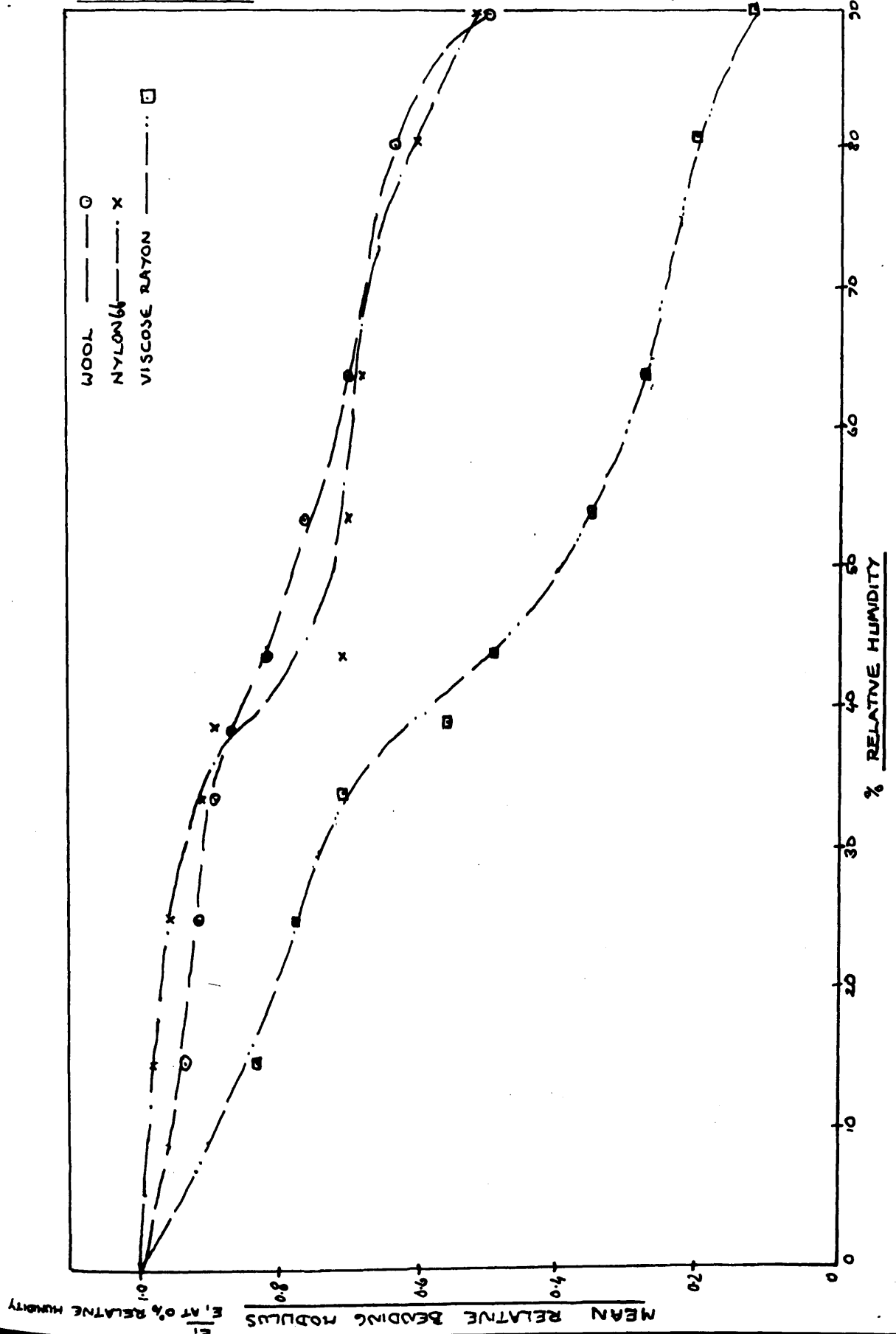
These are presented in a similar manner and with similar notations as in temperature experiment data. The factor F_1 is discussed in the following paragraph.

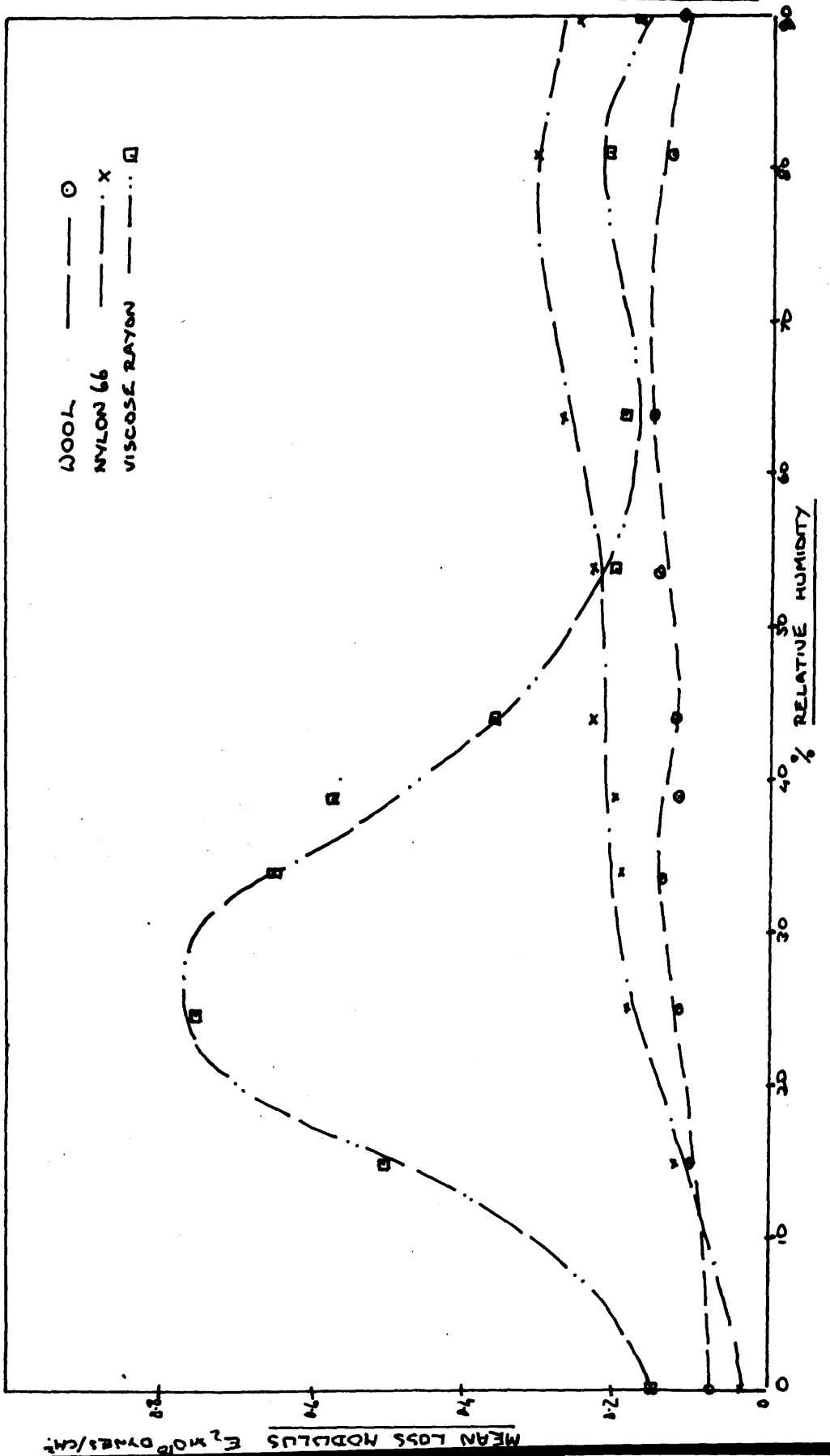
Swelling.

A consequence of moisture absorption by fibres is an

FIG. 55.







WOOL FIBRE 1

Relative Humidity, %	Resonant Frequency, c/s.	Bandwidth, c/s.	Loss Tangent (uncorrected)	Factor F_1	Bending Modulus, $\times 10^{10}$ dynes/cm. ²	Loss Tangent	Loss Modulus, $\times 10^{10}$ dynes/cm. ²
0	229.5	4.0	0.0174	1.0	4.67	0.0174	0.0815
15	225.6	7.9	0.0350	1.006	4.50	0.0248	0.1080
25	221.2	8.7	0.0392	1.003	4.35	0.0294	0.1240
34	220.6	9.4	0.0425	0.999	4.31	0.0321	0.1390
39	216.2	8.8	0.0406	0.992	4.14	0.0298	0.1140
44	211.2	9.4	0.0445	0.982	3.90	0.0335	0.1315
54	209.2	12.2	0.0583	0.960	3.71	0.0473	0.1695
64	203.5	12.8	0.0628	0.935	3.47	0.0502	0.1750
81	183.3	12.2	0.0665	0.898	2.68	0.0523	0.1480
90	152.1	13.5	0.0886	0.832	1.74	0.0720	0.1262

* Dry fibre dimensions: Length = 0.71 cm. Mass/unit length = 19.5 microgrammes/cm.
 0.00412 cm. Density = 1.304 gm./cc.

Shape  0.00475 cm.

* OBTAINED BY APPLYING A REGAIN CORRECTION (IN ALL HUMIDITY EXPERIMENTS). FOR REFERENCES, SEE TABLE 60 AND P.74

WOOL FIBRE 2

Relative Humidity, %	Resonant Frequency, c/s.	Band-width, c/s.	Loss Tangent (uncorrected)	Factor F_1	Bending Modulus, $\times 10^{10}$ dynes/cm ²	Loss Tangent	Loss Modulus, $\times 10^{10}$ dynes/cm ²
0	257.2	5.0	0.0194	1	3.85	0.0194	0.0745
15	245.8	8.8	0.0358	1.006	3.53	0.0298	0.1035
25	242.1	10.4	0.0430	1.003	3.46	0.0361	0.1230
34	243.0	11.9	0.0490	0.999	3.44	0.0419	0.1450
39	242.1	-	-	0.992	~3.25	-	-
44	230.5	10.9	0.0474	0.982	3.04	0.0398	0.1210
54	224.7	11.6	0.0516	0.960	2.83	0.0420	0.1250
64	222.8	12.2	0.0548	0.935	2.71	0.0471	0.1210
81	213.2	12.0	0.0565	0.898	2.37	0.0478	0.1050
90	-	-	-	0.832	-	-	-

Dry Fibre dimensions: Length = 0.65 cm. Mass/unit length = 21.0 microgrammes/cm.

Density = 1.304 gm./cc.

0.00507 cm.

Shape  0.00475 cm.

NYLON 66

Table 56

Relative Humidity, %	Resonant Frequency, c/s.	Bandwidth, c/s.	Loss Tangent (uncorrected)	Factor F ₁	Bending Modulus, x10 ¹⁰ dynes/cm ²	Loss Tangent	Loss Modulus x10 ¹⁰ dynes/cm ²	Relative Bending Modulus
0	222.9	1.44	0.0064	1.00	5.80	0.0064	0.0374	1.00
15	218.1	18.2	0.0835	1.014	5.70	0.0218	0.1170	0.984
25	215.4	21.5	0.1000	1.0195	5.56	0.0332	0.1810	0.960
34	209.1	23.0	0.1100	1.0215	5.29	0.0398	0.1995	0.911
39	206.6	22.8	0.1100	1.0281	5.19	0.0396	0.2038	0.893
44	184.0	25.0	0.1358	1.0294	4.10	0.0571	0.2290	0.705
54	181.4	25.6	0.1410	1.0430	4.10	0.0576	0.2280	0.705
64	178.6	28.0	0.1565	1.0500	4.05	0.0695	0.2750	0.699
81	165.0	31.0	0.1875	1.0570	3.48	0.0923	0.3041	0.600
90	149.0	29.0	0.1943	1.0610	2.84	0.0882	0.2400	0.490

Dry fibre dimensions: Length = 0.54 cm. Mass/unit length = 3.8 microgrammes/cm.

Density = 1.1504 gm./cc.

Shape CIRCULAR 0.00206 cm. DIAMETER

Table 57.

VISCOSE RAYON FIBRE 1

Relative Humidity, %	Resonant Frequency, c/s.	Bandwidth, c/s.	Loss Tangent (uncorrected)	Factor F ₁	Bending Modulus, x10 ¹⁰ dynes/cm. ²	Loss Tangent	Loss Modulus, x10 ¹⁰ dynes/cm. ²
0	272.2	2.7	0.0099	1.0	17.0	0.0099	0.1690
15	253.6	21.4	0.0845	0.972	14.5	0.0331	0.4660
25	246.9	27.2	0.1100	0.957	13.5	0.0588	0.7710
34	239.9	27.6	0.1150	0.943	12.55	0.0628	0.7520
39	215.0	24.9	0.1160	0.930	10.00	0.0561	0.5640
44							
54							
64							
81							
90							

Dry fibre dimensions: Length = 0.50 cm. Mass/unit length = 2.6 microgrammes/cm.

Density = 1.52 gm./cc.

Shape  0.0015 cm.
0.0015 cm.

Table 58.

VISCOSE RAYON FIBRE 2

Relative Humidity, %	Resonant Frequency, c/s.	Band-width, c/s.	Loss Tangent (uncorrected)	Factor F_1	Bending Modulus $\times 10^{10}$ dynes/cm. ²	Loss Tangent	Loss Modulus, $\times 10^{10}$ dynes/cm. ²
0	332.0	3.06	0.0092	1.0	14.22	0.0092	0.1311
15	300.3	25.2	0.0840	0.972	11.50	0.0482	0.5434
25	292.8	28.4	0.0970	0.957	10.67	0.0587	0.6162
34	278.0	27.9	0.1010	0.943	9.53	0.0585	0.5655
39	249.1	30.0	0.1205	0.930	7.54	0.0765	0.5753
44	211.4	21.5	0.1020	0.926	5.41	0.0478	0.2532
54	202.6	20.6	0.1018	0.905	4.86	0.0424	0.2114
64	189.6	20.2	0.1065	0.880	4.16	0.0426	0.1798
81	169.9	23.6	0.1389	0.835	3.17	0.0669	0.2149
90	123.0	26.0	0.2108	0.768	1.57	0.1082	0.1660

Dry fibre dimensions: Length = 0.43 cm. Mass/unit length = 2.80 microgrammes/cm.

0.0015 cm



Shape 0.00167 cm.

Density = 1.52 gm./cc.

NOTE:

- (1) The pressures at which measurements were made, corresponding to the relative humidities are:

Relative Humidity, %	0	15	25	34	39	44	54	64	81	90
Pressure, mm. Hg.	0.005	2.65	4.45	6.05	6.75	7.65	9.45	11.00	14.10	15.80

- (2) The tabulated resonant frequencies and bandwidths are:
- for Wool, fibres 1 and 2, the means for the two major axes,
- for Viscose rayon, fibre 2, the values for vibrations through the major axis only.

Table 59(A)

Wool (Average Values)

Relative Humidity, %	Bending Modulus, $\times 10^{10}$ dynes/cm ²	Loss Tangent	Loss Modulus, $\times 10^{10}$ dynes/cm ²	Relative Bending Modulus
0	4.26	0.0189	0.0780	1
15	4.01	0.0273	0.1057	0.940
25	3.91	0.0327	0.1230	0.918
34	3.88	0.0370	0.1420	0.911
39	3.69	0.0349	0.1160	0.865
44	3.47	0.0366	0.1262	0.815
54	3.27	0.0446	0.1472	0.766
64	2.92	0.0486	0.1480	0.685
81	2.69	0.0500	0.1265	0.631
90	2.05	0.0650	0.1136	0.481

Table 59(B)Viscose Rayon (Average Values)

Relative Humidity, %	Bending Modulus, $\times 10^{10}$ dynes/cm. ²	Loss Tangent	Loss Modulus, $\times 10^{10}$ dynes/cm. ²	Relative Bending Modulus
0	15.61	0.00957	0.145	1.000
15	13.00	0.0406	0.504	0.835
25	12.08	0.0587	0.745	0.774
34	11.04	0.0606	0.658	0.707
35	8.72	0.0663	0.569	0.559
44	7.64	0.0540	0.360	0.487
54	5.41	0.0441	0.200	0.346
64	4.30	0.0432	0.186	0.276
81	3.08	0.0702	0.209	0.198
90	1.64	0.1060	0.174	0.105

anisotropic swelling which gives rise to an increase in length of the order of 1.2% and 4% for nylon and wool, and viscose rayon respectively and an increase in diameter of 5%, 16% and 26% respectively for these fibres, on passing from the dry to the wet state. Due to the magnitude of these dimensional changes and the fact that density and mass per unit length are also affected by the uptake of moisture, a correction factor (F_1) will have to be applied in order to determine the precise bending and loss moduli.

Assuming uniform cross-sectional swelling, the correction factor, at R% relative humidity where R is any relative humidity between 0 and 100% is

$$\frac{m}{l} \frac{(\rho + \delta\rho)^2}{\rho^2} \cdot \frac{(1 + \delta l)^4}{l^4} \cdot \frac{(1 + \delta m)}{(m + \delta m)} \quad (\text{from equation 10})$$

where ρ , l and m are the dry density, length and mass of the fibre,

$\delta\rho$, δl and δm are the increases in ρ , l and m at a relative humidity R,

δm is obtained from the moisture regain data of Fourn and Harris¹³² for wool, nylon and viscose rayon, while the sources for the dimensional and specific gravity changes have been cited previously (p.74). The data required for the calculation of F_1 is presented in Table 60. A detailed calculation of F_1 at 64% relative humidity follows thereafter.

The Damping Correction Factor and Dynamic Parameters for a Partial Vacuum.

Damping effects depend partly on the friction losses in the vibrating body (internal damping) and partly on the

Table 60

WOOL

% Relative Humidity	0	10	20	30	40	50	60	70	80	90
Density, ¹¹⁶ gm./cc.	1.304	1.313	1.315	1.315	1.315	1.314	1.313	1.312	1.306	1.297
Length, cm. ⁹⁹	1.0	1.0044	1.0066	1.0081	1.0092	1.01	1.0104	1.0109	1.0112	1.0113
Regain % ¹³²	0	4.1	6.1	7.95	9.70	11.50	13.45	15.55	18.35	22.50

NYLON

% Relative Humidity	0	10	20	30	40	50	60	70	80	90
Density, ¹¹⁷ gm./cc.	1.1504	1.1515	1.1528	1.1528	1.1550	1.1564	1.1570	1.1570	1.1572	1.1576
Length, cm. ¹¹⁸	1.0	1.0017	1.0038	1.0038	1.0055	1.008	1.012	1.014	1.0158	1.0205
Regain % ¹³²	0	1.1	1.4	1.7	2.3	2.8	3.4	4.1	5.0	5.7

VISCOSE RAYON

% Relative Humidity	0	10	20	30	40	50	60	70	80	90
Density, ¹¹⁹ gm./cc.	1.52	1.525	1.523	1.523	1.522	1.510	1.500	1.485	1.473	1.433
Length, cm. ¹³	1.0	1.001	1.002	1.002	1.003	1.0045	1.006	1.008	1.0105	1.016
Regain % ¹³²	1.0	3.8	5.7	7.3	8.7	10.3	11.9	13.9	16.7	21.5

Example of detailed calculation of Factor, F₁

at 64% relative humidity.

Wool. $\rho + \delta\rho = 1.3126 \text{ gm./cc.}$

$$l + \delta l = 1.0106 \text{ cm.}$$

$$m + \delta m = 1.1425 \text{ gms.}$$

where ρ , l , and m are the dry density, length and mass and equal to 1.304 gm./cc., 1.0 cm., and 1.0 gm. respectively.

$$\begin{aligned} \text{Correction Factor} &= \frac{1.3126^2}{1.304^2} \times \frac{1.0106^4}{1} \times \frac{1.0106}{1.1425} \\ &= \underline{\underline{0.935}} \end{aligned}$$

Nylon. $\rho + \delta\rho = 1.1567 \text{ gm./cc.}$

$$l + \delta l = 1.0151 \text{ cm.}$$

$$m + \delta m = 1.037 \text{ gms.}$$

where ρ , l , and m are the dry density, length and mass and equal to 1.1504 gm./cc., 1.0cm., and 1.0 gm. respectively.

$$\begin{aligned} \text{Correction Factor} &= \frac{1.1567^2}{1.1504^2} \times \frac{1.0151^4}{1} \times \frac{1.0151}{1.037} \\ &= \underline{\underline{1.05}} \end{aligned}$$

Viscose Rayon

$$\rho + \delta\rho = 1.480 \text{ gm./cc.}$$

$$l + \delta l = 1.009 \text{ gm.}$$

$$m + \delta m = 1.127 \text{ gm.}$$

where ρ , l , and m are the dry density, length and mass and equal to 1.52 gm./cc., 1.00 cm., 1.00gm., respectively.

$$\text{Correction Factor} = \frac{1.48^2}{1.52^2} \times \frac{1.009^4}{1} \times \frac{1.009}{1.127} = \underline{\underline{0.88}}$$

damping of the surrounding medium. By working in a vacuum, as in the temperature experiments, the problem of external damping was overcome, but where there is moisture present, only a partial vacuum can be achieved and a correction factor must be applied in order to identify the internal friction of the fibre alone.

Meredith and Hsu¹³³ applied a correction factor, and for a fibre vibrating in air, expressed the dynamic quantities as;

$$E_1 = \frac{\rho A l^4}{I_c^4} \omega_a^2 \left[1 + \frac{1}{2} \left(\frac{\Delta \omega_a}{\omega_a} \right)^2 - \frac{1}{4} \left(\frac{\Delta \omega_a}{\omega_a} \right)^4 \right] (1 + BK) \dots\dots\dots (12)$$

$$E_2 = \frac{\rho A l^4}{I_c^4} \omega_a \left\{ \Delta \omega_a \left[1 - \frac{1}{4} \left(\frac{\Delta \omega_a}{\omega_a} \right)^2 + \frac{3}{32} \left(\frac{\Delta \omega_a}{\omega_a} \right)^4 \right] (1+BK) - BK' \omega_a \right\} \quad (13)$$

$$\tan \delta = \frac{\Delta \omega_a}{\omega_a} \left[1 - \frac{3}{4} \left(\frac{\Delta \omega_a}{\omega_a} \right)^2 + \frac{23}{32} \left(\frac{\Delta \omega_a}{\omega_a} \right)^4 \right] - \frac{BK'}{1+BK} \left[1 - \frac{1}{2} \left(\frac{\Delta \omega_a}{\omega_a} \right)^2 + \frac{1}{2} \left(\frac{\Delta \omega_a}{\omega_a} \right)^4 \right] \dots\dots\dots (14)$$

where ω_a = resonant frequency in air

$\Delta \omega_a$ = bandwidth in air (due to combined effect of air friction and internal damping)

$B = \frac{\rho_a}{\rho}$ where ρ_a is the density of air, ρ fibre density

K and K' are dimensionless functions of a

dimensionless parameter m, which is defined as

$$m^2 = \frac{\rho_a \cdot A \omega}{4 \pi \mu}$$

where μ is the coefficient of viscosity of air, and for values of $m > 0.3$,

$$K = 1 + \frac{\sqrt{2}}{m} \quad \text{and} \quad K' = \frac{\sqrt{2}}{m} + \frac{1}{2m^2}$$

for values of $m < 0.1$

$$m^2(K - 1) = \frac{\pi/4}{L^2 + \pi/4}$$

$$\text{and } m^2 K' = \frac{-L}{L^2 + \pi/4}$$

where $L = 0.577 + \ln.m$

The other parameters in equations 12, 13 and 14, have been defined previously. The equations are reported to hold for values of $\frac{\Delta\omega_a}{\omega_a}$ of less than 0.6.

It has been shown by Lochner⁹⁶ that the resonant frequency of a wool fibre vibrating in air differs by something of the order of 0.2% from the resonant frequency in a vacuum while Stauff and Montgomery⁸⁵ observed a shift of less than 1 c/s at frequencies of about 100 c/s due to air damping of glass filaments. Karrholm and Schroder¹⁰² calculated that the fractional change in the true value of resonant frequency is one half of the ratio of the square of bandwidth to the resonant frequency, while Dusenbury¹⁰⁰ et al. found only a slight difference in bending modulus

between that obtained in air and that in vacuo. For fine fibres, the effect of air damping could be appreciable.

On the other hand, the damping caused by air has greatly increased the bandwidth in previous investigations.^{85,102,133} Hence in a medium, (other than vacuo), an appreciable viscosity and density of that medium will render the internal friction in the fibre small in comparison with the air friction. Thus, a small error of the observed bandwidth in air will cause a large error in the bandwidth of the fibre itself (since the observed bandwidth is due to the combined effect of both internal and air friction).

For this reason, it is desirable to minimise external damping effects, and the dynamic parameters in the present investigation have been determined in a partial vacuum.

Assuming water vapour behaves like a gas, equations (12), (13) and (14) will apply

where ω_a is the resonant frequency in partial vacuum,

$\Delta\omega_a$ is the bandwidth in partial vacuum,

μ is the coefficient of viscosity of water vapour (9.75×10^{-5} poise at 20°C) which is independent of pressure¹³⁴.

ρ_a is the density of water vapour.

ρ_a is dependent on pressure (determined by the aqueous saturated salt solution), and the density of water vapour at a particular pressure is derived from the relationship

$$\rho_a = \rho_o \left(\frac{P}{760} \right) \left(\frac{273.16}{T} \right)$$

where ρ_o (1.86×10^{-4} gm./c.c.) is the density at 0°C and 760 mm. Hg., and T is the absolute temperature¹³⁵.

The calculated value for ρ_a at 100% relative humidity and 20°C is 1.75×10^{-5} gm./c.c. ρ_a is zero at 0% relative humidity and since T is constant in this investigation,

ρ_a will increase linearly from zero at 0% relative humidity to 1.75×10^{-5} gm./c.c. at 100% relative humidity.

Discussion and Conclusions (Temperature Experiments)

According to Fig.29, the ratio of the viscoelastic to the elastic response of a fibre is related to the chemical nature of that particular fibre, e.g. wool, silk and Fibrolane have very similar loss tangent curves, and are all members of the protein family. Consequently, the discussion will be divided into 4 sections dealing with:

- 1) Protein fibres: Wool, silk and Fibrolane
- 2) Cellulose fibres: Ramie and Fortisan
- 3) Modified regenerated cellulose fibres: Acetate fibre and Tricel
- 4) Synthetic fibres: Acrilan A, Acrilan B and polypropylene.

Protein Fibres

Were the loss tangents (Fig.29) the only available data in this investigation from which to draw conclusions, then the three protein fibres would be thought to have extremely similar rheological and structural features. However, further data are available to show that this is not the case, and what is more, a vast amount of previous research has concluded this quite definitely. Fibrillar proteins are known to range in properties from hard, highly

crystalline fibres (such as silk) to the rubber-like contractile elements of muscle. Indeed, Figs. 30 and 31 of relative and absolute bending modulus, and Fig. 32 of loss modulus indicate that wool and Fibrolane are more closely associated with each other, than silk is to either of the other two fibres.

Molecular and structural differences, some of which are highly responsible for the differing mechanical behaviours of these fibres, are discussed by Peters and Woods¹³⁶ and Fox and Foster¹³⁷. Mention is made of the fact that silk is highly crystalline and has a molecular chain configuration almost identical to that of β -keratin, wool is highly non-crystalline, and Fibrolane usually has what might be considered an intermediate structure, being highly non crystalline (like wool) and having extended main chains (like silk). While amplification and modification of the above generalisation will be made, as a first approximation, it would not be unreasonable to find that at normal temperatures, some mechanical properties of Fibrolane should lie between those of silk and wool. This is true of loss tangent, loss modulus and bending modulus. At other temperatures, however, this does not hold, and a much more rigorous investigation is required to account for the relative dynamic behaviours. Before a

detailed comparison of the behaviour can be attempted, a closer examination of the dynamic behaviour of each is necessary; in this process, certain points of comparison are mentioned.

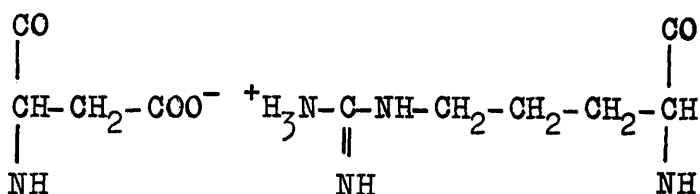
Wool: In Fig. 32 it is seen that wool has a very low loss modulus at all temperatures within the covered range, and this fact requires an explanation.

The loss modulus is proportional to the energy dissipated, which in turn depends on the resistance to bond breakdown and bond rotations in the amorphous regions. On the surface, two possibilities to account for the low loss modulus at all temperatures would appear feasible.

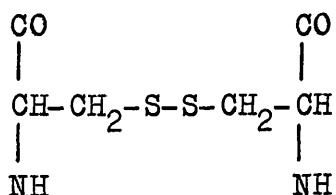
- 1) either there are very few and weak inter-chain bonds and rotational barriers are small or
- 2) a very high degree of inter-chain bonding exists so that thermal agitation encountered in these forced vibration experiments is insufficient to cause any appreciable bond breakdown or tendency for bond breakdown - the rotational barriers are also small.

To determine whether one of the above proposals is plausible, some at least of the salient features of wool structure must be considered. Being a polypeptide with the general formula
$$\begin{array}{c} \text{-NH-CH-CO-} \\ | \\ \text{R} \end{array}$$
 where R is a side chain

and can be one of some twenty or more amino acid groups, many hydrogen bonds are possible on account of the NH and CO groups. A common inter-chain spacing of 4.5 \AA is particularly apt for van der Waals forces to become effective. Of the many side chains, few are inactive, some can give rise to further hydrogen bonding, while an acidic side chain might attract a neighbouring side chain to form a salt linkage e.g.



A further possibility, which is associated with the elastic properties of α -keratin is the cystine bridge



On the grounds of the many hydrogen bonds alone, the fibre may be expected to show considerable and intensive inter-chain interaction, especially if the folded α -keratin model of Astbury and Bell¹³⁸ is accepted, although the possibilities are restricted by the very existence of the above side chains. This model seems, however, to have been superseded by that of Pauling and Corey¹³⁹ who proposed

a helical structure for α -keratin, in which all the NH and CO groups of the peptide chain are mutually satisfied internally, i.e. intra molecularly. The fact that this structure was determined solely on the basis of this intra molecular bonding, without considering side chains is a drawback. More recently the same workers modified their original ideas on the basis of a proposal by Crick¹⁴⁰, that a "coiled coil" of seven helical chains may be the answer. In the light of the results of dynamic responses, such a structure, with side chains also considered, seems very feasible. The "coiled coil" is regarded as being characteristic of the α -keratin chain, and consequently as being common to the "crystalline" and non crystalline regions.

Referring to the loss curves for wool (Figs.29 and 32) a moderate peak at about 60°C and a shoulder at about 125°C are observed. If several chains of helical configuration are intertwined (7 according to Pauling and Corey), then the amorphous regions will consist of many randomly arranged groups of intertwined helices. These groups will be thoroughly consolidated by the many ~~inter~~ and intra chain hydrogen bonds and van der Waals forces capable of being formed, and will behave as quasi crystallites with a quasi elastic response. It is possible that a few of the

polypeptide chains will not exist in coiled coils and will give rise to inter-molecular bonding with each other and some of the active side chains. It is further to be expected that as a result of the "coiled coil" configuration, the side chains will be conferred with a greater degree of rigidity at their "peptide end" by what might be a process of physical restriction; the more so in the case of the chain at the core of the "coiled coil". At their free ends, the side chains will be semi-flexible. The probability is also that they will be drawn into closer alignment with each other and will readily cross-link. Those which form cystine bridges and salt linkages will again behave elastically in the temperature range covered, the former having an activation energy of 60-80 kcal./mole and the latter about 400 kcal./mole¹³⁶. On this basis, the hydrogen bonds and van der Waals forces, of which there will (i.e. those between chains which do not exist in "coiled coils"), be comparatively few, are responsible for the loss features.

The moderately defined peak at 60°C is assigned to the breaking of these hydrogen bonds, but a well defined peak, anticipated at about 75 to 80°C, is rendered impossible by structural limitations. (If the Astbury wool model were accepted, intra molecular hydrogen bonding would be less complete, and subsequent inter molecular hydrogen bonding would give rise to a higher loss modulus than is in fact

realised. In this, there is another reason for supporting a Pauling and Carey model). It is thought that the inactive side chains, being "frozen" and causing a rotational barrier which contributes to the magnitude of the loss modulus up to this temperature are afforded a greater degree of mobility with the increase of free volume space, on increasing the temperature, and simultaneously with the increase of loss modulus due to the straining of the hydrogen bonds, cause a fall in loss modulus, which is the more predominating of the two phenomena above 60°C . It is further suggested, that during this fall in loss modulus, which eventually reaches a minimum value at 106°C , the van der Waals forces have been rendered ineffective, since they have a low activation energy of 2 to 3 kcal./mole and the molecular spacing of 4.5 \AA required for their formation, has been surpassed. The peak due to van der Waals forces is again considered to have been obscured on account of the fast dropping loss modulus, which but for the van der Waals forces, would have reached an even lower energy minimum. At the point of minimum energy loss (106°C) wool may be regarded, as it is in normal conditions by some workers¹⁴¹, as a cross-linked, anisotropic, heterogeneous polymer network, with the exception that at this temperature there are side chain mobilities and unsatisfied amino residues. Hence, the term "crystalline" regions, has been regarded with

suspicion, since the difference between the normal crystalline and amorphous phase is not well defined. In fact it has been suggested that the difference may be one of orientation¹⁴². The shoulder at 126°C, weak as it is, would reflect a preferred state of several less permanent polymorphic states which will occur above 106°C, due in part to the above mentioned side chains and residues acquiring different orientations, and also to the tendency of the "coiled coils" to flow.

The symmetry of the loss peak at 25°C, is indicative of a single mechanism being responsible for its promotion, and is attributed to the arresting of the "coiled coils"; It may be expected to cause a relatively high energy loss. The rate of increase of bending modulus at lower temperatures (see Fig.30) and the partially formed asymmetrical peak at about 60°C, are strongly indicative of a further loss maximum due to the motions of the various side chains. Their semi-rigidity and relative bulk would give rise to considerable energy loss in the process of their arrestment.

The loss tangent and relative bending modulus curves (Figs.9 and 19) show considerable spread. The shapes of the curves are essentially similar, but particularly in the loss curve, maxima and minima are seen to occur at different temperatures from one fibre to the next, and have

significantly differing values. This, however, is not unexpected, since not only is wool a natural fibre and for this reason subject to no small variation between fibres, but also wool has a more complex structure than any other natural fibre. Hence, a difference in the amount of unsatisfied side chains will cause a shift in the apparent loss maximum at 60°C etc. Furthermore, the rate of bond breakdown is related to temperature (see p.9) and conversely, the temperature of bond breakdown is dependent on the rate. Since one of the limitations of the technique of this investigation is that the time which elapses from one temperature to the next, especially below room temperature, cannot be rigidly controlled, another element of inconsistency in the temperature location of transitions is introduced.

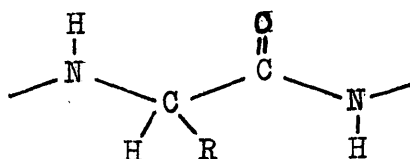
The shape of the bending modulus curve is in accordance with that predicted from the foregoing arguments, and a maximum in the loss curve is always accompanied by a maximum rate of change in the bending modulus.

From Fig.30, it will be seen that below 20°C , the average rate of decrease in bending modulus is slightly greater than the average rate of decrease above 20°C and up to about 80°C , while above 80°C , the average rate of decrease appears to be accelerated. These occurrences are consistent with the loss modulus data, where it will be seen that,

making the same temperature divisions, more energy is dissipated below 20°C than above 20°C and up to 80°C, while above 80°C, the loss modulus rises and will by prediction, continue to do so due to the tendency for macroscopic flow.

A final point is worth noting. Warburton¹⁴³, working at low frequencies and at temperatures of 25°C and 40°C at 70% relative humidity, proposed that over this temperature range, the only effect of heat was to reduce internal friction. This is in accord with the present findings, with the reservation that as the temperature is raised, the total elastic response is reduced by virtue of the fact that certain partially stress bearing elements have become more viscoelastic.

Silk: It would appear almost paradoxical that silk, whose chemical constitution is much simpler than that of wool, exhibits the more complex loss curve. It has a suggested degree of crystallinity of 80%¹⁴² and has fully extended



polypeptide chains which do not assume a coiled configuration, although in crystalline regions may lie in closely packed "pleated sheets"¹⁴⁴. 50% of the side chains (R), are

glycine (-H) and 25% are alanine (-CH₃) which being short do not restrict the formation of crystallites. While these side chains are inactive, serine (-CH₂OH) and tyrosene (-CH₂--OH), which occur with moderate frequency are active on account of their hydroxyl groups. There are relatively few acidic and basic side chains so that salt linkages are rare; cystine bridges do not occur at all.

With reference to Figs. 30 and 31, the relatively high bending modulus, and change thereof with temperature is in keeping with the characteristics of a highly crystalline polymer. The amorphous phase contributing to the bending resistance is small, and it would generally be expected, that even large scale changes in the amorphous regions, would cause a relatively small change in bending modulus. The average rate of increase in bending modulus from high to room temperatures is greater than the rate of increase which occurs from room to sub-normal temperatures. This suggests that the secondary bonds play a greater part in conferring bending stability on the fibre at normal temperatures than do the barriers to rotational movements of segments. A molecular interpretation is put to this feature presently.

The loss modulus assumes a relatively low overall

magnitude (although large when compared with wool, whose low internal friction has been explained). The relatively low magnitude is attributable to the comparative scarcity of secondary bonds since not only is the amorphous domain small but the possibility of secondary bonding is severely limited due to the large number of inactive side groups. Hydrogen bonds will nonetheless exist and as will be seen, the effect of van der Waals forces is considerable.

Two definite peaks and a shoulder are realised above room temperature; at 47°C , 80°C and 117°C respectively. (The fact that the peaks* straddle the apparent hydrogen bond peak of wool almost exactly, appears to be purely coincidental and not related to a unique similarity of the two materials, fibroin and α -keratin). On the other hand, the 80°C peak is attributed to hydrogen bond breakdown, which coincides with the estimated hydrogen bond peak of wool. As the molecules are separated on account of these breakages, the van der Waals forces will be ruptured but do not appear as a higher temperature peak for similar reasons as explain the absence of such a peak in wool. Now, van der Waals forces are known to exist between atoms and molecules even although they are completely uncharged and carry no permanent dipole¹³⁷. Of the side chains in fibroin, many have been termed inactive but for the above

reason, their inactivity is by no means absolute, and van der Waals forces can become effective. As has previously been stated, they are weak, but on account of their number, are regarded as being responsible for the 47°C peak, i.e. van der Waals forces existing between non-hydrogen bonded chains and side chains. The shoulder at 117°C , as in the case of wool, may be the result of a preferred polymorphic phase arising from side and main chain re-arrangement. It will be observed that the average rate of increase of loss modulus above the temperature of the minimum in the loss modulus-temperature curve (100°C for silk), is greater in the case of silk than in the case of wool. This is anticipated since there are many more side chains and main chains, according to the proposed fibre structures of the two fibres, in silk, which are tending to macroscopic flow in the temperature range covered.

The maximum at 0°C in silk will in a similar way to wool, manifest itself as a result of main chain mobility being arrested. Its greater height in relation to that of wool, is a result of the greater number of side chains which can be induced to vibrate, remembering that in wool, the effective number of such chains is greatly reduced by the "coiled-coil" structure. A second low temperature transition is expected with considerable internal friction

on account of the number and relative rigidity of the inactive side chains.

It is normally expected that a large loss peak is accompanied by a high rate of change of bending modulus, and a weak or low loss peak, is accompanied by a low rate of bending modulus change. With silk, the reverse happens, the bending modulus on the average changing more rapidly above room temperature than below. The explanation appears to lie in the overall rigidity of the side chains, which whether arrested or not, contribute considerably to the bending resistance, so that their "freezing" in itself does not add greatly to the bending resistance, while the freezing of the main chains from their partially mobile condition at 20°C to their consolidation at 0°C, is similarly of no great consequence. Above room temperature, the rupture of secondary bonds, weak as they are in the case of van der Waals forces, and few as the hydrogen bonds are, give rise to a greater mobility of side and main chains, and in a broad analogy to the argument of Guthrie¹⁶, who relates a fall in initial tensile modulus with a decrease in crystallinity, the bending modulus can be expected to fall considerably (on account of the amorphous contribution in this investigation).

As in the case of wool, loss maxima are accompanied

by appropriate bending modulus reactions, while the variation from one fibre to the next is accountable for similar reasons as to those proposed for wool.

Fibrolane. To state that the molecular configuration of Fibrolane lies between that of silk and wool is an oversimplification, as would also appear to be the case when Peters and Woods¹³⁶ describe Fibrolane as consisting of β crystallites and comparatively random amorphous domain. Synthetic polypeptides, although not from casein as a source have been produced¹⁴⁵ in the α -keratin mould, while the "~~coiled-coil~~^{cabled}" configuration found in wool keratin is by no means peculiar to that material, and is proposed by Rich and Crick¹⁴⁶ to exist in collagen.

Globular proteins, and casein, from which Fibrolane is produced in its natural form prior to denaturisation, are said to exist in a helical configuration¹⁴⁷ like α -keratin; while Pauling and Corey¹³⁷ suggest that their α -helix may be the basic configuration in at least some, if not all globular proteins. If this is so, then it is quite probable that on stretching during the process of denaturisation, the regenerated protein assumes a β -helical configuration. The periodicity of $7 \overset{0}{\text{Å}}$, found in regenerated proteins, which coincides with that of fibroin, would be due to stretched

α -helices, possibly in "~~coiled coils~~^{cables}", and not to a simple β -keratin, which is^{also} identical in periodicity with fibroin.

Furthermore, from X-ray data¹⁴⁸ of regenerated proteins, the statement is made that "a random or coiled molecular structure is prevalent within the fibre and that there is little or no orientation."

The closeness of the data for wool and Fibrolane indicates that not only are the ratios of the viscoelastic to the elastic components similar, but also that the magnitudes of each are very nearly the same (c.f. silk, whose loss tangent is of the same order of magnitude but the individual components, both plastic and elastic are considerably greater than for wool and Fibrolane). Hence, it would not be unreasonable to find a great deal of similarity in the molecular structures of wool and Fibrolane.

Chemically¹⁴⁹, they differ only slightly, the main feature in this difference being a higher sulphur content in wool and a consequent absence of cystine linkages in Fibrolane.

The loss curves for Fibrolane are interpreted in substantially the same way as the loss curves for wool, bearing in mind that "~~coiled coils~~^{cables}" may exist, but since the molecules are stretched, the hydrogen bonding in these "~~coiled coils~~^{cables}" will be less intra molecular and more inter-molecular as occurs in the silk lattice according to the

"pleated sheet" suggestion.

The apparent hydrogen bond peak at 68°C is expected to truly lie at about 80°C. The low temperature peak at -3°C is much less well defined than that of wool at 2½°C. If the "coiled coils" in wool are α-keratinous and those proposed in Fibrolane are β-keratinous, the latter can be envisaged as long and thin, and the former as short and bulky. As a consequence, the free space per unit volume would be greater in Fibrolane, and account for a lower temperature arrestment. The similar chemical constitution would equalise the rotational barriers and cause a maximum of similar magnitude in both wool and Fibrolane. A second low temperature transition could arise from the motion of the side chains, and it is a side chain mechanism which is thought to be responsible for the vagueness of the -3°C peak, and the continued high loss modulus (in comparison with wool). Since the chains of the "~~coiled coils~~^{cables}" are fully extended, the side chains will be further apart and the possibility of inter side chain bonding proportionately reduced at normal temperatures. Hence on reducing the temperature, and, as it seems, at a temperature below the "~~coiled coil~~^{cable}" maximum, these side chains will form cohesive bonds between neighbouring side chains. Moreover, this phenomenon will add to the energy dissipated due to the

surmounting of rotational barriers as temperature is lowered.

The shape of the bending modulus curve is in accordance with that of the loss curve. The average rates of change of bending modulus with temperature vary in the same way as those of wool, and are accountable for the same reasons. The higher bending modulus of Fibrolane will be mainly due to the extended polypeptide chains being less flexible than the α chains in wool.

The Proteins and Nylon 66.

The fact that every third main chain linkage in the proteins studied is of the polypeptide type, that this linkage is common, in lesser abundance, to nylon, and that consequently these fibres are capable of considerable hydrogen bonding, suggests that certain similarities in dynamic behaviour might be observed.

When the data of Hsu¹ is presented in loss modulus form, a high temperature 120°C peak, a slight 50°C peak, a low -35°C peak, are observed, and a second low temperature peak is predicted.

Of the three proteins examined, it may be expected that in certain respects, nylon should most resemble silk,

since in each, the main chains exist in a planar fully extended form. In as much as silk exhibits two distinct loss modulus peaks at 47°C and 80°C (while only one corresponding peak is detected in wool and Fibrolane), this is true. As in polyethylene, nylon has many van der Waals forces between its adjacent CH_2 groups, and in the light of this, the 50°C peak of nylon would correspond to the 47°C peak of silk - it is due to the van der Waals forces between non hydrogen bonded chains in the amorphous regions. While the 120°C peak is attributed to hydrogen bonds, it can only be assumed that Hsu's¹ particular nylon had some additional constraints conferred upon the chains in the amorphous regions, by the crystallites, for Woodward et al.⁵¹ and Kanaguchi⁵⁰ found hydrogen bond peaks at 77°C and 90°C respectively, which are closer to that of silk at 80°C . The height of this loss modulus peak in nylon is much greater than that of the protein fibres, and reflects the greater degree of hydrogen bonding. This is to be expected if in the "coiled coils" of wool and Fibrolane most hydrogen bonds are satisfied in what are effectively crystalline regions, and in silk, hydrogen bonding is considerably restricted by the many inactive side chains.

In the temperature range from 10° to 60°C the loss modulus of nylon has almost the same value as that for wool

and Fibrolane; the loss modulus of silk is considerably greater. This is expected since the stress bearing elements in the amorphous regions at these temperatures are small in wool and Fibrolane, (for reasons discussed earlier) and also in nylon (the hydrogen bonds are not stressed to any great extent, and the van der Waals forces are known to be weak and do not contribute greatly to the energy loss). In silk however, considerable side chain activity will increase the magnitude of rotational barriers.

As in the proteins, nylon has two low temperature peaks, at -23°C and -77°C ⁵¹, and -40°C and -120°C ⁵⁰. The -23°C , -40°C peak is considered to be due to segmental motions of the non hydrogen bonded amide groups, the -77°C , -120°C to the co-operative movement of the CH_2 groups between amide linkages^{50,51,52,53}. No distinct parallel can be drawn between the low temperature transitions in nylon and the proteins. It is just possible to say that the side chain transition of the proteins is related to the CH_2 transition of nylon, in so far as the amide linkage is absent in both. However, in nylon, a very distinct difference in the number of CH_2 and amide linkages is present, and to relate the low temperature transitions to these is apparently correct. In the proteins, between every amide linkage, there is a CHR group, and it is reasonable to expect

that the main chains will behave with an average rigidity. (CH₂ linkages are semi flexible, amide groups are more rigid which also contributes to the separation of the two transitions in nylon.)

Thus the interpretations of the low temperature transitions in the proteins are thought to be correct, and the reason for their occurrence at higher temperatures than the low temperature transitions of nylon, is the additional side chain constraint.

Cellulose Fibres: Ramie, Fortisan

The dynamic bending moduli of ramie and Fortisan (Fig.31) are high in relation to those of other fibres and reflect the fact that the cellulose chain molecule is very rigid. Moreover, in the case of these fibres, their stiffnesses are the greater for their high degrees of crystallinity which by an X-ray diffraction method were determined as 70% and 50% for ramie and Fortisan respectively (c.f. viscose rayon 30%)¹⁵⁰, and by an acid hydrolysis method as 95% and 83% for ramie and Fortisan respectively (c.f. viscose rayon 68%)¹⁵¹.

A lesser degree of randomness will enhance the promotion of intermolecular hydrogen bonding in amorphous domains,

and will contribute to the high resistance to bending forces. Ramie, high stretch viscose, which can be regarded in this instance as similar to Fortisan, and ordinary viscose, are said to have degrees of orientation of 0.97, 0.88 and 0.54 respectively. These degrees of orientation represent an average orientation of both the crystalline and amorphous regions and vary from unity for full orientation to zero for random orientation.¹⁵²

Due to the fact that ramie has a higher degree of crystallinity and orientation and that the average chain length of molecules in crystalline regions is four times as great in ramie as in Fortisan¹⁵³ it would be expected that a greater difference in the bending moduli of the two fibres should exist. It is however, a well known fact that regenerated fibres possess a hard skin and a soft core and this property of Fortisan would appear to some extent to compensate for its lower degrees of crystallinity and orientation, and shorter chain length; and bring the value of its bending modulus to one approaching that of ramie.

Figs. 30 and 31 show that as the temperature is raised from room temperature to 160°C, the difference between the two bending moduli becomes progressively more pronounced, and that the rate of decrease of the bending modulus of Fortisan with increasing temperature is greater

than that of ramie. This is consistent with the idea that the proportion of amorphous fibre contributing to the bending modulus is present in greater quantity in Fortisan and that the relatively random molecules contained therein, being afforded a greater degree of mobility as a result of hydrogen bond breakage and increased free space for rotation, offer less resistance to the external bending force.

Similarly, on lowering the temperature from room temperature to -60°C , a smaller increase in the bending modulus of ramie than of Fortisan is to be expected since the total amount of molecular rotations to be "frozen" as the free space is reduced, is smaller. (This is explained later.)

The smooth and featureless change in bending modulus with changing temperature would indicate that the consolidation of a three dimensional network in the case of ramie and Fortisan is either a complicated multistep process in which very small differences exist in the mechanical responses of the various polymorphic phases, but are undetectable by this method, or that a continuous and relatively simple process takes place in the range covered. By examining loss tangent or loss modulus data, it is seen that a compromise exists. (Figs.29 and 32).

Hsu¹ reported weak loss maxima at 90°C and -20°C and

proposed the possibility of a still lower peak and a high temperature transition for viscose rayon, while Tokita³⁷ observed a dispersion at 80°C and Dunell and Price³⁶ one at -40°C. No such maxima are observed for ramie and Fortisan in the temperature range -60 to 160°C. The 90°C dispersion may exist and an argument is later put forward in its favour. The cause of its existence in viscose rayon is attributed to the rupture of hydrogen bonding in amorphous regions, while the reason for its experimental absence in ramie and Fortisan may be attributed to the lack of sufficient hydrogen bonding in the comparatively small amorphous space, to render the transition experimentally observable. Moreover, it may be embraced in a higher temperature transition which is predicted by the rapid rate of increase in the loss factor with increasing temperature, and if it exists, is due to motions of whole chains in the amorphous regions.

The low temperature transition of viscose rayon at -20°C is ascribed to the freezing of whole chains in amorphous regions¹. A similar transition in ramie and Fortisan is predicted (from both the loss curves and the bending modulus curves) at a temperature lower than -60°C for ramie and still lower for Fortisan. This proposal of the sequence of occurrence of the loss maxima is further supported

by the fact that minima occur in the loss curves at about 40°C for viscose rayon, 20°C for ramie and 5°C for Fortisan. (These are the temperatures at which the respective fibres assume their most natural molecular configuration.) Although the percentage amorphous area in the fibres diminishes in the order, viscose, Fortisan and ramie, and consequently it might be expected that the low temperature loss peak should occur at the lowest temperature for viscose on account of the fact that more segmental or chain motions are to be arrested in the amorphous area, than in the more crystalline ramie and Fortisan, the reverse happens, as proposed above. This is not surprising in the least, as the amount of hydrogen bonding will diminish in the order viscose, ramie and Fortisan at temperatures of 40°C , 20°C and 5°C , respectively. Due to this, the free space in viscose is smaller than in Fortisan and as the temperature is reduced, the rotational motions of whole chains will be arrested earlier. Similarly, the predicted loss maximum due to the freezing of whole chains will occur at the lowest temperature in the case of Fortisan.

A significant feature of the loss curves of ramie and Fortisan is that they intersect at about 85°C . At normal temperatures, the loss factor for ramie is higher than that for Fortisan. This may be accounted for by the

greater degree of hydrogen bonding as a result of the greater chain length of ramie molecules. Above a temperature sufficiently high for thermal agitation to rupture the hydrogen bonds, the energy dissipated per cycle will be dependent upon the resistance to flow of whole chains. Since the amorphous portion in Fortisan is greater than in ramie, the total molecules resisting flow should be greater and consequently the loss factor higher after rupture of hydrogen bonding. Since this is the case, it would appear that while a loss maximum due to hydrogen bonding cannot be experimentally detected, it does in theory and practice exist, at an estimated temperature of 80°C.

Summarising, the following points can be made. The temperature of the high temperature transition in cellulose, involving the rupture of hydrogen bonds, is highly dependent on the nature of the bond, while the magnitude of the loss maximum depends on the total energy - determined by the number and nature of the bonds, and additional constraints.

	Temperature of maximum	Loss modulus $\times 10^{10}$ dynes/cm ²
viscose rayon	85°C	0.30*
ramie	80°C	0.34
Fortisan	80°C	0.33

* based on data from humidity experiments and Hsu¹.

The above figures show that the maximum attributed to hydrogen bond rupture occurs at a similar temperature for all three cellulose fibres. The presence of a still higher temperature maximum at different temperatures influences the precise location of the hydrogen bond peak.

The loss modulus is of a similar order of magnitude for the three fibres.

A greater number of hydrogen bonds is thought to exist in the rather amorphous viscose rayon, than in ramie and Fortisan, while of the ^{last} ~~latter~~ two fibres, ramie is thought to have a slightly greater degree of hydrogen bonding for reasons proposed earlier.

Since the magnitude of the loss modulus is highly dependent on the number of bonds, it is evident that relatively few as these bonds may be in ramie and Fortisan, a considerable degree of restraint is imposed upon them, probably as a result of the high degrees of crystallinity of these two fibres; and their resultant loss peaks are brought to a similar height as the peak for viscose rayon.

The temperature ^{at which} of a low temperature transition occurs would appear to be ^{depend on} ~~due to~~ the amount of free space and the rotational barriers. Since the rotational barriers will be of the same order for ramie, Fortisan, and viscose (due

to their identical chemical constitutions) the locations of the low temperature maxima will depend on the free space and will occur in the order as previously proposed. The heights of the maxima will be primarily due to the total rotational barriers, but since they occur outwith the temperature range covered in this investigation (in the case of ramie and Fortisan), this proposition cannot be substantiated by fact.

Modified Regenerated Cellulose Fibres: Acetate fibre
and Tricel.

That Tricel has a higher bending modulus than acetate fibre is clearly shown in Fig.31, and that it experiences a greater change in bending modulus, with temperature, is more clearly shown in Fig.30. The higher bending modulus of Tricel is primarily associated with its higher crystallinity. Russell and van Kerpel³⁸ observed a large and possibly greater decrease, with increasing temperature, in the torsional modulus of cellulose acetate, than of cellulose triacetate, and associated this fact with the lower crystallinity of the former. Loss modulus data (Fig.32), however, support the experimental bending modulus data, since they represent the transformation of the properties of stress bearing elements from viscoelastic to elastic

and vice versa. The magnitude of the Tricel loss modulus curve is substantially higher than that of the acetate fibre, which, considering the case of decreasing temperature, indicates that that volume of amorphous fibre which at high temperatures did not contribute to the bending resistance, contributes to a much greater extent at lower temperatures in the case of Tricel - this in spite of its smaller amorphous volume.

This reasoning applies to the results of the present investigation, but may not apply to Russell and van Kerpel's work³⁸. Their polymers may have differed in molecular configuration, and they measured the torsional modulus at low frequencies while this work involved the bending modulus at audio frequencies.

The shapes and heights of the acetate fibre and Tricel loss tangent curves (Fig. 29) are very similar, while the same is true of the shapes of the loss modulus curves. This is not unexpected when the former material has 2.3 acetyl groups per glucose residue and the latter is chemically only slightly different, in that acetylation of available hydroxyl groups is complete. However, certain significant differences do exist, in the dynamic mechanical responses as will become apparent in the following discussion.

In the dilatometric determination of transitions,

Mandelkern and Flory¹⁵⁴ found these to exist at 60°C and 120°C in cellulose acetate and 30°C and 105°C in cellulose triacetate, while in similar experiments, Nakamura³⁹ found corresponding transitions. Russell and van Kerpel³⁸ observed dilatometric transitions at 55°C and 115°C in secondary acetate and at 40°C, 120°C and 155°C in cellulose triacetate. The general agreement between the investigations was good.

In dynamic experiments at audio frequencies Nakamura³⁹ reported a damping peak at 120°C for cellulose acetate and at 60°C and 180°C for cellulose triacetate, while Russell and van Kerpel³⁸ observed damping peaks at -38°C, 120°C (shoulder) and 195°C for acetate and at -48°C, 100°C (shoulder) and 175°C for cellulose triacetate. Certain dilatometric transitions have been associated with damping peaks e.g. Nakamura³⁹ considered his 60°C peak to correspond with Mandelkern and Flory's¹⁵⁴ 30°C dilatometric transition, and Russell and van Kerpel³⁸ related their 175°C peak with their 155°C dilatometric transition for cellulose triacetate. The higher frequency of the mechanical measurements is expected to shift a transition to a higher temperature^{1,38}.

Little molecular interpretation has been put to the results. The transitions observed by Mandelkern and Flory¹⁵⁴

were representative of " 'freezing-in' temperatures for different types of motion", while in parallel reasoning to that of Deutsch, Hoff and Reddish⁷⁰, Russell and van Kerpel³⁸ believed that the low temperature transitions (-38°C , -48°C) were associated with the mobility of acetate groups, while the high temperature transitions (175°C , 195°C) were associated with the movement of groups of atoms in the anhydroglucose chain.

In this work, no definite peaks, but only shoulders, are detected in the loss curves. These occur at 105°C , 60°C and 11°C in the case of acetate fibre and 98°C and 14°C in the case of Tricel. Peaks, however, which lie outside the temperature range covered, are predicted at estimated temperatures of -60°C and 175°C for acetate fibre and -70°C and 165°C for Tricel. The variation of the higher temperature peaks and shoulders, is in accord with a conclusion of Nakamura³⁹, that high temperature transitions occur at lower values with increasing acetyl content.

As a result of acetylation, there are few hydroxyl groups in acetate fibre, and none in Tricel, so that the possibility of hydrogen bonding between chains is considerably reduced in the former, and non-existent in the latter. On this account and due to the different amorphous volumes

in the two fibres, certain differences in the loss curves are expected.

Thus, the shoulder at 60°C in the acetate fibre loss curve, to which no corresponding shoulder is observed in the Tricel loss curve, is attributed to hydrogen bond breakdown, which but for the rupture of van der Waals forces between non hydrogen bonded groups at a lower temperature, and a consequent energy drop due to the liberation of these groups would occur at a slightly higher temperature and take the form of a more pronounced peak.

It is claimed that commercial Tricel has a so-called second order transition at 97°C ¹⁵⁵. The shoulder in the loss tangent curve at 98°C (Fig.29) which appears more pronounced in the loss modulus curve (Fig.32) is regarded as corresponding to this transition, while the higher temperature peak for acetate fibre is thought to be due to a transition of a similar type. It is proposed that in both fibres the mechanism involves a certain amount of main chain movement facilitated largely as a consequence of the removal of the aforementioned restrictions. Presumably, the higher temperature peaks are accounted for by the reasons put forward by Russel and van Kerpel³⁸.

The shoulders reported at 14°C and 11°C for Tricel and acetate fibre, are without precedent and it is doubtful

that they correspond to the dilatometric transitions at 40°C and 55°C respectively for these fibres, since the dynamic maxima are expected to occur at higher temperatures. However, since the predicted high temperature maxima occur at lower temperatures than the determined 175°C , 195°C peaks and are regarded as being due to the same mechanism, it would not be unreasonable to associate the predicted low temperature peaks at -70°C and -60°C with the experimentally determined -48°C and -38°C ³⁸ peaks. The fact that the low temperature peak as found by Russel and van Kerpel³⁸ was sharper in the case of cellulose triacetate, and that the predicted low temperature peak appears sharper in the case of Tricel, further supports this association. The mechanism involved is probably the arresting of the motion of acetate groups. The shoulders at 14°C and 11°C are thought to be due to the early stages of anhydroglucose chain arresting, the development of a more definite peak at a lower temperature being prevented by the onset of the freezing of the acetate groups.

The higher loss modulus of Tricel would perhaps require explanation, since all other factors being equal, the more amorphous material would be expected to yield a higher energy loss on account of the greater number of rotational barriers, secondary bonds etc.

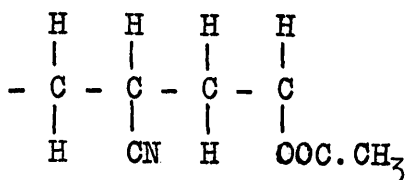
However, the ratio of the degree of polymerisation in acetate fibre to that in Tricel is 9 to 10¹⁵⁶. This fact, together with the greater number of bulky acetate groups in Tricel, causes larger rotational barriers; a fact which apparently more than compensates for the greater amorphous volume usually associated with acetate fibre.

Synthetic Fibres: Acrilan A and Acrilan B.

It was the purpose of this investigation to determine whether any significant difference in the dynamic properties of the two types of Acrilan existed and if so, what could account for it. In previous work, Acrilan B was found to have a significantly higher resilience¹⁵⁷ and an initial static Young's modulus (static at 1% extension) of 24.1 gm./denier compared with an initial static Young's modulus of 19.2 gm./denier for Acrilan A¹⁵⁸. In the course of that work, it was observed that Acrilan B has a 6.9% crimp and Acrilan A, 13.6% crimp - which could have contributed to differences in mechanical behaviour.

If differences in dynamic properties, bending modulus and loss modulus exist, they would normally be the result of a difference in the manufacturing process, in the case of the former, and as a result of fibre composition in the case of the latter¹⁵⁹.

Chemically, it would be assumed that both fibres have the same constitution; i.e. copolymers, 85% acrylonitrile and 15% of vinyl acetate, giving the general formula¹⁶⁰.



On the other hand, it is believed that the copolymer is allowed to stand for a time prior to the spinning of Acrilan A, while Acrilan B is believed to be the product of a completely continuous process.

With reference to the loss curves, the weak shoulders apparent in the loss tangent curves (Fig.29, Table 53) take on much more definite shapes when expressed in the loss modulus form (Fig.32). In the latter curve, high temperature peaks at 110°C and 100°C, and room temperature shoulders at 25°C and 10°C are observed for Acrilan A and Acrilan B respectively. No low temperature transitions are observed throughout the temperature range, and the loss modulus of Acrilan B is higher than that of Acrilan A throughout.

As in the case of Orlon¹⁶¹, hydrogen bonds will be expected to exist between the α hydrogen atom of one chain, and the nitrile nitrogen of its neighbour; the high temperature transitions are attributed to these. The fact that no

low temperature transition is recorded would suggest that the gross entanglement of main chains (such entanglement is considered to exist in certain acrylic polymers⁷¹) is such as to cause the freezing of main chains which are not hydrogen bonded at higher temperatures than are usual.

Localised interaction of side chains and immediately adjacent main chains in acrylic polymers, has previously been regarded as being involved in transitions not far above room temperature. While the room temperature transitions are thought to be due to the freezing of main chains, the location and loss modulus may be affected by such interaction.

Although there is no indication in the loss curves of an imminent low temperature transition, the continuously increasing bending modulus (which is more apparent in the relative bending modulus, Fig.30) suggests that a low temperature transition may in fact occur, far beyond the range covered. If in fact it does, then in parallel reasoning to Hoff, Robinson and Willbourn⁷¹, it would be the result of linear side chains having sufficient flexibility to take up more than one spatial configuration.

The higher bending modulus of Acrilan B is consistent with its better resilience and possibly its higher initial static Young's modulus. It seems likely therefore that the crimp difference of the two fibres was not solely responsible

for the observed differences in mechanical behaviour^{157,158}.

The dynamic data indicate that while the chemical constitutions are thought to be the same, the assumed molecular configurations within the two fibres are not.

An off-white shade observed in Acrilan A would be indicative of a form of degradation of the viscous copolymer having taken place while "standing" prior to spinning. The lower static initial Young's modulus and dynamic bending modulus would support this statement. The lower high temperature loss modulus is indicative of less hydrogen bonding; this could be the result of a reduced degree of polymerisation. On the other hand, a lesser degree of hydrogen bonding would reflect a greater volume of free space and a subsequent lowering of the low temperature transition, while the greater number of rotational barriers (due to the greater quantity of long chain molecules and also to the increased length of the side chains relative to the main chain) would cause a higher loss modulus. As the low temperature transition of Acrilan A is at a higher temperature and has a greater loss modulus than Acrilan B, it is thought that while a form of degradation may assist in the divergence of dynamic behaviour of the two varieties of Acrilan, it is not solely responsible - if at all it exists.

A second possibility is that as the copolymer of Acrilan A is allowed to stand prior to spinning, it "settles down" more uniformly, and Acrilan B has a greater degree of gross entanglement. Hydrogen bonding would again be enhanced in the latter, and promote the experimentally observed higher loss modulus in Acrilan B around the 100°C region. However, applying the same reasoning as for the proposed degraded Acrilan A, to the room temperature loss modulus, a theory based solely on "gross entanglement" cannot be accepted to explain the divergence in dynamic behaviour.

In both of the above arguments, the amorphous volume in each Acrilan has been assumed to be the same. If it is possible for this so-called gross entanglement to be reduced in the amorphous areas of Acrilan A as a result of settling down, so too is it possible that it may assume a higher degree of crystallinity. The fact that the room temperature transition occurs at a higher temperature and with a lower loss modulus could be explained by a lower amorphous content; there is less total free space and fewer total rotational barriers. The high temperature loss modulus would be lower on account of a fewer number of hydrogen bonds. The loss data appear to well satisfy this proposal, but then why should the less crystalline material have the higher bending modulus, and initial static Young's modulus, especially, with

reference to the former mechanical parameter, at 20°C, when the main chain rotations in the amorphous region are frozen in the more crystalline material, thus adding to the bending resistance, while they are still partially mobile in the less crystalline material? If the foregoing arguments can stand, then the degradation of the more crystalline Acrilan A, and the fact that it is not so grossly entangled and thereby less of a quasi three-dimensional network, in amorphous regions than the Acrilan B variety, would appear to be predominating factors over the higher crystallinity of Acrilan A. (It should be remembered that the degree of crystallinity is poor in most acrylic polymers^{1,161}, and that the amorphous regions play a considerable role in the determination of fibre properties). The high temperature transitions are satisfied by all three arguments, but the room temperature transitions, only on the basis of the greater amorphous content of Acrilan B. Hence for the room temperature transitions, the greater amorphous volume of Acrilan B appears to be the dominating factor.

The faster drop in relative bending modulus of Acrilan B above the 100°C region (see Fig.30) is indicative of the onset of motion of a greater number of chains. This corresponds with the higher degree of hydrogen bonding. Approaching room temperatures, and on further reducing the temperature,

the relative bending modulus of Acrilan B shows the sharper rise. This again is consistent with the higher loss modulus of Acrilan B at the room temperature transition and at lower temperatures still.

Acrilan and Orlon

Hsu¹ reported loss tangent maxima at 70°C and 110°C for Orlon, and associated the former peak with rotations of non hydrogen bonded main chains, and the latter peak with hydrogen bond breakdown. A very slight low temperature shoulder was ignored. This, however, takes the same more definite shape of the room temperature Acrilan shoulders, in a loss modulus curve, the point of inflection occurring at about -20°C. Since Orlon is thought to be pure acrylonitrile, and lacking in the bulky acetate groups that occur in Acrilan and effectively hinder rotation in the main chains, a main chain transition in Orlon would be expected to occur at a lower temperature than in Acrilan, and have a lower loss modulus. Both of these requirements are satisfied by the -20°C shoulder, and neither by the 70°C peak.

It is thought that the 70°C peak which like the -20°C shoulder and 110°C peak, was markedly pronounced when transferred from loss tangent to loss modulus as a measure, was due to hydrogen bonding between side chains of non hydrogen

bonded main chains. Being fewer in number, their associated loss modulus was smaller. The occurrence of the first hydrogen bond peak, 40°C earlier than the second, is thought to be due primarily to the additional straining of the hydrogen bonds between the side chains, caused by the chain mobility of the non-hydrogen bonded main chains.

The 110°C peak had a much higher loss modulus than the corresponding Acrilan peaks. This is to be expected since the hydrogen bonds are present in greater quantity due to the absence of the acetate groups present in Acrilan. Unlike Acrilan, Orlon appears to have no very low temperature transition (from the shape of the loss curves and the fact that at -60°C the bending modulus appeared to be approaching a limiting value), which suggests the absence of flexible, non hydrogen bonded side chains present in other acrylic polymers and Acrilan.

Polypropylene

The newness of polypropylene as a commercial fibre, merits a few introductory comments regarding its structure.

Natta and Corradini¹⁶² put forward a theory reasonably widely accepted, that on account of the methyl groups, a planar structure is impossible. "For instance, in the case of polypropylene, a planar structure would result in a

distance of only $2.5 \overset{\circ}{\text{Å}}$ between the nuclei of two carbon atoms of successive methyl groups, which is very unlikely, because certain hydrogen atoms of the methyl groups would be as a result too near to each other, and this situation is in conflict with the requirements of the minimum energy postulate."

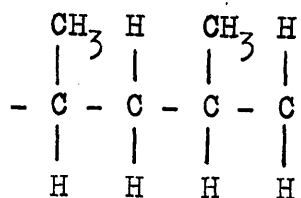
Instead they proposed a helical structure in which the successive monomeric units are arranged on a three fold helix, and that the helices could be left or right handed. The methyl groups were thus suitably accommodated.

Ranby et al.¹⁶³, employing electron microscopy and small angle X-ray scattering determined that crystallisation of polypropylene developed in spirals, pyramids or consecutive layers, but the mechanisms of growth and the nucleation were not clear.

Slichter and Mandell¹⁶⁴ employed a proton magnetic resonance method, which was useful in establishing that the methyl groups were responsible for a low temperature transition believed to exist in polypropylene. Sauer et al.⁵⁷ had, however, attributed a similar low temperature transition to small scale motions of relatively short segments.

To form a basis on which to interpret the results of the present investigation, the structural data of Henstead¹²⁶ are used: namely that the polypropylene is unbranched, has

a density of 0.90 gm./cc., a 75% degree of crystallinity, is isotactic and has the general formula



Referring to the loss curves (Figs.29,32) a very definite room temperature peak (12°C) indicative of a glass transition is observed. This transition has been observed by Sauer et al.⁷⁵ for a 78% crystalline, isotactic polypropylene of density 0.914 gm./cc. at about 25°C , while Reding¹⁶⁵ found such a transition at about -20°C . The main reason for the spread of results is that Reding¹⁶⁵ worked with volume-temperature and stiffness-temperature changes, Sauer et al.⁷⁵ at frequencies of about 1500 c/s., and in this investigation much lower audio frequencies were used. From the rapidly falling bending modulus (see Fig.30) and the increasing loss factor (observed in Fig.29 and predicted from Fig.32) a high temperature peak associated with main chain mobility and the onset of crystalline melting, is predicted. An equivalent peak was observed by Sauer et al.⁷⁵

The comparatively fast increasing bending modulus at -70°C (see Table 51) and the increasing loss tangent and loss modulus (the latter already showed a partial peak) are

strongly indicative of a low temperature peak at about -80°C . Moreover, the height of this loss modulus is such as to suggest considerable motions. Since the degree of branching is considered to be nil¹²⁶, a side chain motion is not involved.

Sauer et al.⁷⁵ observed a small low temperature loss tangent peak at about -50°C . Since the loss tangent represents the ratio of the viscoelastic to the elastic component, it does not represent the energy dissipated. Were a loss modulus peak considered, they would have observed a much higher loss peak as was found in this work, and for this reason their aforementioned mechanism may not be valid - indeed, considerable, and not small scale motion appears to be involved, in which methyl groups, which according to Slichter and Mandell¹⁶⁴ would not couple strongly with mechanical excitation, may only be a contributing factor. It is thought therefore that the -80°C peak is primarily the result of a second glass transition - and it is of interest to note that Sauer and Kline⁷⁴, found such a peak at -100°C . If different crystallites can form according to Rånby et al.¹⁶³, and left handed and right handed helices exist¹⁶², it would not be unreasonable to expect that different degrees of constraint due to the crystalline regions, on the amorphous regions exist. Thus the 12°C peak reflects the

arresting of amorphous chains, not arrested by van der Waals forces, which are considerably restrained by crystallites, and the -80°C peak, amorphous freezing of much lesser restrained chains, in the amorphous regions.

Referring to the polypropylene loss tangent curve, a shoulder at 51°C is observed. A moderately high temperature peak is often associated with secondary bond breakdown, and in polypropylene could only be the result of van der Waals forces. A peak however is largely obscured by the subsequent fast fall in loss modulus after the glass transition.

Polypropylene and Polyethylene

Chemically, these fibres differ only in that the former has a methyl group attached to every second atom, while structurally they differ in that the former molecules take the form of helices, the latter, the normal planar configuration.

As in polypropylene, 3 damping peaks are generally observed in polyethylene^{52,53,57,77,78}. The temperatures at which they occur were established to be -100°C , 0°C and 70°C by Robinson and Oakes⁵⁷, and associated with certain CH_2 links in the main chains, side chain mobility, and large

scale amorphous and crystalline chain motions. The precise location of these peaks will be expected to vary from one polyethylene with more side branches or higher crystallinity, to another with different characteristics, e.g. Deeley et al.⁷⁹ found the low temperature peak at -113°C for a poorly crystalline, low density polyethylene, and at -98°C for a highly crystalline, high density polyethylene, both being unbranched.

The occurrence of the low temperature peak in polypropylene at a higher temperature (-80°C) appears to be the result of additional hindrance to main chain freezing by the methyl groups on every other carbon atom, (since the low temperature peak in polyethylene is ascribed to the same mechanism, and has no such hindrance).

It is interesting to note that Kline et al.⁷⁸ observed a shift of their -103°C peak to higher temperatures with decreased branching while Nielsen⁷⁷ noticed that his -110°C peak shifted to higher temperatures with increasing vinyl acetate copolymer, for polyethylene. The former phenomenon was accounted for by a narrowing of the relaxation times associated with the movement of a small number of CH_2 units, while in the case of the latter, greater hindrance to main chain movement predominated. It seems that the bulky methyl groups, which in some measure cause polypropylene to exhibit

a low temperature transition, at a higher temperature than polyethylene and the bulky acetate groups have a similar effect, while ordinary side branching of the $\text{CH}_2\text{-CH}_2$ type, has the reverse effect. Thus the increase or decrease in the low temperature transition would appear to be connected with the nature of the side groups, or potential impediments to chain motion.

The difference in room temperature peaks is not surprising since the mechanism in polypropylene is main chain freezing and in polyethylene, side chain activity. In fact for polyethylene with negligible branching, the room temperature transition is almost entirely absent⁷⁸.

The high temperature transition in polyethylene is lower than that in polypropylene, the peaks in each case being assigned to large scale mobility of polymer chains in amorphous regions and the onset of crystalline melting. Deeley et al.⁷⁹ observed this transition at 117°C for a high density, 91% crystalline, unbranched polyethylene and at 90°C for a low density amorphous unbranched polyethylene, while the peak in polypropylene (75% crystalline) is about 150°C . Three reasons could account collectively for the much higher polypropylene transition.

1. The considerable restraint on the amorphous regions

by the crystalline regions.

2. The hindrance to chain motions by the CH_3 groups.
3. The likelihood of greater entanglement between helices than between fully extended chains.

Humidity Experiments

Wool

Speakman¹² and Meredith¹³ attributed the fall in the modulus of torsional rigidity of wool fibres to the breaking of hydrogen bonds between CO and NH groups of neighbouring peptide chains, while the polar groups attached to the side chains had no effect on the rigidity of the fibres. The results of this investigation, however, suggest that both the main chains and side chains contribute to the bending modulus.

Meredith¹³ calculated the amounts of water absorbed by polar groups of side chains (a'water) and by polar groups of main chains (a''water) at several humidities. His data are presented below:

Amount of water absorbed (% regain) at different		relative humidities.					
% r.h.	10	30	50	65	75	90	
a'	2.8	4.2	4.7	4.9	5.0	5.1	(x)
a''	0.75	2.3	3.9	5.0	5.8	7.5	(y)

He found a linear relationship between relative rigidity and the amount of a'' water, the former decreasing, with increasing amount of the latter. The same straight line relationship is obtained in plotting relative bending modulus against a'' water absorbed (see Fig.36A). If however, relative bending modulus is plotted against a' water absorbed, two straight lines are obtained with different slopes, and intersecting, by extrapolation, at 45% relative humidity (see Fig.36B).

Now above 45% relative humidity, and up to 90% relative humidity, the bending modulus falls by some 32% (Fig.34 and Table 59A), while only about 10% of the total a' water is absorbed in this range (from (x)) and 55% of a'' is absorbed (from (y)). Clearly, above 45% relative humidity, a'' water is responsible to a great extent for the fall in bending modulus. Below 45% relative humidity, the drop in bending modulus is linearly related to both a' and a'' absorbed water. At 45% relative humidity the fall from dryness is greater (see Fig.34), than that which would be predicted from Fig.36A if only a'' water was responsible. Therefore, the a' water must have a considerable effect on the initial fall in bending modulus at the lower relative humidities.

This trend of thought fits well into the picture of

WOOL

FIG 36A.

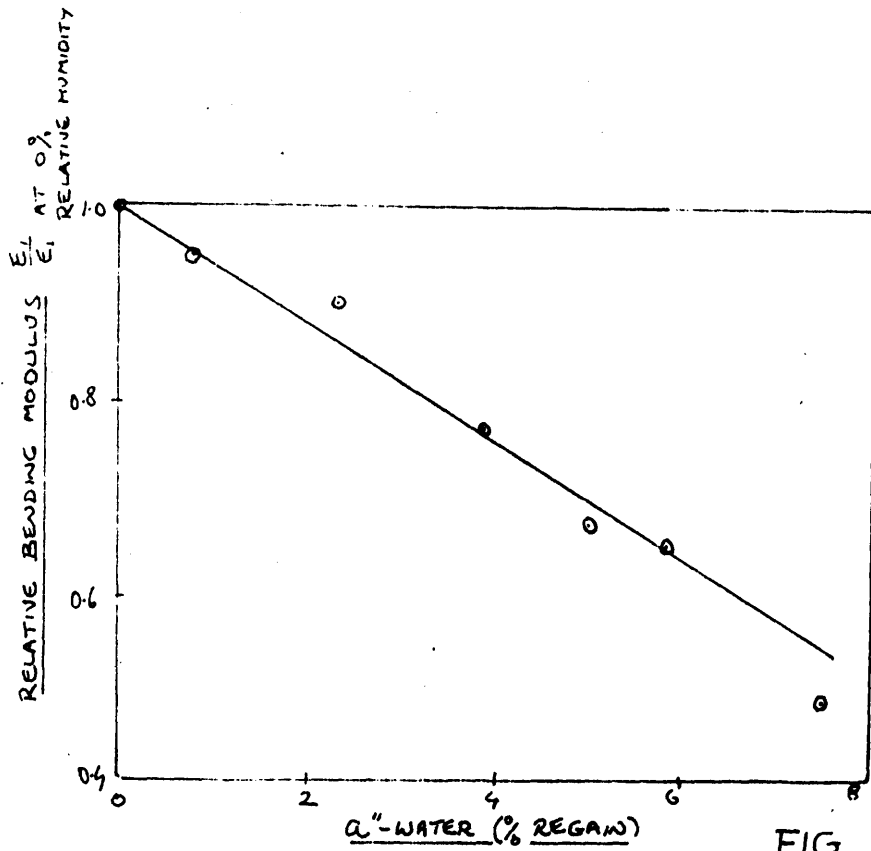
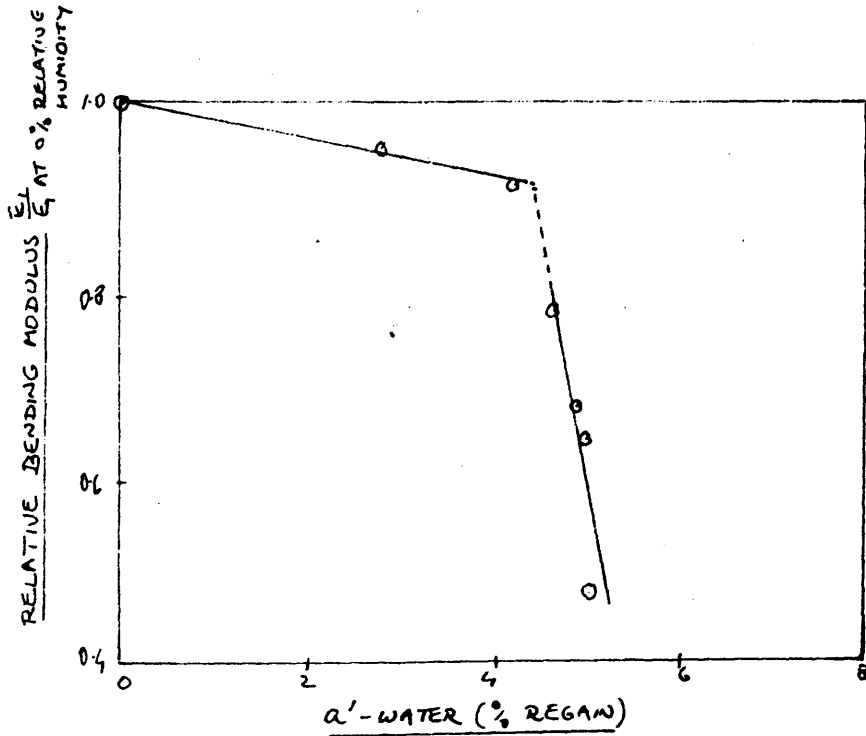


FIG 36B.



the wool structure which was developed from the temperature experiments. Those sites which will initially be available to water molecules are the non-satisfied side chains, and a very few main chains which have not accepted the "coiled coil" configuration. Furthermore, bonded side chains will be more accessible than polar groups in main chains which are thought to lie in a quasi three dimensional crystalline manner, as "coiled coils". Thus at lower relative humidities, more a' water is expected to be absorbed than a'' water and this is shown ((x) and (y)), quite clearly.

At humidities of over 45% relative humidity, when the majority of sites available to a' water are occupied, the water molecules will then be attracted to the hydrophilic groups in the quasi crystalline "coiled coils" main chains which had hitherto been less penetrable. Thus above 45% relative humidity, a large fall in bending modulus (31% from 45 to 90% relative humidity - Fig.34..) can be expected since it is due mainly to inter and intra molecular hydrogen bond breakage between main chains.

In Fig.30, a drop in bending modulus of dry wool from a relative value of 1 at 20°C to 0.9 at 80°C, is observed. At this temperature hydrogen bonding in all parts of amorphous regions, other than "coiled coils", is thought to be broken. In Fig.34 a drop from 1 to 0.8 in relative bending

modulus is observed between 0% and 45% relative humidity, at about which humidity, the "coiled coils" are thought to begin to accept moisture. The great difference in loss of bending strengths under the two conditions must be due to the fact that the effect of temperature on the "coiled coils" is in fact negligible - as it is on the salt linkages, while up to 45% relative humidity (from 0%) the "coiled coils" will be very slightly affected and the salt linkages disrupted⁷. A point worth noting at this stage is that van Wyk¹¹ found that the bending modulus of wool was reduced in the ratio of 3:1 from dryness to saturation. The shape of the curve was similar to that found in this work, while the ratio of the dry bending modulus to that at saturation is estimated to be about 2.8 : 1. in this work.

Warburton⁸ measured the logarithmic decrement for wool with increasing moisture content, and stated it increased continuously suggesting a "large increase in plasticity with regain". Close examination of the curve he produced reveals that very slight shoulders at 8% and 20% regain might exist (about 40 and 80% relative humidity respectively). If in fact they do, they would correspond reasonably with loss tangent shoulders at 35 and 70% relative humidity (Fig.33). These shoulders develop as peaks in the loss modulus curves (Fig.35) at about 33% and 70% relative humidity respectively.

The 33% peak is thought to be the result of previously mentioned secondary bonds being broken (below 45% relative humidity). The fact that the loss modulus is about twice as great as that of the 80°C peak in the temperature experiments is explained in the same way as the differences in fall of relative bending modulus i.e. in the humidity range, the internal friction will be greater since salt linkages and a very few "coiled coils" are bearing stress, while in the temperature experiment, up to 80°C, these elements do not bear stress.

The second loss modulus peak at 70% relative humidity is due mainly to the gradual breaking of hydrogen bonds in the "coiled coils" up to the point of the maximum, while beyond the maximum, sufficient chain mobility at the expense of little external force, causes a fall in modulus in spite of some further hydrogen bond breaking at higher humidities.

The value of 45% relative humidity, extrapolated in Fig.36B appears to be very significant. It is seen to coincide with that relative humidity at which the energy dissipated is a minimum (Fig.35) and lies between the loss modulus maxima. In other words, it seems to support the previous argument that two mechanisms are involved during the moisture absorption of wool, the details of which have been described. Moreover, the mechanism responsible for

the higher humidity "transition", while involved to a small extent in the lower humidity transition, only becomes really effective above 45% relative humidity, above which the mechanisms responsible for the lower humidity transition are almost ineffective.

Nylon 66

Figs. 33 and 35 indicate that two definite dispersions in the dynamic mechanical response of nylon 66 to increasing moisture content exist. A loss tangent shoulder at 40% relative humidity (loss modulus shoulder at 35% relative humidity) which in previous work^{9,56} was undetected, is accompanied by a rapid change in the bending modulus, and its existence as a dispersion cannot be doubted. A loss tangent peak at 85% relative humidity (loss modulus peak at 80% relative humidity) has a location and magnitude which is thought to correspond with the single peak that Quistwater and Dunell^{9,56} observed. The aforementioned workers experimented at three temperatures and to emphasise the good agreement between this work and theirs, the data for this single peak is presented below.

Temperature of Experiment °C	Loss modulus value dynes/cm ² x 10 ¹⁰	Location of loss modulus peak % Relative Humidity
9	0.38	90 [✓]
20	0.32	80 [*]
35	0.26	60 [✓]
60	0.23	35 [✓]

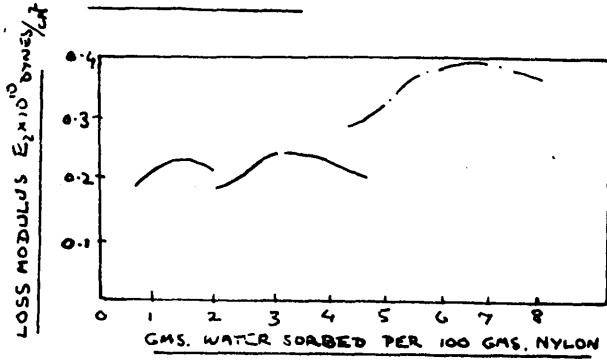
* This investigation.

✓ Quistwater and Dunell^{9,56} - see Fig.37A.

The value of $\tan \delta$ at this peak varied from 0.05 to 0.10 in the work of Quistwater and Dunell^{9,56} and they associated it with the 77°C peak of Woodward et al.⁵¹ who obtained a peak at 77°C, when working over a wide temperature range, with a value of 0.035. The mechanism responsible for the peak was therefore segmental motion due to hydrogen bond weakening. In the present work, the peak at 80% relative humidity has a value of 0.32×10^{10} dynes/cm.² for loss modulus, and since the fibre was from the same yarn as used by Hsu¹, would be due to the same mechanism as caused a peak at 120°C with a value of 0.25×10^{10} dynes/cm., by parallel reasoning to Quistwater and Dunell^{9,56}. The mechanism is the same as the one responsible for the 77°C peak of Woodward et al.⁵⁷, and varies in temperature on account of

NYLON 66

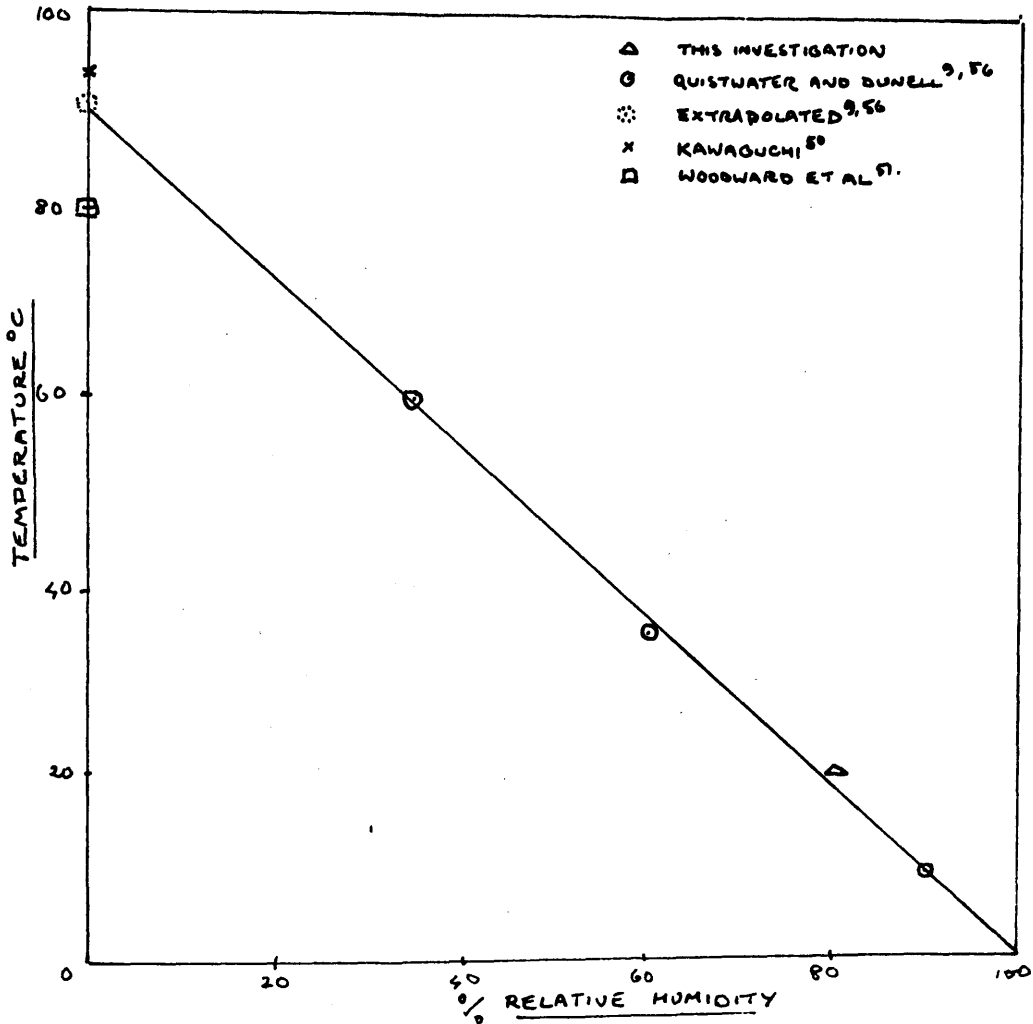
FIG. 37A



DATA OF QUISTWATER AND
DUNELL SHOWING LOSS MODULUS
MAXIMA AS A RESULT OF THE
WATER SORPTION OF NYLON 66

AT 9°C - - - -
35°C - - - -
60°C - - - -

FIG. 37B



structural differences¹.

The shoulder at 35% relative humidity has a loss modulus value of 0.21×10^{10} dynes/cm.² which could correspond to the -35°C peak of Hsu¹, which had a corresponding value of 0.28×10^{10} dynes/cm.² and was ascribed to segmental motion involving non hydrogen bonded amide groups.

Analysing the complete curve, it would appear that initially absorbed water is attracted to non hydrogen bonded carbonyl groups in the amorphous regions and effectively heightens rotational barriers to main chain rotation (carbonyl and amide portions probably). Motions would thus be "arrested" were it not for the simultaneous plasticising action of water vapour and the onset of diminishing effectiveness of hydrogen bonds, causing molecular chain motion. At the same time, this chain motion increases internal friction and prevents a true peak from forming. When hydrogen bonds are virtually disrupted segmental motion is more fully facilitated but a drop in loss modulus, subsequent to the 80% relative humidity peak, occurs since the force required to cause this motion decreases rapidly with intermolecular constraints removed.

The bending modulus data support the loss modulus data, but it is perhaps surprising to find such a large decrease in bending modulus of the hydrophobic nylon 66 as

relative humidity is increased. However, by comparing the effect of temperature on dry nylon 66¹, with that of humidity, it is seen that in the former case the relative bending modulus drops in the ratio 2:1 as temperature is increased from 20°C to 120°C (hydrogen bond peak) - Fig.30, while in the latter case, accounting for dimensional changes the relative bending modulus drops in the ratio of 2 : 1.14 on increasing the relative humidity from 0% to 75% (hydrogen bond peak) - Fig.34. Since over these ranges the molecular mechanisms are essentially the same, it is not surprising to find similar drops in bending modulus. Moreover, it suggests that the molecular interpretations are correct. A further point worth noting is that the hydrogen bonds must play a considerable part in the bending resistance to small forces (van der Waals forces will also be important). The fact that a second "peak" has been established at 35% relative humidity, which Quistwater^{9,56} and Dunell did not observe, would indicate that measurements in bending vibration are more sensitive than those in longitudinal vibration. This is quite feasible since on the application of a small tensile stress the main chains bear the brunt of the force², while in bending stress the secondary forces will respond more effectively. Hence at any particular temperature or humidity the effect of these conditions will probably be assisted by the bending force, more than by the tensile

force, thus assisting rather than obscuring, the detection of the mechanism involved.

Predicting and Estimating the Hydrogen Bond

Dispersion in Nylon 66.

(1) The location: by extrapolating the results of Quistwater and Dunell^{9,56} (see Figs.37A and 37B), a maximum in loss modulus would occur at 0% relative humidity at an experimental temperature of about 90°C, (and would have a magnitude of the order of 0.18×10^{10} dynes/cm.²). This is obtained by assuming that a straight line relationship exists between the relative humidity at which the peak occurs and the experimental temperature. The assumption would appear to be correct for on extending the assumed straight line, it intersects the ordinate in the 90°C temperature region which corresponds with the temperature of the hydrogen bond peak for dry nylon obtained by Kawaguchi⁵⁰ and Woodward et al.⁵¹ (see Fig.37B). The loss modulus value of 0.18×10^{10} dynes/cm.² (see Fig.38) is smaller than that obtained by Hsu¹, but he found that this particular peak existed at 120°C, due to structural differences. Normally, however, 0.18×10^{10} dynes/cm.² would be a reasonable value to expect. (Hsu¹ determined a rather high bending modulus of 6.0×10^{10} dynes/cm.² at 20°C

and 0% relative humidity, which was confirmed in this work.)

Thus, for nylon 66, if the temperature of the experiment is known, and constant, the location of a relative humidity peak can be theoretically predicted. Conversely, if the relative humidity is known, and constant, the location of a temperature peak can be theoretically predicted.

The straight line graph (Fig.37B) has the simple equation

$$y = -ax + b$$

where y is proportional to the temperature and x to the relative humidity.

- (2) The magnitude: the height of the loss modulus peak can be estimated in either an experiment involving changing humidity at constant temperature, or changing temperature at constant humidity.

Accepting that the magnitude of the loss modulus peak is of the order of 0.18×10^{10} dynes/cm.² in an experiment at 0% relative humidity (and from the combined data of Hsu¹, Kawaguchi⁵⁰, and Woodward et al.⁵¹, it seems reasonable) then by plotting the loss modulus values of "relative humidity" peaks, obtained in experiments conducted at different constant temperatures, against these temperatures, curve (i) in Fig.38 is obtained. (The curve is deduced from the

data of Quistwater and Dunell^{9,56} - Fig.37A and of this work.) From the same data, the loss modulus values of "temperature" peaks, obtained in experiments conducted at different constant relative humidities, can be plotted against these relative humidities, and curve (ii) in Fig.38 can be obtained.

Thus, if the temperature of the experiment is constant, the location of the relative humidity at which a peak occurs is obtained from Fig.37B, and the magnitude of the loss modulus from Fig.38 curve (i). The magnitude of the "temperature" loss modulus peak for an experiment at constant relative humidity is obtained from Fig.38, curve (ii).

The equation for Fig.38(ii) is of the type

$$y = ax^2 + b$$

where y is proportional to the loss modulus,
and x to the relative humidity.

Viscose Rayon.

Considerable investigation of the effects of moisture on the dynamic tensile and torsional moduli of cellulose fibres has been carried out, e.g. by Meyer and Lotmar²² who found that the tensile modulus of bone dry viscose rayon was

was about 11 times that of wet viscose rayon, by Meredith¹³, who observed that the modulus of torsional rigidity of dry viscose rayon was 33 times that of viscose rayon at 100% relative humidity. Comparatively little work has been done on the effect of moisture on the internal friction of viscose rayon. Price et al.⁵⁵, in forced longitudinal vibration experiments found only a small increase in internal friction on increasing the relative humidity from 28% to 98% and suggested that hydrogen bonding was not of great consequence in the mechanism of energy loss in viscose rayon.

By extrapolating the results of Tokita³⁷, (see Fig. 39A), who worked over a wide temperature range at several constant relative humidities, the loss tangent varied considerably with relative humidity for a constant temperature of 30°C. The value of loss tangent was about twice as great at 80% relative humidity as at 0% relative humidity. The shape of the calculated loss tangent curve is almost identical with that obtained in this work (see Fig. 33), the main difference being that the observed maximum is at a lower relative humidity of about 25%. This, however, is expected since the maximum at 35% relative humidity (Fig. 33) was obtained in an experiment conducted at 20°C. The loss tangent maximum at 35% becomes apparent as a loss modulus

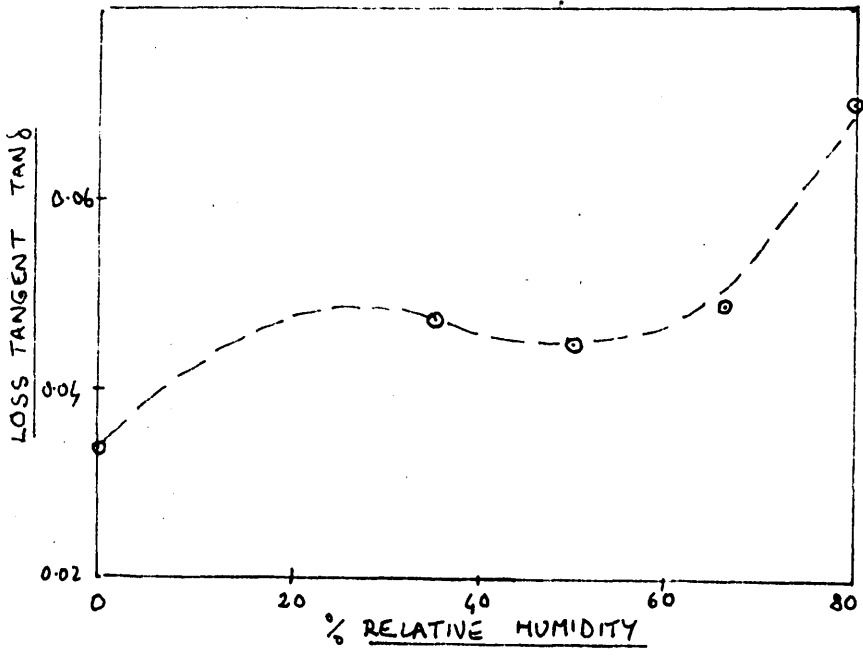
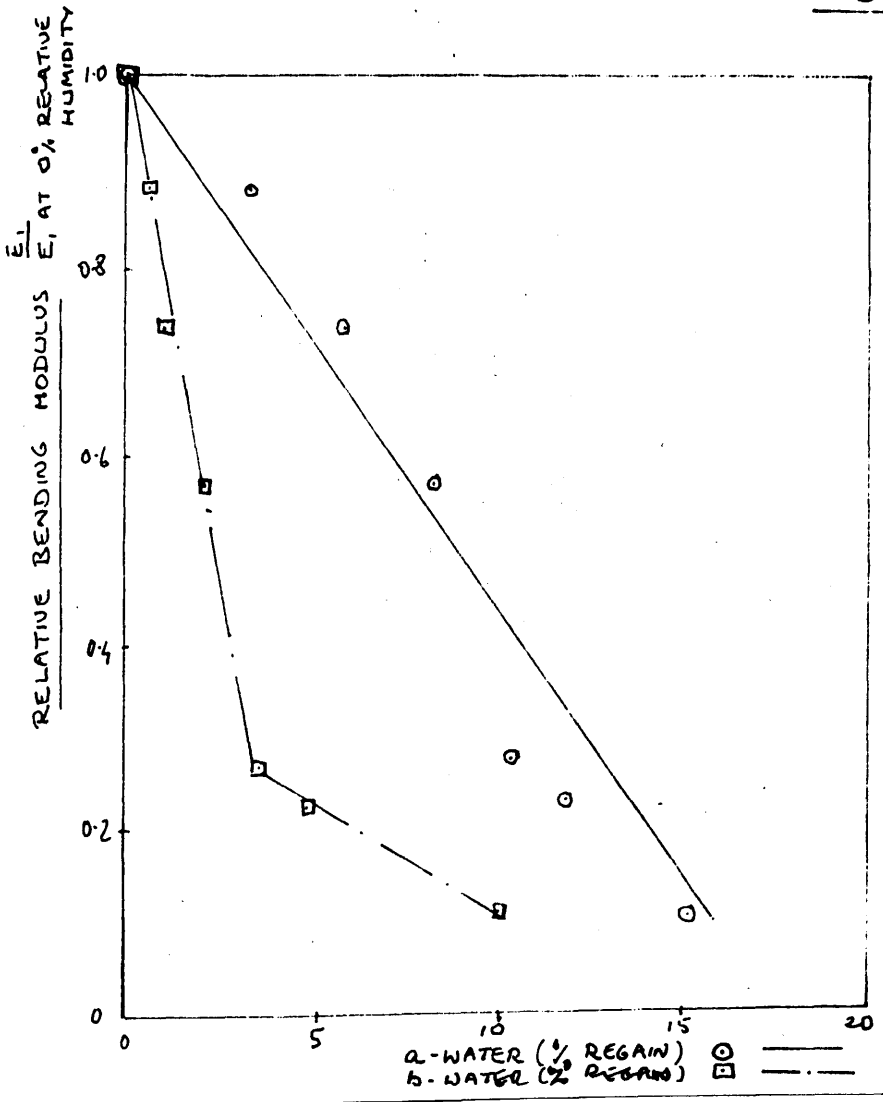


FIG 39B



maximum at 30% relative humidity, and since the loss modulus gives the actual internal friction, interpretation will later be put to this curve. (Fig.35).

The amorphous portion of the fibre is that which is accessible to moisture, the moisture being attracted to the hydrophilic hydroxyl groups. Now, according to Peirce's¹⁶⁶ two phase sorption theory, water vapour is absorbed in two ways

- (1) each molecule of water is associated with a definite group in the fibre molecule, as in a chemical compound (a - water)
- (ii) water molecules fill the spaces available under attractive forces like those in a liquid (b - water)

The relative amounts of each type of water absorbed at different humidities can be estimated from the data of Meredith¹³, which is presented below

Relative Humidity%	0	10	30	50	65	75	90
Total % Regain	0	3.4	6.8	10.4	13.7	16.7	25.5
a-water absorbed (% regain)	0	3.1	5.8	8.3	10.2	11.7	15.0

Thus at lower relative humidities, the ratio of a-water to b-water absorbed is great, and at higher humidities relatively small. Clearly then, the dispersion at low humidities should be chiefly due to a-water, while if one exists, (and it does

(see Fig.35)) at higher humidities both a-water and b-water could be responsible (since the amount of a-water absorbed is still increasing, but the amount of b-water absorbed is increasing at a faster rate).

Before analysing the loss modulus curve, a look at the plot of relative bending modulus against a-water and b-water absorbed may be enlightening (Fig.39B). The linear relationship which Meredith¹³ found between relative rigidity and a-water absorbed, is similarly obtained with the relative bending modulus - a-water plot. By plotting relative bending modulus against b-water absorbed, as in the case of wool, two straight lines of different gradients are obtained, whose point of intersection occurs at a value of absorbed b-water equivalent to 65% relative humidity. The same type of effect was found in the case of wool, but for viscose rayon, it appears that at low humidities (below 65% relative humidity), the b-water contributes little to the reduction of bending modulus, while above this value of relative humidity, the effect of b-water may not be negligible.

Now considering the process of moisture sorption, the greater part of initially absorbed moisture, as the data of Meredith¹³ show, is attracted to the available non hydrogen bonded, and hydrogen bonded, hydroxyl groups. Thus at low

humidities the internal friction increases on two accounts.

- (i) straining (and eventual breaking) of hydrogen bonds
- (ii) increased chain mobility as a result of this breaking, and so-called "plasticisation".

Thus with reference to the loss modulus curve sufficient hydrogen bond breakage must have occurred at 30% relative humidity, to allow further molecular mobility at the expense of little applied force. Hence the occurrence of the maximum. Since the relative bending modulus is linearly related to the a-water absorbed, hydrogen bond breakage continues up to 90% relative humidity (the limit of this investigation), but down to a minimum of dissipated energy at 65% relative humidity, does not cause a continuing rise in loss modulus, again due to the considerable and increasing mobility which requires little force. Above 65% relative humidity the loss modulus rises, reaching a maximum at about 80% relative humidity (see Table 59B and Fig.35). It is highly unlikely that suddenly, a greater number of hydrogen bonds per unit rise in relative humidity ^{is} ~~are~~ being strained. It is thought therefore that the now fast increasing amount of absorbed water is filling empty space sufficiently to hinder motion rather than to plasticise, and assists the straining of certain hydrogen bonds in causing a rise in loss modulus. The decelerated fall in bending modulus (Fig.34)

supports the proposal that some hindrance is occurring. The second loss modulus peak then occurs at 80% relative humidity accompanied by a rapid fall in bending modulus - the result of further hydrogen bond straining (breakage), but now accompanied by renewed chain mobility at little expense of force.

Again it is of interest to note that the extrapolated value of 65% relative humidity (Fig. 39B) is significant. It marks that stage at which the b-water becomes influential in the reduction of bending modulus with increasing moisture content, and coincides with that relative humidity at which the internal friction is a minimum, lying between two maxima. This supports previous arguments that the b-water as was previously pointed out, has little effect at low humidities, but at higher humidities the amount of absorbed b-water is proportional to bending modulus (as is the a-water) to such a degree that it assists in the fall of bending modulus.

A comparison of humidity results with temperature results may appear to be complex since there are two hydrogen bond peaks in the former investigation and only one at 90°C ¹ in the latter. Moreover, the energy dissipated is of the order of 0.75 and 0.22×10^{10} dynes/cm.² for the low and high relative humidity peaks respectively, and an estimated 0.30×10^{10} dynes/cm.² at the 90°C peak of dry viscose rayon.

(Thus the total energy dissipated is some 3 times greater for the two humidity peaks together, than for the temperature peak.)

This great difference could be due to one of two factors, or both;

- (a) the viscose rayon used by Hsu¹ was more crystalline and consequently the total number of hydrogen bonds in amorphous regions was smaller, thereby causing a smaller energy loss
- (b) the conferred chain mobility due to moisture sorption is such that as certain hydrogen bonds are broken, others can reform.

The second reason is feasible and at the same time, does not necessitate an alteration of the interpretation of the loss modulus curve.

The greater fall in bending modulus, as a result of moisture sorption (1:0.75 from 0% relative humidity to 30% relative humidity, and 1:0.88 from 20°C to 90°C according to Hsu¹) is expected, since although in moisture sorption, new hydrogen bonds appear to form, so assisting bending resistance, the chain mobilities in non hydrogen bonded sections are so great as to cause the more rapid fall.

References

1. Hsu, B.S., Ph.D.Thesis Manchester University, 1958.
2. Maxwell, B., J.Polymer Sci., 20, 551, 1956.
3. Mark, H., p.217 in High Polymers Vol.V.
Cellulose and Cellulose Derivatives, Part I.
Ed. Ott,E., Spurlin,H.M., Grafflin,M.W.,
Interscience Publish. Inc., N.Y. London.
4. Gordon, M., p.31 in The Structure and Physical Properties of High Polymers., Ed. Gordon,M.,
Wilson, Guthrie & Co., 1957.
5. Tobolsky,A.V., p.61 in The Properties and Structure of Polymers. Ed. Tobolsky,A.V., John Wiley
& Sons Inc.,
6. Onogi,S., and Ui,K,, J.Colloid.Sci., 11, 214, 1956.
7. Feughelman, M., J.App.Polymer Sci., 2, 189, 1959.
8. Warburton, F.L., J.Text.Inst., 39, P297, 1948.
9. Quistwater,J.M.R., and Dunell, B.A., J.Polymer Sci.,
28, 309, 1958.
10. Kawai, H, and Tokita, N., J.Phys.Soc.Japan, 6, 367, 1951.
11. van Wyk, C.M., S.Afr.J.Sci., 48, 127, 1951.
12. Speakman, J.B., Trans.Farad.Soc., 40, 6, 1944.
13. Meredith, R., J.Text.Inst., 48, T163, 1957.
14. Brown, A., Text.Res.J., 25, 891, 1955.
15. Bryant, G.M., and Walter, A.T., ibid., 29, 211, 1959.
16. Guthrie, J.C., J.Text.Inst., 48, T193, 1957.

17. Suleimanova, Z.I., and Kargin, V.A., Zhur.Fiz.Chem., 32, 811, 1958.
18. Kaswell, E.R., Amer.Dyes Rep., 38, 127, 1949.
19. Rigby, B.J., J.Text.Inst., 49, T379, 1958.
20. Peters, L. and Woods, H.J., p.186 in The Mechanical Properties of Textile Fibres. Ed. Meredith, R. N.Holland Publishing Co., Amsterdam 1956.
21. Bueche, F., J.Polymer.Sci., 22, 113, 1956.
22. Meyer, K.H. and Lotmar, W., Helv.Chim.Acta, 19, 68, 1936.
23. Tipton, H., J.Text.Inst., 46, T323, 1955.
24. Palandri, G., Rubber Age, 64-65, 45, 1948-49.
25. de Vries, H., in On the Elastic and Optical Properties of Cellulose Fibres. Schotanus and Jens, Utrecht, 1953.
26. de Vries, H., Ann.Sci.Text.Belges., No.4, 286, 1955.
27. Hamburger, W.J., Text.Res.J., 15, 295, 1948.
28. Fujino, K., Kawai, H., and Horio, T., Text.Res.J., 25, 722, 1955.
29. Kawai, H. and Tokita, N., J.Phys.Soc.Japan, 5, 17, 1950.
30. Dunell, B.A. and Dillon, J.H., Text.Res.J., 21, 393, 1951.
31. Lyons, W.J., and Prettyman, I.B., J.App.Phys., 19, 473, 1948.
Lyons, W.J., Text.Res.J., 19, 123, 1949.
32. Chaikin, M., and Chamberlain, N.A., J.Text.Inst., 46, T25 and 44, 1955.
33. Asmussen, R.W., and Andersen, F., Trans.Dan.Acad.Tech.Sci., No.5, 1947.
34. Andersen, F. ibid., No.13, 1950.
35. Ballou, J.W., and Silverman, S., Text.Res.J., 14, 282, 1944.

36. Dunell, B.A. and Price, S.J.W., J.Polymer Sci., 18, 305, 1955.
37. Tokita, N., ibid., 20, 515, 1956.
38. Russell, J., and van Kerpel, R.G., ibid., 25, 77, 1957.
39. Nakamura, K., Chem.High Polymers, Japan, 13, 47, 1956.
40. Tokita, N., and Kanamura, K., J.Polymer Sci., 27, 255, 1958.
41. Mackay, B.H., and Downes, J.C., J.App.Polymer Sci., 2, 32, 1959.
42. Ree, T., Chen, M.C., and Eyring, H., Text.Res.J., 21, 789 and 799, 1951.
43. Smith, J.C., McCrackin, F.C., and Schiefer, H.J., J.Text. Inst., 50, 755, 1959.
44. Eyring, H., Alder, H.G., Rossmassler, S.A., and Christensen, C.J., Text.Res.J., 22, 223, 1952.
45. Adams, N., J.Text.Inst., 47, T531, 1956.
46. Fujino, K., Kawai, H., Horio, T., and Hiyamoto, K., Text.Res.J., 26, 852, 1956.
47. Kawaguchi, T., Chem.High Polymers, 14, 176, 1957.
48. Thompson, A.B., and Wood, B.W., Trans.Farad.Soc., 46, 459, 1950.
49. Kawaguchi, T., J.Polymer Sci., 32, 417, 1958.
50. Kawaguchi, T., J.App.Polymer Sci., 2, 56, 1959.
51. Woodward, A.E., Sauer, J.G., Deeley, A.W., and Kline, D.E., J.Colloid.Sci., 12, 363, 1957.
52. Schmieder, K., and Wolf, K., Kolloid Z., 127, 65, 1952.
53. Schmieder, K., and Wolf, K., ibid., 134, 149, 1953.

54. Woodward, A.E., Crissman, J.M., and Sauer, J.A.,
J. Polymer Sci., 44, 23, 1960.
55. Price, S.J.W., McIntyre, A.D., Pattison, J.D., and
Dunell, B.A., Text.Res.J., 26, 276, 1956.
56. Quistwater, J.M.R., and Dunell, B.A., J.App.Polymer Sci.,
1, 267, 1959.
57. Robinson, D.W., and Oakes, W.G., J.Polymer Sci., 14,
505, 1954.
58. Reddish, W., Trans.Farad.Soc., 46, 459, 1950.
59. Ward, I.M., ibid., 56, 648, 1960.
60. Nohara, S., Kobunshi Kagaku, 14, 318, 1957.
61. Ecker, R., Kautschuk u. Gummi, 6WT, 127, 1953.
62. Nolle, A.W., J.App.Phys., 19, 753, 1948.
63. Nolle, A.W., J. Polymer.Sci., 5, 1, 1950.
64. Sack, H.S., Hotz, J., Raus, H.L., and Work, R.N.,
J.App.Phys., 18, 450, 1947.
65. Cunningham, J.R., and Ivey, D.G., ibid., 27, 967, 1956.
66. Fukada, E., J.Phys.Soc., Japan, 6, 254, 1951.
67. Gordon, M., p.43 in The Structure and Physical Properties
of High Polymers. Ed.Gordon,M., Wilson, Guthrie
and Co., 1957.
68. Yamamoto, K., and Wada, Y., J.Phys.Soc., Japan, 12, 374
1957.
69. Kawaguchi, T., Chem.High Polymers, 13, 287, 1956.
70. Deutch, K., Hoff, E.A.W., and Reddish, W., J.Polymer Sci.,
13, 565, 1954.
71. Hoff, E.A.W., Robinson, D.W., and Willbourn, A.H., ibid.,
18, 161, 1955.

72. Sharpe, E.B., and Maxwell, B., Modern Plastics, 33,
No.4, 137, 1955.
73. Newman, S., J.App.Polymer Sci., 2, 333, 1959.
74. Sauer, J.A., and Kline, D.E., J.Polymer Sci., 18,491,1955.
75. Sauer, J.A., Wall, R.A., Fuschillo, N., and Woodward, A.E.,
J.App.Phys., 29, 1385, 1958.
76. Baccareda, M., and Butta, E., J.Polymer Sci., 22, 217,1956.
77. Nielsen, L.E., ibid., 42, 357, 1960.
78. Kline, D.E., Sauer, J.A., and Woodward, A.E., ibid.,
22, 455, 1956.
79. Deeley, C.W., Sauer, J.A., and Woodward, A.E., J.App.Phys.,
29, 1415, 1958.
80. Butta, E., and Charlesbury, A., J.Polymer Sci., 33, 119,
1958.
81. Koppelman, J., Kolloid Z., 144, 12, 1955.
82. Fitzgerald, E.R., J.App.Phys., 29, 1442, 1958.
83. Sheldon, F., J.Colloid Sci., 14, 147, 1959.
84. Shinohara, Y., J.App.Polymer Sci., 1, 257, 1959.
85. Stauff, D.W., and Montgomery, D.J., J.App.Phys., 26, 540,
1955.
86. Eischen, G., C.r.Acad.Sci.Paris, 248, 3160, 1959.
87. Sen, K.R., J.Text.Inst., 39, T339, 1948.
88. Khayatt, R.M., and Chamberlain, N.H., ibid., 39, T185,1948.
89. Roder, H.L., Bull.Inst.Text.France, 49, 61, 1954.
90. Kawakami, T., and Ikeda, S., Bull.Text.Res.J., Japan, 32
14,

91. Carlene, P.W., J.Text.Inst., 41, T159, 1950.
92. Prins, J., Rayon Review, 9, 54, 1955.
93. Isshi, T., J.Text.Mach.Soc., Japan, 3, No.2, 48, 1957.
94. Friedermann, W., Deutsche Textilberichte, 7, 159, 1957.
95. Peirce, F.T., J.Text.Inst., 20, T133, 1929.
96. Lochner, J.P.A., ibid., 40, T220, 1949.
97. Lincoln, B., ibid., 43, T158, 1952.
98. Woods, H.J., Leeds Lit. and Phil.Soc., 3, 577, 1940.
99. Speakman, J.B., Trans.Farad.Soc., 25, 92, 1929.
100. Dusenbury, J.H., Wu, C.N., and Dansiger, C.I., Text. Res.J., 30, 277, 1960.
101. Guthrie, J.C., Morton, D.H., and Oliver, P.H., J.Text. Inst., 45, T913, 1954.
102. Karrholm, E.M., and Schröder, B., Text.Res.J., 23, 207 1953.
103. Karrholm, E.M., ibid., 25, 756, 1955.
104. Okajima, S., and Suzuki, S., J.Soc.Text. and Cell. Ind., Japan, 15, 809, 1959.
105. Schröder, G., Melliand Textilberichte, 5, 418, 1953.
106. Horio, M., Onogi, S., Nakayama, C., and Yamamoto, K., J.App.Phys., 22, 566, 1951.
107. Horio, M., and Onogi, S., ibid., 22, 977, 1951.
108. Wakelin, J.H., Voong, E.T.L., Montgomery, D.J., and Dusenbury, J.H., ibid., 26, 786, 1956.
109. Marlow, P.F., J.Text.Inst., 49, T40, 1958.

110. Onogi, S., and Ando, S., J.Soc.Text. and Cell.Ind.,
Japan, 9, 617, 1953.
111. Patterson, W.I., Geiger, W.B., Mizell, L.R., and
Harris, M., J.Res.Nat.Bur.Stand., 27,89,1941.
112. Bull, H.B., J.Amer.Chem.Soc., 66, 1499, 1944.
113. Handbook of Textile Fibres. Ed. Cook, Gordon,J.,
Merrow Publ.Co., 1959.
114. Steffens, W., Textil Praxis, 10, 3, 1955.
115. de Witt Smith, H., Proc.A.S.T.M., 44, 543, 1944.
116. King, A.T., J.Text.Inst., 17, T53, 1926.
117. Starkweather, H.J., Jnr., J.App.Polymer Sci., 2,
129, 1959.
118. Abbott, N.J., and Goodings, A.C., J.Text.Inst., 40,
T232, 1949.
119. Meredith, R., Ch.XIII in Fibre Science. Ed.Preston,J.M.,
Text.Inst., 1953.
120. Stern, F., Private communication.
121. Goodings, A.C., and Turl, L.H., J.Text.Inst.,31,769,1940.
122. Man Made Textile Encyclopedia, Ed.Press, J., Inter-
science Publ.Co.Inc.New York 1959.
123. p.66 in "Contribution to the Physics of Cellulose
Fibres", Ed. Hermans, P.H., Elsevier 1946.
124. Hermaan, P., and Herzog, A., in "Mikroskopische und
Mechanisch Technische Textiluntersuchungen"
1931.
125. p.467 in Fibres from Synthetic Polymers, Ed. Hill, R.,
Elsevier 1953.

126. Henstead, W., J.Text.Inst., 52, P148, 1961.
127. Herstenberg, J., and Mark, H., Z.Kryst., 69, 271, 1929.
128. Passaglia, E., and Koppehele, H.P., J.App.Polymer Sci., 1, 28, 1959.
129. Howard, W.H., J.App.Polymer Sci., 5, 303, 1961.
130. Dannis, M.L., J.App.Polymer Sci., 1, 121, 1959.
131. Boyer, R.F., and Spencer R.S., J.App.Phys., 15, 398, 1944.
132. Fourt, L., and Harris, M., p.306 in Physiology of Heat Regulation and the Science of Clothing. Ed. Newburgh, L.H., W.B.Saunders Co. 1949.
133. Meredith, R., and Hsu, B.S., in the press.
134. p.220 in "Heat and Thermodynamics" Ed. Roberts, J.K., Blackie & Sons, London and Glasgow. 1933.
135. Beranek, L.L., p.3-57 in Americal Institute of Physics Handbook, McGraw-Hill Co. New York-London.1957
136. Peters, L., and Woods, H.J., Chapter VIII in "Mechanical Properties of Textile Fibres." Ed.R.Meredith, N.Holland Publishing Co., Amsterdam. 1956.
137. Fox, S.W., and Foster, J.F., Chapter 16 in "Introduction to Protein Chemistry". Eds. Fox, S.W., and Foster, J.F., New York, John Wiley and Sons Inc. 1957.
138. Astbury, W.T., and Bell, F.O., Nature, 147, 696, 1941.
139. Pauling, L., and Corey, R., Proc.Natl.Acad.Sci.U.S., 37, 205, 261, 729, 1951.
140. Crick, F.H.C., Nature, 170, 882, 1952.
141. Speakman, P.T., Review of Textile Progress, 11, 70, 1959.

142. p.80 in Artificial Fibres. Ed. Moncrieff, R.W., London National Trade Press Ltd., 1954.
143. Warburton, F.L., J.Text.Inst., 1959, 50, T1.
144. Pauling, L., and Corey, R., Proc.Natl.Acad.Sci.U.S., 37, 251, 1951.
145. Bamford, C.H., Hanbey, W.E., and Hapßey, F., Proc.Roy.Soc., A205, 30, 1951.
146. Rich, A., and Crick, F., Nature, 176, 915, 1955.
147. Bragg, L., Andrew, J.C., and Perutz, M.F., Proc.Roy.Soc., A203, 321, 1350.
148. p.98 in Handbook of Textile Fibres. Ed. Harris, M., Harris Research Laboratories Inc. 1954.
149. p.20 in Artificial Fibres. Ed. Moncrieff, R.W. London. National Trade Press Ltd., 1954.
150. p.70 in Contribution to the Physics and Chemistry of Cellulose Fibres. Ed. Hermans, P.H., Elsevier, N.Y. 1946.
151. Philipp, H.J., Nelson, M.C., Ziefle, H.M., Text.Res.J., 17, 585, 1947.
152. p.28 in Mechanical Properties of Textile Fibres. Ed. Meredith, R., N.Holland Publ.Co. Amsterdam, 1956.
153. Morehead, T., Text.Res.J., 20, 549, 1950.
154. Mandelkern, C., and Flory, P.J., J.Amer.Chem.Soc., 73, 3206, 1951.
155. Tricel Technical Service Manual, British Celanese Ltd.
156. p.16 in Man Made Textile Encyclopedia. Ed. Press, J., Interscience Publ.Co. Inc., New York, 1959.
157. Meredith, R., private communication.

158. Turner, D.J., Diploma Thesis, Royal College of Science and Technology, Glasgow. 1961.
159. p.460 in Fibres from Synthetic Polymers. Ed. Hill, R., Elsevier 1953.
160. p.66 in Handbook of Textile Fibres. Ed. Harris, M., Harris Research Laboratories Inc., 1953.
161. Ham, G.E., Text.Res.J., 24, 597, 1954.
162. Natta, G., and Corradini, P., J.Polymer Sci., 39, 29, 1959.
163. Ranby, B.G., Morehead, F.F., Walter, N.M., J.Polymer Sci., 44, 349, 1960.
164. Slichter, W.P., and Mandell, E.R., J.App.Phys., 29, 1438, 1958.
165. Reding, P.F., J.Polymer Sci., 21, 547, 1956.
166. Peirce, F.T., J.Text.Inst., 14, T1, 1923.

\$\$\$\$\$\$\$\$\$\$\$\$

bonded main chains. Being fewer in number, their associated loss modulus was smaller. The occurrence of the first hydrogen bond peak, 40°C earlier than the second, is thought to be due primarily to the additional straining of the hydrogen bonds between the side chains, caused by the chain mobility of the non-hydrogen bonded main chains.

The 110°C peak had a much higher loss modulus than the corresponding Acrilan peaks. This is to be expected since the hydrogen bonds are present in greater quantity due to the absence of the acetate groups present in Acrilan. Unlike Acrilan, Orlon appears to have no very low temperature transition (from the shape of the loss curves and the fact that at -60°C the bending modulus appeared to be approaching a limiting value), which suggests the absence of flexible, non hydrogen bonded side chains present in other acrylic polymers and Acrilan.

Polypropylene

The newness of polypropylene as a commercial fibre, merits a few introductory comments regarding its structure.

Natta and Corradini¹⁶² put forward a theory reasonably widely accepted, that on account of the methyl groups, a planar structure is impossible. "For instance, in the case of polypropylene, a planar structure would result in a